SAPIENZA
UNIVERSITÀ DI ROMA

From root extract to antiarthritic facts: trip across a novel therapeutic approach to inflammation and pain

PhD in Biochemistry

Department of Biochemical Sciences
"A. Rossi Fanelli"

PhD Candidate

Alessia Mariano

Supervisor
Prof. Anna Scotto d'Abusco

Coordinator
Prof. Stefano Gianni

XXXV cycle
Triennium: 2019-2022

Index

3

Abstract

Osteoarthritis (OA) is a chronical-degenerative and inflammatory disease affecting joints and involving several cellular and molecular processes in different cell types, as chondrocytes, osteoblasts, synoviocytes and immune cells. In OA the cartilage, a specialized tissue that allows the sliding between the two joint heads, is degraded, and, in the joint, the bones have friction each other causing pain and their own remodeling. Synovial membrane cells secrete inflammatory mediators and a greater amount of synovial fluid, resulting in synovial membrane thickening and contributing to the joint damage. To date, there is no specific anti-OA therapy, and so painkillers, anti-inflammatory drugs and intra-articular injections of corticosteroids are administered. However, considering painkilling and anti-inflammatory drug contraindications, in addition to chondroprotectors that preserve cartilage from degeneration, nutraceuticals are often introduced in therapies for their efficacy and less side effects than traditional drugs. Among them, *Harpagophytum procumbens,* known as Devil's claw, is one of the most used herbs as an anti-OA remedy. Its secondary roots contain several bioactive compounds able to relieve patient symptoms decreasing inflammation and joint pain. In order to understand its activity on pain and inflammatory pathways, in the present study, a *H. procumbens* root extract (HPE) was characterized for its phytochemical composition and effects on Fibroblast-like synoviocytes (FLSs) from OA patients. The dry HPE was solubilized in different solvents, deionized water (HPE_{H2O}), DMSO (HPE_{DMSO}), 100% v/v ethanol ($HPE_{EtOH100}$), and 50% v/v ethanol (HPE_{EtOH50}), chosen based on their biocompatibility and ability to dissolve different classes of phytochemical compounds. Preliminary phytochemical analyses have shown

that the highest polyphenol levels were found in HPE$_{DMSO}$ and HPE$_{EtOH50}$, whereas different volatile bioactive compounds, mainly β-caryophyllene and eugenol, were detected in all the extracts except for HPE$_{H2O}$. Since these compounds have been described to mitigate pain through an agonism on endocannabinoid type 2 (CB2) receptors and considering the involvement of CB2 in OA pathogenesis demonstrated through our histochemical analyses, it was decided to analyse the HPE analgesic effect on OA FLSs. However, even if both HPE$_{H2O}$ and HPE$_{DMSO}$ were able to enhance CB2 receptor expression, only the latter has been used for subsequent experiments. Considering the CB2 receptor association with G$_i$ protein in cell membrane, the HPE$_{DMSO}$ effectiveness to affect CB2 pathways was studied by analysing the cAMP modulation, the protein kinase A (PKA) and Extra-regulated kinase (ERK) activation and the correlated matrix metalloproteinase (MMP) production. In line with what expected, HPE$_{DMSO}$ was able to inhibit cAMP production and PKA activation, also showing a reduction in ERK1/2 phosphorylation that surprisingly disagreed with the extract effect on PKA. Interestingly, although it is not due to CB2 receptor stimulation, the effect on the MAPK pathway generates a decrease in some extracellular matrix degrading enzyme and pro-inflammatory interleukin expression, suggesting the HPE antiarthritic role. Moreover, to clarify the effects of bioactive constituents and the possible interactions occurring in the phytocomplex, harpagoside, the *H. procumbens* root extract biomarker, and the main volatile compounds detected at the phytochemical analysis, have been studied in comparison to the whole extract. It was observed that β-caryophyllene, α-humulene, eugenol and harpagoside alone were always less effective than the *H. procumbens* whole extract and the Mix that contained all the individual compounds. However,

7

the surprising result is that the mixture was also always less effective than HPE$_{DMSO}$ whole extract. This evidence suggested the existence of synergistic interactions between each analysed compound and other molecules not identified in phytochemical analyses that contribute to the entire extract bioactivity.

In our most recent analyses, HPE$_{DMSO}$ has demonstrated a role in the inhibition of the phosphoinositide specific-phospholipase C (PI-PLC) γ1 mRNA splicing process. Sanger sequencing analysis revealed some retained introns in HPE$_{DMSO}$ treated FLSs. However, studies describing the *H. procumbens* ability to interfere with the splicing process were not available in scientific literature. On the other hand, the accurate analysis of the PI-PLC γ1 gene, only carried out by the Human and Vertebrate Analysis and Annotation (HAVANA) group, identified the intron retention phenomenon in PI-PLC γ1 gene. Our results were perfectly in line with what described by the HAVANA group. However, during our analysis we highlighted a lack of HPE$_{DMSO}$ effect on intron retention phenomenon in some FLS samples from different OA patients. This inter-individual variability led us to consider more carefully some data obtained in our previous experiments. Surprisingly, it was shown that HPE$_{DMSO}$ was ineffective in inhibiting MMP gene expression in those samples where the intron retention phenomenon in PI-PLC γ1 mRNA was absent. This result suggested that the decrease of PI-PLC γ1 protein, due to lack of splicing, could be associated with the decrease of MMP production.

List of abbreviations

2-AG: 2-arachidonoyl glycerol

ADAMTS: A Disintegrin and Metalloproteinase domain with Thrombospondin motifs

AEA: arachidonoyl ethanolamide

ANOVA: analysis of variance

AP-1: activator protein-1

cAMP: cyclic-AMP

CB1: endocannabinoid type 1 receptor

CB2: endocannabinoid type 2 receptor

CREB: cAMP response element-binding protein

Ct: threshold cycle

CTL: control/ untreated cells

DAG: diacylglycerol

DAMPs: Damage-Associated Molecular patterns

DMSO: dimethyl sulfoxide

ECM: extracellular matrix

ELISA: Enzyme-Linked Immunosorbent Assay

ERK1/2: Extra-regulated kinase 1/2

EtOH: ethanol

FAAH: Fatty Acid Amide Hydrolase

FLSs: Fibroblast-like synoviocytes

GAGs: glycosaminoglycans

GC-MS: Gas Chromatography-Mass Spectrometry

GPCR: G protein coupled receptor

HAVANA: Human and Vertebrate Analysis and Annotation

HPE: *Harpagophytum procumbens* extract

HPE$_{DMSO}$: HPE dissolved in DMSO

HPE$_{EtOH100}$: HPE dissolved in 100% v/v EtOH

HPE$_{EtOH50}$: HPE dissolved in 50% v/v EtOH

HPE$_{H2O}$: HPE dissolved in deionized water

ICAM-1: intercellular adhesion molecule-1

IKKs: IκB kinases

IL: interleukin

IP$_3$: inositol triphosphate

IκB: NF-κB inhibitors

JNK: c-Jun NH$_2$-terminal Kinase

MAPK: mitogen-activated protein kinase

MAPKK: MAPK kinase

MAPKKK: MAPK kinase kinase

MCP-1: monocyte chemoattractant protein-1

MLSs: Macrophages-like synoviocytes

MMPs: matrix metalloproteinases

MTS: 3-(4,5-dimethylthiazol-2–yl)-5- (3-carboxymethoxyphenyl)-2- (4-sulfophenyl)-2H-tetrazolium

NF-κB: nuclear factor-kappa-light-chain-enhancer of activated B cells

NSAIDs: nonsteroidal anti-inflammatory drugs

OA: osteoarthritis

PAMPs: Pathogen-Associated Molecular Patterns

PBS: phosphate buffer saline

PH: pleckstrin homology

PIP2: phosphatidyl inositol 4,5 bisphosphate

PI-PLC: phosphoinositide-specific PLC

PKA: protein kinase A

PKC: protein kinase C

PLA: phospholipase A

PLB: phospholipase B

PLC: phospholipase C

PLD: phospholipase D

Pro-MMPs: pro-matrix metalloproteinases

PRRs: Pattern Recognition Receptors

QE: quercetin equivalent

RTK: tyrosine kinase receptor

RT-PCR: Real Time-Polymerase Chain Reaction

SPME: solid phase microextraction

TAE: tannic acid equivalent

TIC: total ion current

TIM: triose phosphate isomerase

TL-Rs: Toll like-receptors

TNF-α: Tumor Necrosis Factor-α

Δ-9-THC: (−)-*trans*-Δ^9-tetrahydrocannabinol

1. Introduction

1.1 Osteoarthritis

Osteoarthritis (OA) is a chronic-degenerative and inflammatory disease which affects joints causing pain and functional limitation to patients. For several years, OA disease was called Arthrosis and just considered a pathology linked to aging process. Recently, scientific evidence demonstrated the inflammation involvement in OA pathogenesis and now is officially recognized as Osteoarthritis. Etymologically, the desinence "itis" indicates quantitatively variable inflammation which is present in each phase of the disease [1,2].

However, the prevalence of the disease is closely related to aging, that is considered as the primary risk factor for OA. Worldwide, the OA incidence is about 7.6% in the population aged 18-44, 29.8% in the population aged 45-64, and over 50% in the population over 65 years old [3]. Among people with OA, there are twice as many women as men, especially for those with arthritis affecting knees and hands. Symptoms typically begin to appear in women around 40-50 years old, and the disparity becomes even greater after age 55, when women enter menopause. Indeed, during menopause period, estrogen levels drop off and this phenomenon may contribute to accelerate the OA process [4]. In addition to age and gender, other risk factors include obesity, genetics, diet, and mechanical joint traumas. OA is a leading cause of disability in older adults and responsible for impairment of mobility in the elderly population. Pain is the predominant symptom, aggravated by joint use and alleviated by rest which usually leads affected patients to seek medical care [5]. OA is responsible for a very high number of primary healthcare

visits, knee and hip replacement surgery and hospital costs in general. However, also considering the disease onset in working age, the socio-economic OA burden is not only limited to the direct costs of healthcare use but also includes significant non-healthcare-related costs. These take the form of productivity losses and the cost of care associated with the limited independence of people with OA [6].

Initially, OA was considered a disease that involved exclusively articular cartilage, but recent research has shown that all the intra and peri-articular tissues are affected by the inflammatory condition. The central element in OA pathogenesis still remains the progressive cartilage degradation that causes subchondral bones exposition. Cartilage is a specialized tissue with a support function, absorbing and distributing mechanical loads applied to the entire joint and covering the articular ends allowing a sliding between subchondral bones. When the cartilage is degraded, exposed subchondral bones have friction each other causing pain and remodelling of bones themselves. These mechanical alterations are responsible for variable degrees of synovial inflammation, ligaments degeneration, joint capsule hypertrophy, and changes in the periarticular muscles, in the nerves, purse and local fat pads [7,8]. OA affects mainly diarthrosis of the body, but often is observed a multiple joint involvement. The most affected are those of knees, hands, hips, and spine [9].

1.2 Joints

Joints, also known as articulations, are a form of connection between bones in the body providing stability to the skeletal system as well as allowing specialized movement. In the human body, there are about 360 joints, which

are distinguished by shape and degree of mobility [10]. Consequently, joints can be categorized both structurally and functionally. According to joint structural classification that takes into account the type of binding tissue connecting the bones to each other, fibrous and cartilaginous joints, and synovial ones can be distinguished. Fibrous and cartilaginous joints are respectively characterized by the presence of fibrous connective tissue or cartilage, responsible for anchoring the bones each other. Otherwise, in synovial joints bone heads are not directly connected, but come into contact each other within a joint cavity that is filled with a lubricating fluid [11]. Instead, in the functional classification the degree of movement available between the joint heads is described. According to this classification, fibrous and cartilaginous joints are further distinguished in synarthrosis, or motionless joints, and amphiarthrosis, or slightly mobile joints. On the contrary, synovial joints are the most mobile in the human skeleton and are also called diarthrosis [12,13]. Anyway, the available movement for each joint is related to the functional requirements for the specific articulation and depends on its localization in the body.

1.3   Diarthrosis or synovial joints

A synovial joint is the most common one in mammals that provides the majority of body movements. In the human body there are many types of synovial joint and, even if the exact structure of the singular synovial joint varies depending on its function, the general anatomic structure is the same. A synovial joint is a solid organ that extends from the *periosteum* of the bone, includes articular cartilage that covers subchondral bones, and is encapsulated by the articular capsule made by fibrous membranes separated

by fat deposits. Inside the articular capsule, a *synovial membrane* delimits and covers the joint cavity, and secrets a specialized fluid, called synovial fluid. This fluid creates a lubricating cushion between the two bones, allowing them to glide smoothly past each other [11,14].

Synovial joints comprise most of the extremity joints allowing skeleton movements, and are the most accessible joints to direct inspection and palpation [15]. These can be found in the elbow, knee and ankle, allowing for flexion and extension; in the shoulder and hip, where movements are possible in almost any direction; and in the neck allowing only rotation [16].

1.3.1 Articular cartilage

Articular cartilage is the most highly specialized connective tissue of diarthrodial joints. It is a resilient and smooth elastic tissue, rubber-like padding that covers and protects the ends of long bones in joints.

For its unique viscoelastic characteristics, the main functions consist in providing a smooth, lubricated surface for low-friction articulation and facilitating the transmission of loads to the subchondral bones [17]. It is an avascular tissue type, so its microarchitecture is less organized than bone's one, and is not innervated and therefore relies on diffusion to obtain nutrients [18]. Articular cartilage consists of two phases, a fluid phase and a solid one, which together are responsible for the tissue biomechanical properties. The liquid phase is composed of water, that represents about 80% of the articular cartilage weight, and electrolytes (Ca^{2+}, K^+, Na^+, Cl^-). The solid phase is composed of collagen type II, a protein that forms a network of fibres responsible for the overall shape of the tissue. This network is filled with glycosaminoglycans (GAGs), proteoglycans, and in a minor part with

glycoproteins. These two phases constitute the so-called extracellular matrix (ECM), that responds to tensile and compressive forces to which the cartilage is subjected [19].

Cartilage is composed by a single cell population, the chondrocytes, responsible for ECM production and maintenance of homeostasis. Chondrocytes derive from specialized mesenchymal cells and occupy only 2% of the total articular cartilage tissue. They are located in matrix cavities, called *lacunae*, connected to each other by small *canaliculi*, which create a rich connectivity between cells [20]. Since cartilage is an avascular tissue, chondrocytes live in a low-oxygen environment and obtain nutrients and metabolites from the surrounded extracellular matrix by diffusion [21].

Chondrocytes, in healthy adult tissue, are differentiated cells that maintain tissue balance by synthesizing a very low level of ECM to replace damaged matrix molecules, preserving the structural integrity of cartilage [22]. However, during aging and joint disease, this equilibrium is disrupted and the rate of loss of matrix may exceed the rate of deposition of newly synthesised molecules, exposing the collagen network to irreversible destruction. The damage may lead to aberrant chondrocyte behaviour that is reflected in changes in quantity or composition of matrix proteins. These alterations are associated with significant loss of cartilage mechanical functions and with an increase in friction between joint bone surfaces [23,24].

1.3.2   Synovial membrane

The synovial membrane is a specialized mesenchymal tissue lining the diarthrodial joint spaces, bursae (fluid-filled sacs between tendons and bones), and tendon sheaths. On its outside surface, it makes direct contact

16

with the articular capsule fibrous membrane, while on its inside surface it has contact with the lubricant synovial fluid [25]. Together with bones, articular cartilage, tendons, and ligaments, it represents an important component of the joint. As such, it not only has its own specific functions but also interacts with other tissues both structurally and functionally. Indeed, from a functional point of view, the synovial membrane promotes skeletal movement by producing synovial fluid responsible of cartilage and tendon surfaces lubrication, decreasing joint friction [26]. Moreover, unlike articular cartilage, the synovial membrane is vascularized, and this is an important communication channel to transport cartilage nutrients, immune cells, and inflammation mediators in the joint [27]. This tissue is composed by a more external part or *intima* consisting of a luminal layer 1-3 cells deep, a capillary plexus and a deeper lymph vessel network, and by a more internal part or *subintima* composed by adipose, areolar, or fibrous tissue [28].

The *intima* contains synoviocytes, the characteristic cells of synovial membrane, that were histologically analysed for the first time by Barland et al. in 1962 [29]. Over the years, a controversy has arisen in the scientific community about the classification of synoviocytes in the synovial membrane. In the past, some studies highlighted the presence of three different types of synoviocytes: type A synoviocytes, type B synoviocytes and a third type with intermediate morphology among the other two. However, transmission electron microscope (TEM) observations in 1982 disproved the existence of the third cell type by describing it as a variant of the other two cell lines. Today, it is officially recognized that only two type of morphologically different synoviocytes are present in the human synovial membrane [27,30,31].

17

Type A synoviocytes, also called Macrophages-like synoviocytes (MLSs) are non-fixed cells, morphologically and functionally similar to macrophages. From the morphological point of view, they are round, rich in ripples and invaginations of the cytoplasmic membrane, with the cell surface covered by microvilli, similar to blood macrophages. TEM analysis evidenced a variable number of empty appearing vacuoles and pinocytotic vesicles, whose function has not been fully defined yet [27,29]. They are immunoreactive to several antibodies against macrophages and express the major complex of histocompatibility type II (MHC II) molecules, which plays a fundamental role in the early stages of the immune response. MLSs contain lysosomal enzymes, esterases, phosphatases and cathepsin B, D and L, which are used as markers to identify this cell type and whose expression is increased in the case of inflammation. The release of these enzymes in the ECM is responsible of tissue damage [27,32–34]. MLSs are involved in phagocytotic mechanism by absorbing and degrading extracellular constituents or cell debris through their well-developed vesicular system [35].

The second synovial membrane cell population (type B) is represented by mesenchymal-origin cells defined Fibroblast-like synoviocytes (FLSs). In addition to the typical fibroblast elongated morphology, FLSs display many fibroblast characteristics such as the expression of type IV and V collagens, vimentin, and CD90 [36]. Moreover, they have some unique properties that allow them to be distinguished from many other fibroblast lineages, including synovial fibroblast. For instance, they express VCAM-1, an adhesion molecule, and show a higher activity of uridine diphosphate glucose dehydrogenase than fibroblast cells, which is associated to their ability in hyaluronan production [35]. Unlike type A synoviocytes, FLSs have a less

rippled membrane, fewer vesicles and an extensive wrinkled endoplasmic reticulum distributed into the cytoplasm, where protein synthesis takes place. Furthermore, histochemical analyses have shown that these cells have long cytoplasmic extroflexions, with different dimensions and shapes that make a complex network in the synovial membrane *intima* layer. Unfortunately, the functional role of this distinctive network is not totally known, but several evidence makes this cellular characteristic correlated to the synoviocytes type B secretory function. Indeed, through these cytoplasmic processes, FLSs are able to reach the synovial membrane surface and to connect the *intima* to the joint cavity, where proteins and small molecules are secreted [27]. They are responsible for the synthesis and secretion of a diverse array of proteins that contribute to the synovial membrane properties, as well the composition of the synovial fluid. These molecules include collagen, glycosaminoglycans, lubricin, pro-matrix metalloproteinases (pro-MMPs), interleukins (IL), and eicosanoids, but also hyaluronic acid, a proteoglycan presents in high concentrations in the synovial fluid of healthy joints [37].

1.3.2.1 Synovial membrane in OA pathogenesis

The involvement of the synovial membrane in OA pathogenesis is often not emphasized, more focus being focused on the articular cartilage and bone. Recently, many clinical studies have considered abnormal synovial changes, both in its structure and function, as one of the characteristic features in OA onset and progression [38]. The hallmark of OA is macroscopically visible change to the synovial tissue which becomes inflamed, hyperplastic, and invasive of the closer cartilage and bone [39]. Under physiological conditions, synoviocytes do not actively divide in the synovial membrane,

while in joint disease, such as in OA, rapidly proliferate leading to *intima* hyperplasia and thickening [40]. The lining expands from 1-3 cells deep to a depth of up to 10-20 cells, with an inversion of the normal ratio between type A and B synoviocytes [36].

Interestingly, MLS amount serve as a sensitive biomarker of disease since the number of infiltrating macrophages within the inflamed synovial membrane correlates with joint destruction and pathology progression [41–43]. They show a highly activated phenotype and are dynamic in producing pro-inflammatory cytokines, chemokines, growth factors as well as reactive nitrogen and oxygen species contributing to synovial damage [44–46]. Additionally, macrophages infiltrate the synovial space with other cells; therefore, interaction between the different cell types is likely to be critical. The activation of FLSs into the *intima*, indeed, is driven by MLS products that in turn induce the release of array of mediators, especially interleukins and MMPs [47,48]. These molecules travel through the synovial fluid to the joint heads causing cartilage ECM degradation [49]. In particular, MMPs and other proteases are responsible of the dysregulation of chondrocyte functions, thus causing an imbalance between anabolic and catabolic processes that allow ECM to maintain its structural integrity under physiological conditions [50–52]. Wear particles, soluble cartilage-specific antigens, and microcrystals are all released into the synovial fluid by the damaged cartilage and phagocytosed by MLSs. This process generates a vicious cycle of continuous synovial inflammation and cartilage degradation [50].

Additionally, the FLS secretory function is altered, affecting the synovial fluid composition. They produce a lower amount of lubricant molecules, in particular hyaluronic acid and lubricin, that rapidly diffuse out of the joint

because of the enhanced inflamed synovial permeability. Therefore, fluid synovial viscosity is reduced and its lubrication property diminished, leading to increased friction and mechanical forces on the cartilage and finally contributing to the tissue damage [53,54].

1.4 Inflammation

For a long time, OA has been considered as an inevitable consequence of aging and joint "wear and tear" due to mechanical stress. However, according to some recent studies, it is now clear that alongside the joint mechanical damage, the inflammation plays a key role in the OA pathogenesis. Consequently, the description of this condition with the widely used term "degenerative joint disease" denotes only the inevitability of the process, does not express its true complexity. [55].

Inflammation in OA is very different than the one observed in rheumatoid or psoriatic arthritis that are characterized by an autoimmune response. OA inflammation is defined as an innate immune response that typically includes cells and mechanisms involved in defending against infections from other organisms in a non-specific way. In the joint it is activated following mechanical, physiological and biochemical changes [56] and has a role in the maintenance of tissue homeostasis [57]. Innate immune cells express receptors ("Pattern Recognition Receptors" or PRRs) that can recognize exogenous Pathogen-Associated Molecular Patterns (PAMPs) and endogenous Damage-Associated Molecular Patterns (DAMPs) released from injured tissue or dying cells [58]. Ligand binding to these receptors results in activation of inflammatory signalling pathways including Nuclear Factor-κB

(NF-κB), Mitogen-Activated Protein Kinase (MAPK) as well as the release of cytokines and chemokines [59].

1.4.1   NF-κB pathway

NF-κB is the short name of Nuclear Factor kappa-light-chain-enhancer of activated B cells, that was firstly detected in B cells and linked to the gene enhancer for the immunoglobulin κ chain, in 1986 by Sen et al. [60]. It represents a family of inducible transcription factors, which regulates several genes involved in different processes of the immune and inflammatory responses. This family is composed of five structurally related members, including p50, p52, RelA (or p65), RelB and c-Rel, which work in homo- or heterodimer form [61]. The common feature of all these transcription factors is a shared N-terminal Rel Homology Domain (RHD) that is responsible of the dimerization process, interactions with NF-κB inhibitors (IκB), nuclear translocation and DNA binding on target genes [62]. Under unstimulated conditions, all the NF-κB members in dimeric form are inactive and located in the cytoplasm bound to IκB molecules. Following stimulation, IκB are phosphorylated by IκB kinases (IKKs) and degraded by the proteasome, allowing free NF-κB dimers to translocate into the nucleus modulating the expression of pro-inflammatory cytokines, chemokines, adhesion molecules, and growth factors [63].

In recent years, the existence of two different NF-κB signalling pathways has been demonstrated (Fig. 1). The "canonical" pathway that is mainly triggered by proinflammatory cytokines, usually leads to activation of RelA or c-Rel complexes, while the "non-canonical" one, activated by lymphotoxin β, CD40 ligand and B cell activating factor (BAFF), involves RelB/p52

complex [62]. The initial step is common to the two pathways and consists in IKK complex activation. The IKK complex consists of two kinase subunits, IKKα and IKKβ, and a regulatory subunit IKKγ or NEMO [64]. In order to be activated, these kinases need a double phosphorylation on two serine residues located in an activation loop, but the exact mechanism of activation is not clear [65]. Therefore, IKKβ phosphorylation is mainly involved in the canonical pathway activation through the phosphorylation of two IκB N-terminal serine residues, causing its dissociation from the heterodimer p65-p50 [66]. The active heterodimer moves into the nuclear compartment, activating the transcription of several factors among them pro-inflammatory mediators and IκB, its inhibitory subunit, generating an auto-feedback loop [67,68]. On the other hand, IKKα is the only kinase required for the non-canonical pathway activation through the phosphorylation and processing of p100, the precursor for p52. p100 is usually associated with RelB, so that its proteolytic processing induces the formation of an active dimer RelB/p52 able to translocate into the nucleus where activates the gene transcription [69].
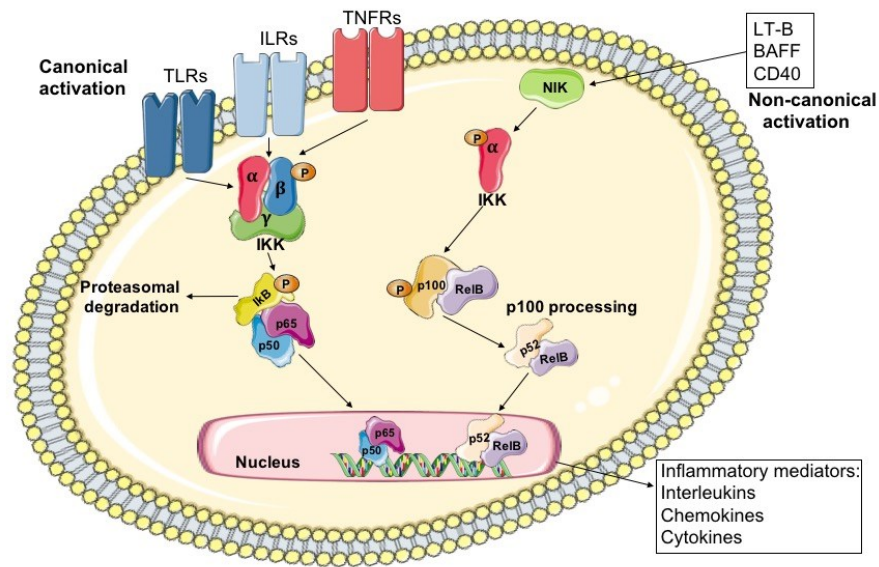
Figure 1. General schematic representation of canonical and non-canonical NF-κB pathways.

In OA, the activation of NF-κB pathway plays a key role in synovial inflammation and cartilage breakdown. In chondrocytes, NF-κB transcription factors mediate the secretion of many degrading enzymes, such as MMPs and the aggrecanases "A Disintegrin and Metalloproteinase domain with Thrombospondin motifs" (ADAMTS) 4 and 5, causing the disorganization and catabolism of both the collagen and proteoglycan component of ECM, thus leading to tissue damage and functional failure. In synovial membrane, synoviocytes, stimulated by matrix fragments from cartilage degradation and cell stress products, react by enhancing the canonical NF-κB pathway in a positive feedback cycle. Cellular Toll like-Receptors (TL-R) and chemokine

surface receptors mediate the synthesis of chemokines (IL-8), cytokines (IL-1β, IL-6 and Tumor Necrosis Factor-α (TNF-α)), and angiogenic factors (Vascular-Endothelial Growth Factor or VEGF) causing further cartilage degradation and synovial neoangiogenesis both contributing to tissue inflammation [62].
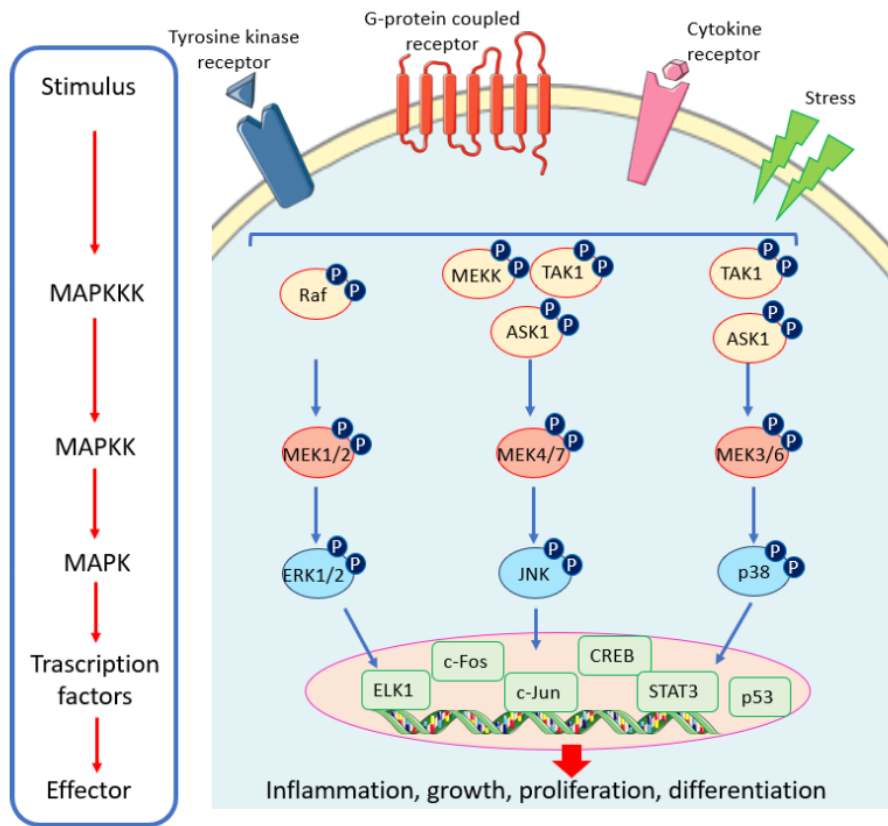
1.4.2 MAPK pathway

The MAP kinases are Serine/Threonine kinases ubiquitously expressed and evolutionarily conserved in eukaryotes. They regulate important cellular processes such as proliferation, stress responses, apoptosis and immune defence [70]. The MAPK signalling pathway is activated by different stimuli including cytokines, growth factors, and matrix proteins that bind to tyrosine kinase receptors, G protein coupled receptors, cytokine receptors, and integrins on cell membrane. Basically, the MAPK cascade activation occurs in a module of consecutive phosphorylations. MAPK kinase kinase (MAPKKK) phosphorylates a MAPK kinase (MAPKK) which then, in turn, activates a MAPK by double phosphorylation. Once activated, the MAPK translocates into the nucleus and interacts with specific targets modulating the gene expression in response to the extracellular stimulus [71] (Fig. 2). MAPK can be divided into 4 subfamilies that include Extracellular Regulated Kinase (two isoforms - ERK 1 and 2), c-Jun NH_2-terminal Kinase (three isoforms - JNK 1, 2, and 3), p38 (four isoforms - α, β, γ and δ), and ERK5. [72]. Generally, ERK is activated in response to growth factors, hormones and proinflammatory stimuli, while JNK1/2/3 and p38 α, β, γ, and δ are activated by cellular and environmental stresses [70,73]. ERK5, rather, is poorly studied and its role in cells is not well understood yet [74].

The activation of the ERK cascade is mostly initiated at the membrane receptors, transmitting the signal by recruiting adaptor proteins and exchange factors. They, in turn, induce the activation of Ras, a small G protein at the plasma membranes [75,76]. Ras recruits to the membrane and activates the serine/threonine protein kinase, Raf, a MAPK kinase kinase. This enzyme activates the MAPK kinase, MEK, that, in turn, double phosphorylates the MAPK, ERK, at both threonine and tyrosine residues [70]. Phospho-ERK translocates to the nucleus where activates multiple transcription factors such as cAMP response element-binding protein (CREB), c-Fos and c-Jun proto-oncogenes, also known as activator protein-1 (AP-1) complex, and the ternary complex factor Elk-1 [77]. These factors regulate their target gene transcription and thereby change the expression of specific proteins, ultimately leading to the regulation of cellular metabolism and function [78].

The JNK pathway includes a MAPK which belongs to the stress-activated protein kinase, a group of kinases that can be activated by any internal or external stimuli that cause cell stress [79]. Several MAPKKKs have been reported to activate the JNK signalling pathway. These include members of the MEKK group, the mixed lineage protein kinase group, the ASK group, TAK1 and Tpl2 [77]. The JNK phosphorylation is carried out by two MAPK kinases, MKK4 and MKK7 through a dual phosphorylation of threonine and tyrosine [80]. Activated JNK can translocate into the nucleus and phosphorylate a variety of transcription factors including c-Jun, STAT3 and p53. The first identified JNK substrate is c-Jun, whose activation is mediated by a double phosphorylation in its N-terminal region. Further, phosphorylated c-Jun interacts with c-Fos, which can mediate the

transcriptional activity of numerous genes playing an important role in apoptosis, inflammation, cytokine production, and metabolism [81].

The third and most recently characterized member of the MAPK family is the stress-kinase p38. In comparison to the JNK pathway but in contrast to ERK, the p38 pathway is not commonly activated by mitogens but it is induced by environmental stress [82]. The p38 MAPKs consist of four isoforms with distinct substrate specificities and tissue distributions: p38α (MAPK14), p38β (MAPK11), p38γ (MAPK12), and p38δ (MAPK13) [83]. Comparably to the others MAPK, extracellular stimuli affect the canonical phosphorylation cascade, involving sequential activation of a MAPK kinase kinase, a MAPK kinase, and finally the p38 MAPK. p38-specific MAPK kinases are MKK3 and MKK6 responsible of threonine and tyrosine residue phosphorylation [84]. Once p38 MAPK is activated, it translocates from the cytosol to the nucleus to regulate cellular functions by modulating downstream transcriptional targets such as AP-1 complex, STAT1, NF-κB, ELK1, and CREB [83]. As JNK, p38 pathway is implicated in the regulation of apoptosis, cell survival, differentiation, and inflammation. Therefore, although JNK and p38 pathways may have similar functions, are cell-specific and context dependent [85].

Figure 2. General schematic representation of MAPK pathways.

Accumulating evidence supports a key regulatory role of the MAPK in mediating inflammatory and matrix degrading processes that contribute to joint tissue destruction in OA. In chondrocytes, MAPK are mainly involved in the reduction of proteoglycan synthesis and in the induction of MMP release stimulated by extracellular matrix fragments generated during the cartilage damage [86]. In synoviocytes, besides a role in regulating processes relevant to joint tissue destruction, mounting evidence suggests that MAPK are also important mediators in pain signals [87]. For this reason, they have been taken into consideration as a possible therapeutic target, to reduce both

pain and structural progression in OA. Among the three MAPK, ERK1/2 inhibitors are those that received less attention. This is due to the potential toxicity of systemic ERK1/2 inhibition because of its involvement in a multitude of growth factor signalling pathways that regulate cell proliferation and tissue homeostasis. On the contrary, JNK and p38 are most commonly activated by stress-induced signals and so inhibition of these pathways have a better risk-benefit ratio than ERK1/2 inhibition [72].

1.4.3 Phospholipases

Phospholipases are enzymes that hydrolyse phospholipids into fatty acids and other lipophilic substances. Acids trigger the release of bound calcium from cellular stores and the consequent increase in free cytosolic calcium ions (Ca^{2+}), an essential step in calcium signalling to regulate intracellular processes [88]. Phospholipid hydrolysis is stimulated by cytokines, growth factors, neurotransmitters, hormones and other extracellular signals [89]. Cleavage products include second messengers, such as arachidonic acid, inositol triphosphate (IP_3) and diacylglycerol (DAG), which are implicated in cellular responses by activating protein kinase C (PKC) and inducing the release of Ca^{2+} [90].

There are four major classes of phospholipases, termed A, B, C, and D, which are distinguished by the type of reaction which they catalyse. The phospholipases A (PLAs) are acyl hydrolases classified according to their hydrolysis of the 1-acyl ester (PLA1) or the 2-acyl ester (PLA2). Some phospholipases can hydrolyse both acyl groups and are called phospholipase B (PLB). Cleavage of the glycerophosphate bond is catalysed by phospholipase C (PLC), while the removal of the base group is catalysed by

phospholipase D (PLD). The PLC and PLD are therefore phosphodiesterases [88] (Fig. 3).
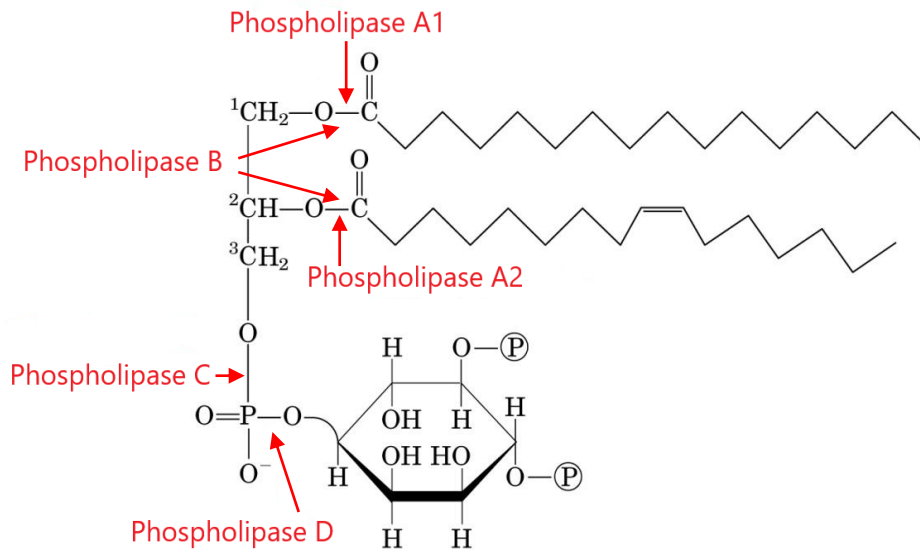
Figure 3. Phospholipase sites of action.

Unlike the other phospholipases, PLCs have a specific target. They utilize only phosphatidyl inositol 4,5 bisphosphate (also known as $PI(4,5)P_2$ or PIP_2), a minor but essential constituent of plasma membranes as substrate, hence, they are called phosphoinositide-specific PLCs (PI-PLCs) [91]. The two PIP_2 cleavage products, DAG and IP_3, are critical second messengers to mediate cell signalling. DAG, which remains membrane bound, activates the PKC, which then phosphorylates downstream effectors to activate an array of cellular functions like the regulation of cell proliferation, cell polarity, learning, memory, and spatial distribution of signals. The second product, IP_3 is a small water-soluble molecule, which diffuses from the membrane

through the cytosol to bind its receptor on the endoplasmic reticulum inducing the release of Ca^{2+}. In turn, the cytoplasmic calcium levels are quickly elevated [92]. Finally, Ca^{2+} activates downstream transcription factors responsible of gene modulation [93].

There are thirteen different PI-PLC family members that can be divided into six classes based on their primary structures: β, γ, δ, ε, η and ζ [94]. There is no α form of PI-PLC, since the protein that was originally described as the α form turned out to be an isomerase without phospholipase activity [95]. PI-PLC β, γ, δ, ε, η and ζ isoforms are distinct according to tissue distribution, cell localization, expression, and regulation. PI-PLC β and PI-PLC γ are typically activated by extracellular stimuli and are termed primary PI-PLCs, whereas PI-PLC δ, ε, η and ζ are activated by intracellular stimuli and known as secondary PI-PLCs [96]. The two primary PLC families possess distinct mechanisms of activation. PI-PLC β isoforms are activated by G_{α} of the G_q subfamily and $G_{\beta\gamma}$ subunits of all heterotrimeric G proteins, whereas PI-PLC γ isoforms are activated by tyrosine kinase receptors (RTK) [97,98]. Regarding the secondary PI-PLC isoforms, the activation mechanisms are various. PI-PLC ε isoform can be activated by both G proteins coupled receptors (GPCR) and RTK systems, while both PI-PLC δ and PI-PLC η are activated by GPCR-mediated calcium mobilization. About PI-PLC ζ, its nuclear activation and translocation mechanisms remain unknown but it has been described as a sperm-specific protein [99].

1.4.3.1 PI-PLC β

The four isoforms of the PI-PLC β family (PI-PLC β1, β2, β3, and β4) are an important family of mammalian enzymes that differ for their expression

pattern. The same cell type can express more than one isoform. PI-PLC β1 and β4 are mostly expressed, although not exclusively, in the nervous system. PI-PLC β2 can be found in the hematopoietic lineage, while PI-PLC β3 is more widely distributed [100].

From a structural point of view, PI-PLC β proteins share a highly conserved catalytic core composed of an N-terminal pleckstrin homology (PH) domain, four tandem EF hand repeats, a triose phosphate isomerase (TIM)-like barrel domain which houses the active site, and a C2 domain. The PI-PLC β PH domain only weakly contributes to membrane association and is responsible of the interaction with $G_{\beta\gamma}$ subunits of G protein and with phospholipids. Instead, the EF hands do not bind Ca^{2+}, contrary to their role in other well-known proteins, but they are involved in the interaction with G_α subunit of G proteins [101] (Fig. 4). All the PI-PLC β are universally activated by the G_α and $G_{\beta\gamma}$ subunits of GPCRs, but the four isoforms differ in their affinity for activators. PI-PLC β1 and PI-PLC β3 bind G_α with larger affinity compared to PI-PLC β2 or PI-PLC β4. While $G_{\beta\gamma}$ subunits have a good effect on PI-PLC β3 and PI-PLC β2, a small effect on PI-PLC β1 and do not bind PI-PLC β4 [100,102].
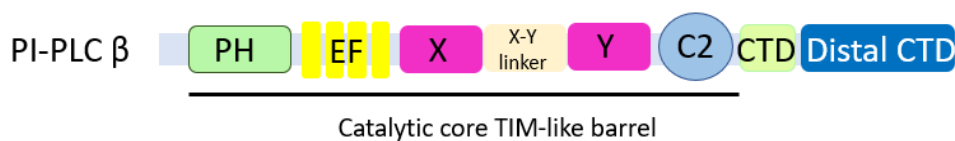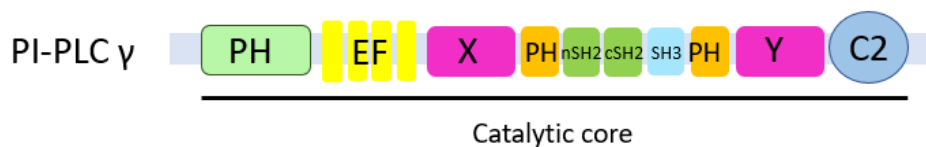

Figure 4. Domain organisation of PI-PLC β enzymes

1.4.3.2   PI-PLC γ

The PI-PLC γ family comprises two isoforms of PI-PLC, γ1 and γ2, that share high sequence homology. PI-PLC γ1 is ubiquitously expressed, whereas PI-PLC γ2 is predominantly expressed in hematopoietic cells [102]. Structurally, PI-PLCs γ are characterized by a multidomain insert between the X domain and Y domain, which consists of a split PH domain, N-terminal SH2 (nSH2) domain, C-terminal SH (cSH2) domain, and SH3 domain [99,103]. Through the nSH2 domain, PI-PLC γ interacts with phosphorylated tyrosine residues in activated RTK, leading to the phosphorylation of a conserved tyrosine residue in PI-PLC γ sequence. For this reason, nSH2 domain has a key function in enzyme activation. On the other hand, the cSH2 domain has a regulatory role (Fig. 5). Indeed, following the phosphorylation, this domain is removed from the catalytic PI-PLC γ active site, allowing PIP_2 access and catabolism [98,103].

Figure 5. Domain organisation of PI-PLC γ enzymes

1.5 Pain

The International Association for the Study of Pain defines pain as "an unpleasant sensory and emotional experience associated with actual or potential tissue damage, or described in terms of such damage" [104].

Pain is the OA hallmark symptom, that contributes to functional limitations and drives patients to seek medical attention [105]. OA pain is classically considered a nociceptive pain condition due to joint damage and described by patients in different ways according to the different stages of the disease [106]. It is generally described as intermittent but severe, or constant background pain. Intermittent intense pain has the greatest impact on quality of life and is typical of the early stages of OA, whereas constant pain at rest, particularly during the night, occurs in the middle stages of OA [107]. Moreover, unlike structural joint damage, pain perception is subjective with natural variability among patients in terms of sensitivity and tolerance, and is influenced by biological, psychological and social factors [105,106,108].

Although articular cartilage is seen as the main target in OA, this is an aneural tissue, so its damage cannot be responsible for the nociceptive stimulus. Conversely, subchondral bone, synovium, ligaments, and joint capsule are all richly innervated tissues and contain nerve endings. It is therefore believed that degenerative changes and stress on these sensitive structures are the basis of joint pain [109,110]. Diarthrosis joints contain sympathetic and sensory nerves [111]. Sympathetic fibres regulate joint blood flow through varying the articular blood vessel vasoconstrictor tone. While, sensory nerve fibres are distinguished by large diameter myelinated fibres that transmit proprioceptive signals, such as sensations of movement or sense of position, and medium diameter fibres responsible for the

transmission of the painful impulse. The pain-sensitive nerve fibres have a diameter of less than 5 μm and can be unmyelinated or myelinated with an unmyelinated nerve termination where it is believed that the joint pain originates [112,113]. In healthy joints, these nociceptors are quiescent with a high threshold of activation; however, following tissue injury or inflammatory process, they become active, joint nociceptor threshold is reduced and afferent nerves become hyper-responsive to both normal and detrimental movement [113]. As result, nociceptors continuously send nociceptive information to the central nervous system generating allodynia and hyperalgesia, typical features of OA inflammation [114].

1.5.1 The endocannabinoid system

The endocannabinoid system is a neuromodulator system that plays important roles in nervous system development, synaptic plasticity, and the response to endogenous and environmental insults [115]. It comprises endogenous cannabinoids or endocannabinoids, cannabinoid receptors, and the enzymes responsible for the synthesis and degradation of endocannabinoids [116]. Endocannabinoids are endogenous lipids that bind cannabinoid receptors, generating effects similar to those produced by the psychoactive components of cannabis Δ-9-THC ((−)-*trans*-Δ^9-tetrahydrocannabinol). The first discovered endocannabinoids are anandamide or arachidonoyl ethanolamide (AEA) and 2-arachidonoyl glycerol (2-AG) [117] (Fig. 6).

Arachidonoyl ethanolamide (AEA)   2-arachidonoyl glycerol (2-AG)
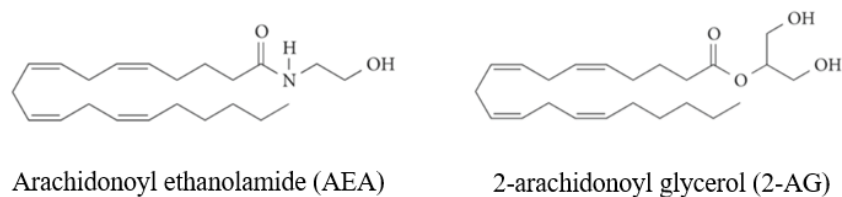
Figure 6. Chemical structures of arachidonoyl ethanolamide (AEA) and 2-arachidonoyl glycerol (2-AG)

These two endocannabinoids possess distinct properties. AEA binds with a high affinity endocannabinoid receptors and acts as a partial agonist of the endocannabinoid type 1 receptor (CB1), while is almost inactive to endocannabinoid type 2 receptor (CB2). On the contrary, 2-AG is as a complete agonist in both receptors, but with moderate affinity [116,118]. Unlike most neurotransmitters, AEA and 2-AG are not stored in vesicles but rather their precursors are present in lipid membranes. Upon demand, endocannabinoids are synthetized and then released into the extracellular space [119]. Both AEA and 2-AG are produced from cell membrane lipids via different biosynthetic pathways. The canonical pathway for AEA production starts from the precursor phosphatidylethanolamine and requires the action of two enzymes, N-acyltransferase and PLD. The first enzyme converts phosphatidylethanolamine, into N-acyl-phosphatidylethanolamine (NAPE), then PLD cleaves NAPE to yield anandamide [120,121]. On the other hand, the canonical pathway to synthetize 2-AG is a 2-step pathway that involves removal of the IP_3 from arachidonoyl-containing PIP_2 mediated by a PI-PLC β, followed by the deacylation by a DAG lipase [122]. Once synthetized and released into the extracellular space, endocannabinoids move from the postsynaptic neuron backward across the synapse, bind presynaptic

36

CB1 receptor, and suppress neurotransmitter release [123]. After completing their biological role as retrograde messengers, the endocannabinoids are inactivated by enzymatically regulated mechanisms of degradation or recycling. The enzyme responsible for the AEA hydrolysis is the Fatty Acid Amide Hydrolase (FAAH) that in some conditions is also responsible for the 2-AG metabolism, for which, however, there are also other more or less selective hydrolases [124].

The effects of endocannabinoids are primarily mediated by CB1 and CB2 cannabinoid receptors. Histological studies have revealed that these receptors display a highly divergent pattern of distribution throughout the organism [118,125]. CB1 is mainly present in the central nervous system and participates in a variety of brain function modulations, including executive, emotional, reward, and memory processing interacting with the glutamatergic, GABAergic and dopaminergic systems [126]. CB2 is considered as a "peripheral" cannabinoid receptor since is distributed in peripheral and immune cells [127].

1.5.1.1 Endocannabinoid receptor signalling

Both CB1 and CB2 receptors are G protein-coupled receptors (GPCR), exhibiting approximately 44% amino acid similarity overall and 68% homology in the transmembrane region which contains the binding sites for cannabinoids [128]. GPCR is a family of eukaryote membrane receptors that translate external signals into specific cellular responses. GPCRs comprise an extracellular N-terminus domain, seven transmembrane α-helices and an intracellular C-terminus domain. Generally, ligand binding induces a conformational change in the receptor, causing activation of a heterotrimeric

G protein docked to the internal face, then initiating a specific cellular process [128]. Heterotrimeric G proteins consist of catalytic G_α and closely associated regulatory subunits of $G_{\beta\gamma}$ [129]. G proteins are classified into four families according to their α subunit: G_i, G_s, $G_{12/13}$, and G_q. The G_s and G_i families regulate adenylyl cyclase activity, while G_q activates PI-PLC β and $G_{12/13}$ can activate small GTPase enzymes [129,130]. CB1 and CB2 receptors are coupled to G proteins of the G_i and G_q classes [121]. Their stimulation is respectively responsible of the adenylyl cyclase enzyme inhibition or the PI-PLC-Ca^{2+} pathway stimulation [131] (Fig. 7). Adenylate cyclase enzyme, normally located in the cell membrane, catalyses the conversion of ATP into cyclic-AMP (cAMP) and pyrophosphate. cAMP works by activating protein kinase A (PKA), that is a normally inactive tetrameric holoenzyme, consisting of two catalytic and two regulatory units. The binding of four cAMP molecules on the regulatory units of PKA causes the dissociation between the regulatory and catalytic subunits, thus leading to the release of active catalytic subunits, which may then phosphorylate target proteins [132]. One of the main targets of PKA-mediated phosphorylation is CREB protein that once activated binds to certain DNA sequences called cAMP response elements (CRE), thereby increasing or decreasing the transcription of the downstream genes [133]. In addition to CREB, the cAMP/PKA pathway may also influence the gene transcription by modulating the MAPK activity [134]. Different studies have demonstrated that the inhibition of PKA activity leads to the activation MAPK signalling pathways, with the activation of ERK1/2, JNK, and p38 [116,135]. On the other hand, another mechanism for MAPK activation following GPCR stimulation is proposed. G_i proteins result able to stimulate the MAPK signalling pathway by mechanisms that involve the

disassociated βγ-subunits of heterotrimeric G proteins. Even if $G_{βγ}$ is generally described as a regulatory subunit for the absence of a catalytic site, recent evidence allows to describe this dimer as involved in protein-protein interactions [136,137]. In this case, $G_{βγ}$ released from G_i-heterotrimer activates Ras in a mechanism that seems to involve PI-PLC β enzymes [138]. CB1 and CB2 receptors are also described as responsible of modulation of intracellular Ca^{2+} concentration that represents a key element for synaptic plasticity and nervous transmission. The stimulation of G_q class receptors induces elevation in intracellular Ca^{2+} concentration through the activation of PI-PLC-Ca^{2+} pathway. PI-PLCs β cleave a specific plasma membrane phospholipid, PIP_2, producing IP_3 and DAG, which are required for Ca^{2+} mobilization. IP_3 diffuses to bind to IP_3 receptors, specialized Ca^{2+} channels in the endoplasmic reticulum that only allow the passage of the ion from the endoplasmic reticulum into the cytoplasm [139,140]. DAG together with released Ca^{2+}, works to activate PKC, which phosphorylating target molecules leads to further altered cellular responses [141]. Once again, MAPK signalling is one of the most affected pathways, suggesting a complex and multiple involvement of these kinases in the cellular metabolism [138].
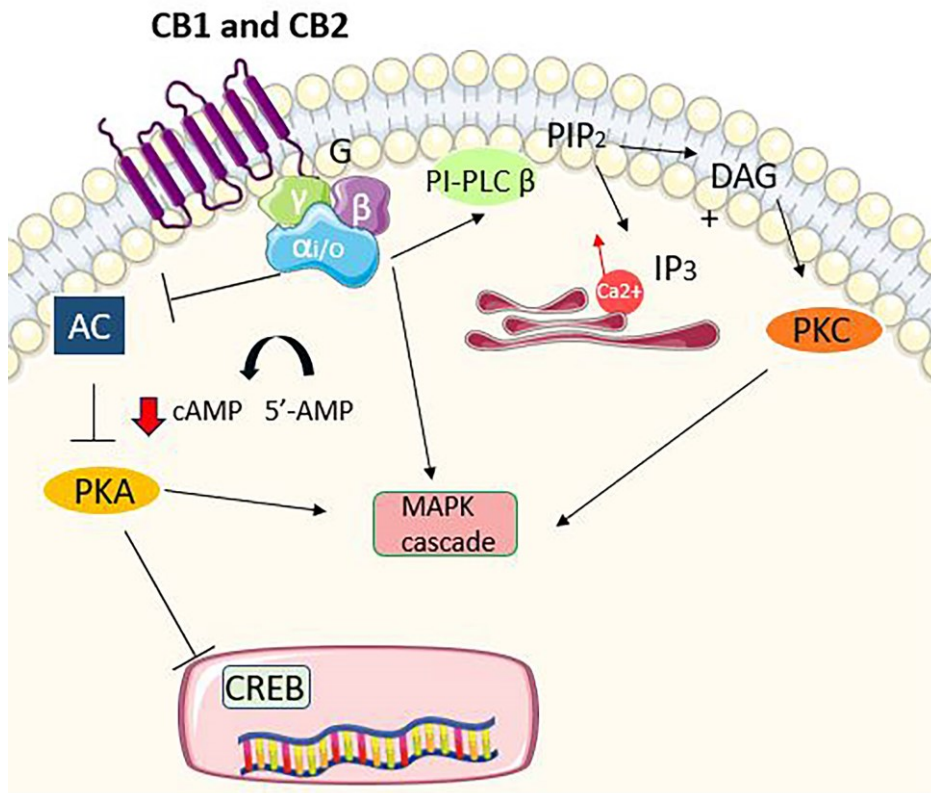
Figure 7. General schematic representation of endocannabinoid receptor signalling

1.6 OA treatment

Osteoarthritis (OA) is a debilitating joint disease that causes pain and functional limitation with a strongly negative impact on patients' quality of life. Nowadays there is no resolutive treatment against OA disease, but a series of therapies can be undertaken aimed at reducing pain and inflammation, improving the functioning of the joint and limiting the progress of the disease [142,143]. OA therapies, usually, need to be individualized according to the level of function and activity of the patient, the professional needs, the joints involved and the severity of the disease and any medical problem coexisting [144].

Current treatment options consist of both non-pharmacological and pharmacological modalities. Non-pharmacological treatments are the first-line therapeutic options that should be considered for mild disease before exploring pharmacological approaches. These treatments are based on patient education and self-management, exercise programs, weight loss, and the use of assistive devices [145,146]. Pharmacological therapy, rather, is used in patients with progressive disease who fail to respond to non-pharmacological remedies [145]. NSAIDs or nonsteroidal anti-inflammatory drugs are among the most commonly administered analgesics in the world, often used as first-line medications for joint pain. They are relatively inexpensive drugs that show not only an analgesic effect, but also an anti-inflammatory and anti-pyretic one [147–149]. However, although they are largely used, caution should be taken in prescribing NSAIDs by carefully evaluating the patient's medical history. Prolonged use of these drugs is a risk factor for gastrointestinal, hepatic or renal side effects, especially in elder populations [150]. For this reason, OARSI guidelines recommend topical application of

41

NSAIDs for local treatment of joint pain when symptoms are relatively mild, as a safer option than oral administration [151,152].

Patients who do not respond or cannot tolerate NSAIDs and continue to have severe pain may be considered as candidates for other therapeutic approaches, such as opioid therapy. Nevertheless, tolerance, dependence, and other adverse effects, including sedation, dysphoria, respiratory depression, and constipation, may occur with opioid use. These are the reasons why most international OA guidelines recommend the use of opioids for severe pain management only in exceptional circumstances, and their use should be avoided for long-term treatment [151,153–155].

In recent years, chondroprotective drugs have also been included in OA therapy of a growing number of patients [156]. This new strategy for OA drug development is focused on modifying the structural progression of the disease, using substances that protect cartilage from degeneration, by the stimulation of the anabolic activity of chondrocytes and by the inhibition of catabolic enzymes [157–159]. This approach could potentially cause retardation, a complete halt or a reversion in disease progression and even the prevention of disease development [160]. The European Medicines Agency (EMA) classifies chondroprotective drugs as Symptom Modifying Drugs (SMD), that act on symptoms with no detectable effect on the structural changes of the disease, or as Symptomatic Slow Acting Drugs for OA (SySADOA), that have also a beneficial impact on structural disease progression [161]. Chondroprotective substances most commonly used in OA therapy are the glucosamine, chondroitin sulphate and hyaluronic acid, the latter intra-articularly administered as viscous supplementation [159,162–164].

In patients with severe OA where the combination of non-pharmacological and pharmacological treatments has been tried for a long period of time without satisfactory results, arthroprosthesis surgery may be necessary [165]. This surgery aims to restore the stability and correct mechanical function of the joint, thereby improving the quality of life of the patients [166].

1.6.1 *Harpagophytum procumbens*

Nutraceutical is a food providing health improvements in addition to its nutritional value that contains bioactive compounds with a pharmacological effect [167]. The term nutraceutical is composed by 'nutrition', as dietary supplement, and 'pharmaceutical', according to its physiological benefits. However, the term nutraceuticals is not recognized by the US Food and Drug Administration (FDA), which uses the term 'dietary supplements' [168]. During last years, nutraceuticals have been largely assumed in addition to traditional drugs as an alternative OA treatment for the early stage of pathology, considering their safety and efficacy.

One of the most widely used nutraceuticals in OA treatment is *Harpagophytum procumbens*, an herbal drug used in Europe during the last decades against joint disease [169,170]. *Harpagophytum procumbens* (Burch.) DC. ex Meisn., 1840, also known as Devil's claw, is native to the southern part of the African continent and may be found in Namibia, Botswana, South Africa, Angola, Zambia, and Zimbabwe [171,172]. It is a tuberous perennial herbaceous plant with visually distinctive fruits. They have numerous characteristically long protrusions, like ramps, which give the plant the colloquial name of Devil's claw [173]. The parts usually used for the development of pharmaceutical preparations are the secondary roots that

43

contain an higher percentage of bioactive components than the primary roots [174] (Fig. 8). They contain a large amount of iridoid glycosides (mainly harpagoside, harpagide and procumbide), sugars, triterpenoids (oleanolic, ursolic acids), phytosterols (β-sitosterol), aromatic acids (caffeic, cinnamic, chlorogenic), and flavonoids (luteolin, kaempferol). Iridoid glycosides, that are the most abundant molecules among these components, show anti-inflammatory and analgesic effects and for this reason are considered to be the active substances of the plant [175]. However, it should be pointed out that different studies have demonstrated that whole *H. procumbens* extract exerts greater effects than these isolated single components. Therefore, it can be assumed that the other constituents such as the flavonoids and terpenoids contribute to the pharmacological actions of the herbal drug [176].
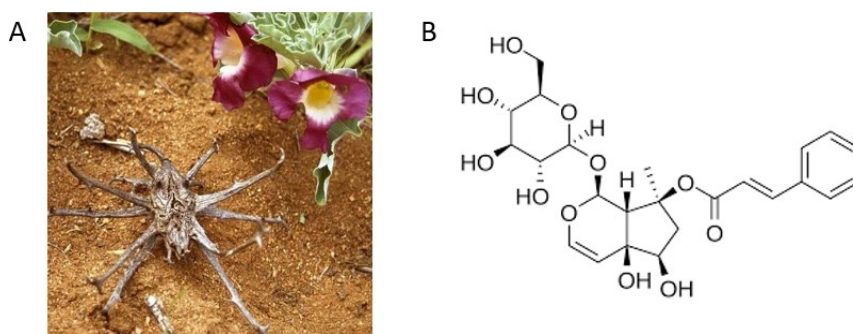
Figure 8. *Harpagophytum procumbens* plant (A). Harpagoside chemical structure (B)

Over the years, the anti-inflammatory and analgesic effect of *H. procumbens* extract was clearly demonstrated in various studies [177]. These researches have shown that the roots extracts have the ability to inhibit the release of

nitric oxide, pro-inflammatory cytokines, as IL-6, IL-1β and TNF-α, and to counteract the action of prostaglandins contributing to the inhibition of the inflammatory cascade of arachidonic acid [178,179]. In addition, harpagoside, the most expressed iridoid glycoside, was able in *in vitro* studies to reduce the expression of iNOS and COX-2 by inactivation of the NF-κB complex [180].

These scientific findings represent a great step forward in the study of this nutraceutical. Although *H. procumbens* is a remedy used since the time of traditional medicine, still little is known about the biochemical mechanisms underlying its pharmacological effect in OA treatment.

.

2. Aim of the work

Osteoarthritis (OA) is an inflammatory joint disease characterized by the progressive joint structure degeneration, that can affect one or more anatomical districts. In OA patients the cartilage, a specialized tissue with a supporting function, comes to be damaged leaving exposed the subchondral bones. As a result, the bones have friction each other causing pain and remodelling of bones themselves. Since it is a very disabling disease that often has an early onset, several studies aim to identify molecules that can slow its progression improving patient life quality.

In recent years, indeed, chondroprotective substances that protect cartilage from degeneration, stimulating chondrocyte anabolic activity and inhibit catabolic enzymes, have been introduced in OA therapies. However, especially during the disease initial stages, in addition to chondroprotectors, nutraceuticals are often introduced in therapies for their efficacy and less side effects than traditional drugs.

Among them, *Harpagophytum procumbens,* known as Devil's claw, is one of the most used herbs as an anti-OA remedy. Its secondary roots contain several bioactive compounds able to relieve patient symptoms decreasing inflammation and joint pain. Although its therapeutic properties are well known, the biochemical mechanisms at the cellular level responsible for its pharmacological effects are still not well identified. For this reason, aim of this work was to analyse the *H. procumbens* extract (HPE) effect on human primary Fibroblast-like synoviocytes (FLSs) from OA patients to understand its activity on pain and inflammation metabolic pathways. Moreover, it aimed

to investigate the therapeutic role of single bioactive compounds in root extract in order to compare their effects to those of the whole phytocomplex.

3. Materials and methods

3.1 *Harpagophytum procumbens* Extract

The dry aqueous extract from *H. procumbens* root (HPE) was provided by Ambiotec S.A.S. The extract was a fine, brown-coloured powder with characteristic smell and taste, containing 1.2% (w/w) harpagoside. The powder was stored at room temperature in dry and dark conditions until use. In order to evaluate antiarthritic activity and to highlight possible bioactive constituents, HPE was further dissolved in different solvents, including dimethyl sulfoxide (DMSO), 100% v/v ethanol (EtOH), 50% v/v EtOH, and deionized water. These solvents were chosen based on their biocompatibility and ability to dissolve different classes of phytochemicals, mainly focusing on volatile compounds and polyphenols. Particularly, DMSO possesses high solubilizing properties for both polar and nonpolar compounds, thus, being able to dissolve the entire phytocomplex. Conversely, deionized water and ethanol recover mainly polar and nonpolar molecules, respectively, whereas 50% v/v ethanol can collect compounds dissolved by both solvents.

3.2 Phytochemical analysis

3.2.1 Determination of Total Polyphenols, Tannins, and Flavonoids

Total amounts of polyphenols and tannins in the tested extracts were determined spectrophotometrically by the Folin-Ciocalteu method. Briefly, to evaluate total polyphenols, each sample (100 µg/mL) was mixed with the Folin-Ciocalteu reagent (100 µL; 10% v/v) and incubated for 5 min. Then, a

sodium carbonate solution (80 µL; 7.5% w/v) was added, shaken, and incubated for 2 h again.

Regarding tannins, samples (1 mg/mL) were mixed with polyvinylpyrrolidone (100 mg/mL) and centrifuged at 1100 rpm for 10 min to allow the phenolic compound precipitation. Then, polyphenol content was measured in the supernatant as described above. The tannin content was determined by subtracting the polyphenol amount in the supernatant to the total polyphenol amount. For both polyphenols and tannins, the absorbance was measured at 765 nm, and the amount was calculated as tannic acid equivalent (TAE) per milligram of dry HPE extract.

Furthermore, total flavonoids and its subclass flavonols were measured by applying the aluminium chloride method. Specifically, total flavonoids were measured after mixing equal volumes of each extract (2 mg/mL) and aluminium trichloride (2% w/v in methanol), whereas the content of flavonols was determined by mixing 50 µL extract (4 mg/mL), 20 µL aluminium trichloride (10% w/v in methanol), 60 µL sodium hydroxide (1 M), 10 µL sodium nitrite (5% w/v in deionized water), and 70 µL deionized water. After a 10 min incubation, the absorbance was measured at 415 nm, and the total contents of flavonoids and flavonols were determined and expressed as quercetin equivalent (QE) per milligram of dry HPE extract.

3.2.2 Solid Phase Microextraction (SPME)

For the extraction of volatile compounds, solid phase microextraction (SPME) holders and coating fibers (Supelco; Bellefonte, PA, USA) were used. The sampling was performed with an SPME fiber (50/30 µm) divinylbenzene/carboxen/polydimethylsiloxane. Before sampling, the SPME

fiber was conditioned by heating in the injector of a gas chromatograph at 270 °C for 30 min in order to remove traces of contaminants. Prior to analysis, a fiber blank was run to confirm the absence of contaminant peaks. To obtain a better extraction, SPME conditions, such as the most suitable temperature and equilibration time, were adjusted. Each sample was placed in a septum-sealed glass vial. The fiber was exposed to the headspace of the sample for 20 min at 40 °C. During this time, samples were stirred with a magnetic stirrer. After equilibration, the fiber was removed from the sample and immediately inserted into the GC injection port for the thermal desorption (2 min) at 270 °C.

3.2.3 Gas Chromatography-Mass Spectrometry (GC-MS)

The extracts were analysed using a GC-MS Perkin Elmer Clarus 500 instrument (Perkin Elmer, Waltham, MA, USA) equipped with a flame ionization detector (FID). Chromatographic separations were performed on a Varian FactorFour VF-1 fused-silica capillary column (length 60 m x 0.32 mm ID x 1.0 µm film thickness). The oven temperature program was as follows: 60 °C for 2 min, then, a gradient of 6 °C/min to 250 °C for 10 min, and an injector temperature of 270 °C. Helium was used as the carrier gas with a flow rate of 1 mL/min. Split injection with a split ratio of 1:20 was used. The electron-impact ionization mass spectrometer was operated as follows: ionization voltage, 70 eV; ion source temperature, 200 °C; scan mode, 30.0 to 500.0 mass range. The volatile compounds were identified by comparing mass spectra with those in the NIST02 and Wiley libraries. Furthermore, linear retention indices of each compound were calculated using a mixture of n-alkane hydrocarbons (C8-C30, Ultrasci, Ultra Scientific

Italia, Bologna, Italy) injected directly into GC injector using the same temperature program reported above. Semiquantitative analysis was performed by normalizing the peak area generated in the FID (%) without using correction factors (relative response factors). All analyses were repeated twice.

3.2.4 Quantification of Chemical Constituents by GC-FID

β-caryophyllene, α-humulene, and eugenol, which were the principal volatile compounds detected in the extract, were quantified by Perkin Elmer Clarus 500 gas chromatography equipped with FID using the internal standard (nonane solution) method. Chromatographic separations were performed as described above.

In order to calculate absolute quantitative data, the response factors for each compound were calculated by injections of pure analytical standards of β-caryophyllene, α-humulene, and eugenol at the concentration of 1 µg/mL.

3.2.5 UHPLC-MS Analyses

LC-MS determination of harpagoside concentration was performed on a Waters Acquity H-Class UHPLC system (Waters, Milford, MA, USA), including a quaternary solvent manager, a sample manager with flow-through needle system, a photodiode array detector, and a single-quadruple mass detector with electrospray ionization source (ACQUITY QDa). Chromatographic analyses were performed on a Kinetex C18 column (Phenomenex, 100 mm x 2.1 mm i.d., 2.6 µm particle size). Solvent A was 0.1% formic acid in water, and solvent B was 0.1% formic acid in CH_3CN. Flow rate was set at 0.5 mL/min and column temperature at 25 °C. Elution

51

was isocratically performed for the first minute with 2% solvent B; from min 1 to min 6, solvent B was linearly increased to 55%, then, in 0.5 min, solvent B was set at 100% and maintained for 2 min. The column was re-equilibrated with 98% solvent A and 2% solvent B for 4 min before next injection. Harpagoside was identified by retention time, mass, and UV-Vis spectra, using a commercially available standard. The calibration curve was prepared as follows. Harpagoside at concentration of 0.01 mM was prepared in 0.1% aqueous formic acid/acetonitrile (95:5) (Merck Life Science, Darmstadt, Germany), and then 0.5 µL, 1 µL, 2.5 µL and 5 µL were injected. HPE$_{DMSO}$ at concentration of 0.1 mg/mL was prepared in the same solvent, and 10 µL or 20 µL were injected. In the above-described chromatographic conditions, harpagoside has a retention time of $\approx$ 4.9 min. Mass spectrometric detection was performed in the negative electrospray ionization mode using nitrogen as nebulizer gas. Analyses were performed in Total Ion Current (TIC) mode in a mass range 100-1200 m/z. Capillary voltage was 0.8 kV, cone voltage 15 V, ion source temperature 120 °C, and probe temperature 600 °C. Calibration curves were generated with pure single compound, harpagoside (Sigma-Aldrich, St. Louis, MO, USA), by monitoring the H-ion (m/z 493.14).

3.3 Human tissues

Human synovial membranes were isolated from OA patients and non-OA (fractured) patients that underwent total knee arthroplasty surgery. Full ethical consent was obtained from all donors and the Research Ethics Committee, ASL Lazio 2 (#005605/2019, 3 March 2019) approved the study.

3.3.1 Immunohistochemistry

The tissues were fixed in 4% paraformaldehyde in 0.1 M phosphate buffer pH 7.2 immediately after removal from patients and embedded in paraffin. Histological sections (about 2 to 5 μm thick) were stained with haematoxylin and eosin for morphologic evaluation or were used for immunohistochemical analysis.

Histological sections for immunohistochemical analysis were deparaffinized and rehydrated in graded ethanol (100°-100°-95°). Endogenous peroxidase activity was blocked by 3% hydrogen peroxide for 10 min. Antigen retrieval was performed in 10 mM sodium citrate buffer (pH 6.0) for 15 min. The sections were then incubated with anti-CB1 and anti-CB2, (Santa Cruz Biotechnology, Inc., Dallas, TE, USA), both diluted 1:50, overnight at 4 °C. After incubation, specimens were washed and incubated with the secondary-biotinylated antibody and subsequently, with streptavidin-biotin-peroxidase (DAKOLSAB Kit peroxidase; DAKO, Carpinteria, CA, USA). The signals were developed by incubating with freshly prepared 3,3'-diaminobenzidine substrate-chromogen buffer at room temperature. Slides were mounted with permanent mounting media. Negative controls were used in each experiment. The samples were scored semi-quantitatively using a score based on the intensity and distribution: 0, undetectable; 1+, weak staining; 2+, medium staining; 3+, strong staining [181].

3.3.2 Human Primary Cell Isolation

Human primary Fibroblast-like synoviocytes (FLSs) were isolated from synovial membranes, obtained, as above described, from patients who underwent a total knee and hip arthroplasty. In brief, the synovial membrane

fragments were minced and treated with 1 mg/mL collagenase type IV and 0.25% trypsin for 2 h, at 37 °C in agitation. Then, cells were grown to 80% confluence in Dulbecco's Modified Eagle Medium (DMEM) high glucose (HyClone, Logan, UT, USA) supplemented with L-glutamine, penicillin/streptomycin (Sigma-Aldrich), and 10% fetal bovine serum (FBS) and cultured at 37 °C and 5% CO_2. All experiments were carried out with synoviocytes at first passage (p1), isolated from at least 3 different donors.

3.4 Cell treatment

Cells were left untreated (CTL) or treated, for the required time, with 0.1 mg/mL of HPE dissolved in deionized water (HPE$_{H2O}$), DMSO (HPE$_{DMSO}$), 100% v/v EtOH (HPE$_{EtOH100}$), and 50% v/v EtOH (HPE$_{EtOH50}$). Solvents alone were tested, too. Experiments were independently repeated at least three times.

In order to analyse the effect of single HPE$_{DMSO}$ components on FLSs, cells were treated for 24 h with β-caryophyllene (Santa Cruz Biotechnology, Inc, sc-251281A; ≥98% purity), α-humulene (Merck Life Science cod. 53675; ≥96% purity), eugenol (Merck Life Science, cod. W246700; ≥98% purity) and harpagoside (Merck Life Science, cod. 68527; ≥95% purity), according to the levels detected by phytochemical analysis in 0.1 mg/mL HPE$_{DMSO}$. Moreover, it was prepared a mixture containing all four components at concentrations determined in 0.1 mg/mL of HPE$_{DMSO}$.

3.5 Cell viability assay

To assess HPE potential cytotoxic effect on FLSs at different concentrations and time points, an MTS (3-(4,5-dimethylthiazol-2–yl)-5-(3-

carboxymethoxyphenyl)-2-(4-sulfophenyl)-2H-tetrazolium) based colorimetric assay was performed (Promega Corporation, Madison, WI, USA). Briefly, 8 x 10^3 cells per well were seeded in a 96-well plate. The day after seeding, cells were starved overnight in reduced serum medium, in order to align cell cycle progression. Cells were then left untreated (CTL) or treated with HPE for 24, 48, and 72 h. After each time point, 100 µL MTS solution was added to the wells. Spectrophotometric absorbance was directly measured at 492 nm after 3 h incubation.

3.6 RNA Extraction and Reverse-Transcription

Total RNA was extracted from untreated and treated FLSs, with Blood/Tissues Total RNA extraction kit (Fisher Molecular Biology, Trevose, PA, USA), and the reverse transcription was performed according to the manufacturers' instructions by Improm II enzyme (Promega Corporation).

3.7 Quantitative-Real Time-PCR

Quantitative-Real Time-Polymerase Chain Reaction (RT-PCR) analysis was performed using an ABI Prism 7300 (Applied Biosystems, Thermo Fisher Scientific, Waltham, MA, USA). Amplification was carried out using SensimixPlus SYBR Master mix (Bioline, London, United Kingdom). Primers (Table 1) synthesized by Bio-Fab research (Rome, Italy), were designed using Primer Express software v1.4.0 (Applied Biosystems). Data were analysed by $2^{-\Delta\Delta Ct}$ method, determining the transcript abundance relative to 18S rRNA housekeeping gene [182].

Table 1. RT-PCR primer sequences

GENE	PRIMER SEQUENCES (Fw-Rv)
CB1 **NM_016083**	5'-TTCCTTCTTGTGAAGGCACTG-3' 5'-TCTTGACCGTGCTCTTGATGC-3'
CB2 **NM_009924**	5'-ATGCTGTGCCTCATCAACTC-3' 5'-CTCACACACTTCTTCCAGTG-3'
FAAH **NM_001441**	5'-CAGCTTTCCTCAGCAACATG-3' 5'-CAATCACGGTTTTGCGGTAC-3'
c-FOS **NM_005252**	5'-CGAGCCCTTTGATGACTTCCT-3' 5'-GGAGCGGGCTGTCTCAGA-3'
MMP-13 **NM_002427**	5'-TTCTTGTTGCTGCGCATGA-3' 5'-TGCTCCAGGGTCCTTGGA-3'
CREB **NM_004379.5**	5'-ATTGCCCCTGGAGTTGTTATG-3' 5'-TTCTACGACACTCTCGAGCTG-3'
MMP-3 **NM_002422.5**	5'-CCTGGTACCCACGGAACCT-3' 5'-AGGACAAAGCAGGATCACAGTT-3'
ADAMTS-5 **NM_007038.5**	5'-GCACTTCAGCCACCATCAC-3' 5'-AGGCGAGCACAGACATCC-3'
IL-6 **NM_000600**	5'-GATGGATGCTTCCAATCTG-3' 5'-CTCTAGGTATACCTCAAACTCC-3'
IL-8 **NM_000584**	5'-GACATCAAAGAAGGACTTG -3' 5'- GCCACAATTTCAGATCCTG-3'
IL-1β **NM_000576**	5'-ACAGAATCTCCGACCACCACTA-3' 5'-TCCATGGCCACAACAACTGA-3'
PI-PLC β2 **NM_004573.3**	5'-AGAAGCTGGAGGAGAAGCAG-3' 5'-TTCATCCTGGCCTCGTACTC-3'
PI-PLC β3 **NM_000932.5**	5'-CGTGATGATCTCATCGCCAG-3' 5'-TTGTGACCTCGGAGCTCATC-3'
PI-PLC β4 **NM_000933.4**	5'-GTCCAGCTTGAACATCTAG-3' 5'-CCATCTGCTGCATCTCCTTC-3'
PI-PLC γ1 (204) **DQ297143.1**	5'-GCCATGTGCCATCTCTATTG-3' 5'-CATAAACAGACTCCAACGGC-3'
PI-PLC γ1 (205) **DQ297143.1**	5'-AGCCTGTCCCACAGGTCAG-3' 5'-CTGAGAACAGGCAGAGTCAG-3'
PI-PLC γ1 (207) **DQ297143.1**	5'-CAAGGACCTGAGAACATGC-3' 5'-GGCAGTCAGATCTTAAGAGG-3'
PI-PLC γ1 (208) **DQ297143.1**	5'-TGACCATTGGTGGGCTTTG-3' 5'-AATCTGACAAGCCGGCACAT-3'
PI-PLC γ1 (212) **DQ297143.1**	5'-AGCTTTGCCGAGTGTCCCTTC-3' 5'-CAATGTCAGCCCAGCCATAC-3'
18S **NM_003286**	5'-CGCCGCTAGAGGTGAAATTC-3' 5'-CATTCTTGGCAAATGCTTTCG-3'

3.8 Semi-Quantitative-PCR

PCR was used to study the modulation of PI-PLC enzymes in HPE$_{DMSO}$-treated FLSs. PCR reactions were performed with MyTaq DNA Polymerase (Bioline) following manufacturers' instructions. Cycling conditions were performed with 95 °C initial denaturation step for 1 min, followed by 30 cycles consisting of 95 °C denaturation (30 sec), annealing (30 sec) at 56 °C and 72 °C extension (1 min) in Mastercycler^{TM} (Eppendorf, Hamburg, Germany) thermocycler. Primers (Table 2) synthesized by Biofab research, were designed using Primer Express software v1.4.0 (Applied Biosystems). Amplified PCR products were analysed by 1.5% agarose gel electrophoresis using Glyceraldehyde 3-phosphate dehydrogenase (GAPDH) as housekeeping gene. Image acquisitions were performed by ChemiDoc Instrument (Bio-Rad Laboratories, Hercules, CA, USA).

Table 2. PCR primer sequences

GENE	PRIMER SEQUENCES (Fw-Rv)
PI-PLC β1 OMIM*607120	5'-AGCTCTCAGAACAAGCCTCCAACA-3' 5'-ATCATCGTCGTCGTCACTTTCCGT-3'
PI-PLC β2 OMIM *604114	5'- AAGGTGAAGGCCTATCTGAGCCAA-3' 5'- CTTGGCAAACTTCCCAAAGCGAGT-3'
PI-PLC β3 OMIM *600230	5'- TATCTTCTTGGACCTGCTGACCGT-3' 5'- TGTGCCCTCATCTGTAGTTGGCTT-3'
PI-PLC β4 OMIM *600810	5'- GCACAGCACACAAAGGAATGGTCA-3' 5'- CGCATTTCCTTGCTTTCCCTGTCA-3'
PI-PLC γ1 OMIM *172420	5'- TCTACCTGGAGGACCCTGTGAA-3' 5'- CCAGAAAGAGAGCGTGTAGTCG-3'
PI-PLC γ2 OMIM *600220	5'- AGTACATGCAGATGAATCACGC-3' 5'- ACCTGAATCCTGATTTGACTGC-3'
PI-PLC δ1 OMIM *602142	5'- CTGAGCGTGTGGTTCCAGC-3' 5'- CAGGCCCTCGGACTGGT-3'
PI-PLC δ3 OMIM *608795	5'- CCAGAACCACTCTCAGCATCCA-3' 5'- GCCA TTGTTGAGCACGTAGTCAG-3'
PI-PLC δ4 OMIM *605939	5'- AGACACGTCCCAGTCTGGAACC-3' 5'- CTGCTTCCTCTTCCTCATATTC-3'
PI-PLC ε OMIM *608414	5'- GGGGCCACGGTCATCCAC-3' 5'- GGGCCTTCATACCGTCCATCCTC-3'
PI-PLC η1 OMIM *612835	5'- CTTTGGTTCGGTTCCTTGTGTGG-3' 5'- GGATGCTTCTGTCAGTCCTTCC-3'
PI-PLC η2 OMIM *612836	5'-GAAACTGGCCTCCAAACACTGCCCGC-3' 5'-GTCTTGTTGGAGATGCACGTGCCCCTT-3'
GAPDH NM_02046	5'- CGAGATCCCTCCAAAATCAA -3' 5'- GTCTTCTGGGTGGCAGTGAT -3'

58

3.9 Immunofluorescence analysis

Proteins were visualized by immunofluorescence. Cells, plated at a density of $8 \times 10^3/cm^2$, were left untreated (CTL) or treated, for the required time, as specified for each individual experiment. Then, cells were washed in phosphate buffer saline (PBS), fixed in 4% paraformaldehyde in PBS for 15 min at 4 °C, and permeabilized with 0.5% Triton-X 100 in PBS for 10 min at room temperature. After blocking with 3% bovine serum albumin in PBS for 30 min at room temperature, cells were incubated at 1 h, at room temperature, with primary antibodies. Cells were washed with PBS and then, incubated for 1 h, at room temperature, with Alexa Fluor secondary antibodies (Table 3). Slides were washed and then, stained with DAPI (Invitrogen, Thermo Fisher Scientific) to visualize the nuclei. The images were captured by a Leica DM IL LED optical microscope, using an AF6000 modular microscope (Leica Microsystem, Milan, Italy).

Table 3. Antibodies for immunofluorescence analysis

PROTEIN	PRIMARY ANTIBODY	SECONDARY ANTIBODY
Vimentin	Mouse monoclonal antibody (Proteintech Group, Manchester, UK) 1:50	Alexa Fluor 488 donkey anti-rabbit antibody (Invitrogen, Thermo Fisher Scientific) 1:300, green
CB2	Mouse monoclonal antibody (Santa Cruz Biotechnology) 1:150	Alexa Fluor 488 donkey anti-goat antibody (Invitrogen, Thermo Fisher Scientific) 1:600, green
p-PKA	Rabbit oligoclonal antibody (Invitrogen, Thermo Fisher Scientific) 1:250	Alexa Fluor 595 donkey anti-rabbit antibody (Invitrogen, Thermo Fisher Scientific) 1:400, red
p-ERK1/2	Rabbit monoclonal antibody (MyBioSource, San Diego, CA, USA) 1:1000	Alexa Fluor 488 donkey anti-rabbit antibody (Invitrogen, Thermo Fisher Scientific) 1:400, green
PI-PLC γ1	Mouse monoclonal antibody (Santa Cruz Biotechnology) 1:50	Alexa Fluor 595 donkey anti-rabbit antibody (Invitrogen, Thermo Fisher Scientific) 1:300, red

3.10 Western Blot analysis

Western Blot experiments were performed to analyse the effect of HPE$_{DMSO}$ on phosphorylation of ERK1/2 and c-Fos. Cells, untreated and treated with HPE$_{DMSO}$, were washed with PBS and lysated by protein extract kit (Active Motif, Carlsbad, CA, USA) in accordance with manufacturers' instructions. Extracts were resolved on Mini-protean TGX precast gels (Bio-Rad Laboratories) and transferred to Polyvinylidene difluoride (PVDF) membranes (Bio-Rad Laboratories) and probed with specific antibodies in accordance with the manufacturers' instructions. Rabbit anti-ERK1/2 and anti-p-ERK1/2 antibodies (MyBioSource) were used at 1:1000; rabbit anti-c-Fos and anti-p-c-Fos antibodies (Cell Signaling Technology, Danvers, MA, USA) at 1:500 and mouse anti-actin (Merck Life Science) at 1:1000. The secondary antibodies HRP-conjugate, both anti-rabbit and anti-mouse (Immunological Sciences, Rome, Italy) were used at 1:5000. The blots were revealed by ECL detection system (Advansta, Menlo Park, CA, USA). Image acquisitions were performed by ChemiDoc Instrument (Bio-Rad Laboratories).

3.11 Measurement of cAMP

The amount of cAMP in untreated (CTL) and treated cells was measured by the Direct cyclic AMP Enzyme-Linked Immunosorbent Assay (ELISA) kit (Enzo Life Sciences, New York, NY, USA), according to the manufacturers' instructions. Briefly, 10×10^4 cells per well were seeded in 24-well plates and cultured for 5 min, 10 min, 20 min, 1 h, 24 h, and 48 h in presence of HPE$_{DMSO}$. The effects of HPE$_{DMSO}$ were also studied under the stimulation of

61

Forskolin (7-beta-Acetoxy-8, 13-epoxy-1a, 6b, 9atrihydroxy-labd-14-en-11-one), which is a potent, rapid, and reversible stimulator of adenylate cyclase activity and consequently an agent responsible of the cAMP increase [183]. The cells were treated with Forskolin for 20 min or pre-treated with the extract for 1 h and then stimulated with Forskolin for 20 min.

3.12 MMP-13 ELISA

The amount of MMP-13 in the cell supernatant was determined using ELISA kit (Fine Test ELISA, Fine Biotech Co., Ltd., Wuhan, China) according to the manufacturers' instructions. Optical Density (O.D.) absorbance was measured at 450 nm by a microplate reader (NB-12-0035, NeBiotech, Holden, MA, USA).

3.13 Calcium assay

The intracellular Ca^{2+} has been measured by Calcium Green-1 AM (Invitrogen, Thermo Fisher Scientific) following the manufacturers' instructions, using 3 x $10^4/cm^2$ cells treated with HPE_{DMSO} for 20 min, 1 h, and 24 h. The assay is based on the use of molecules that exhibit an increase in fluorescence upon binding Ca^{2+}.

3.14 FAAH inhibition assay

The potential ability of the tested extract to inhibit fatty acid amide hydrolase (FAAH) was evaluated using a commercial fluorescence-based kit (Cayman's FAAH Inhibitor Screening Assay Kit, Vinci Biochem, Vinci (FI), Italy), according to the manufacturers' instructions. The fluorescence of the

FAAH-catalysed product was measured at an excitation wavelength of 340 to 360 nm and an emission wavelength of 450 to 465 nm by a BD Accuri. C6 flow cytometer (BD Biosciences, Milan, Italy). Suitable control wells treated with vehicles (maximum FAAH activity) and with the known FAAH inhibitor JZL 195 (maximum FAAH inhibition) were included. Each treatment was assayed at least in triplicate and at least in two different experiments. The enzyme activity was evaluated as % inhibition with respect to the vehicle.

The Hill equation $E = E_{max}/ (1+(10^{LogEC50/A}) HillSlope)$ (E, effect at a given concentration; E_{max}, maximum activity; EC_{50} or IC_{50}, concentration giving a 50% inhibition; A, concentration of agonist; HillSlope, slope of the agonist curve) was applied to obtain a concentration-response curve.

3.15 Spheroids culture

In order to mimic FLS physiological conditions, cells were cultured in 3D by performing spheroid culture. 3×10^5 FLSs were pelleted by centrifuging for 5 min, at 250 x g, and then cultured in DMEM high glucose with 10% FBS, in presence of 50 μg/mL of ascorbic acid. Spheroids were left untreated (CTL) or treated with 0.1 mg/mL of HPE$_{DMSO}$ and were cultured for 21 days. Then were fixed with 4% paraformaldehyde and paraffin embedded. Sequentially sections were used for immunohistochemical analysis, staining them with mouse monoclonal anti-CB2 antibody, anti-PI-PLC β2, anti-PI-PLC β3, and anti-PI-PLC β4 (all Santa Cruz Biotechnology, Inc) all diluted 1:50.

Section stained with anti-CB2 antibody were incubated with the secondary-biotinylated antibody and subsequently, with streptavidin–biotin–peroxidase (DAKOLSAB Kit peroxidase). The signals were developed by incubating

63

with freshly prepared 3,3'-diaminobenzidine substrate-chromogen buffer at room temperature. Slides were mounted with permanent mounting media.

Sections stained with anti-PI-PLC β2, anti-PI-PLC β3, and anti-PI-PLC β4 antibodies were incubated with Alexa Fluor secondary antibodies. PI-PLC β2 and β3 were stained in red with Alexa Fluor 595 donkey anti-rabbit antibody 1:300, while PI-PLC β4 was stained in green with Alexa Fluor 488 donkey anti-rabbit antibody (all Invitrogen, Thermo Fisher) 1:300. Slides were washed and stained with DAPI (Invitrogen, Thermo Fisher Scientific) to visualize the nuclei. The images were captured by a Leica DM IL LED optical microscope, using an AF6000 modular microscope (Leica Microsystem).

3.16 Densitometric analysis

To perform the densitometric analysis of protein production, the free software ImageJ v1.52t (https://imagej.nih.gov/ij/) was used. For each cell culture condition, the integrated density values of chemiluminescence and fluorescence obtained in Westerns Blot and in immunofluorescence experiments, respectively, were considered.

3.17 Statistical analysis

All data were obtained from at least three independent experiments, each performed either in duplicate or in triplicate. Data were statistically analysed with two-way repeated measures analysis of variance (ANOVA) with Bonferroni's multiple comparison test, using Prism 5.0 software (GraphPad Software, San Diego, CA, USA). p value < 0.05 was considered significant.

4. Results and Discussions

4.1 Histological comparison between non-OA and OA synovial membrane

Osteoarthritis (OA) is the most common type of arthritis worldwide, characterized by pain and decline in physical function. While classically it has been considered only as an articular cartilage "wear and tear" pathology, it is currently recognized that OA is a whole-joint disease with a complex aetiology that also involves the synovial membrane and surrounding tissues. However, the involvement of the synovial membrane in OA pathogenesis is often not emphasized in scientific publications, which place more attention on the articular cartilage and bone.

For this reason, this study began with a first preliminary and exploratory histological analysis of the synovial membrane from non-OA and OA patients. Synovial tissues were explanted by a team of orthopedists during arthroplasty surgery from both non-OA and OA patients who underwent total knee replacement. By staining the histological sections of non-OA synovial membrane with haematoxylin and eosin, it resulted that synoviocytes, coloured in blue, were immersed in an amorphous granular matrix, and lied mainly on synovial membrane intimal part forming from one to three layers. On the other hand, the subintimal area contained mainly loose connective tissue with collagen and elastin fibers as well as fibroblasts, macrophages, and adipocytes. OA synovial membranes, rather, showed some morphological abnormalities typical of chronic inflammation. These included the hyperplasia of the lining cell layer with a dense cellular infiltrate composed largely of lymphocytes and monocytes that contribute to the

synovial inflammation and pannus formation (Fig. 9). However, it should be noted that in non-OA synovial membranes, deriving from patients undergoing arthroplasty surgery following traumatic fractures, the inflammatory infiltrate is not entirely absent. This is due to a condition of acute inflammation developed as a result of the experienced trauma and is less intense than the typical chronic inflammatory infiltrate of OA.
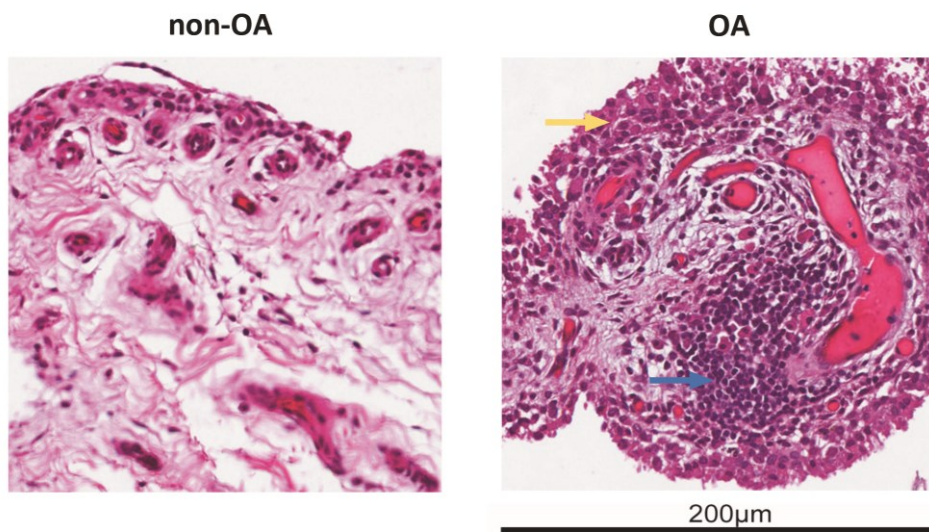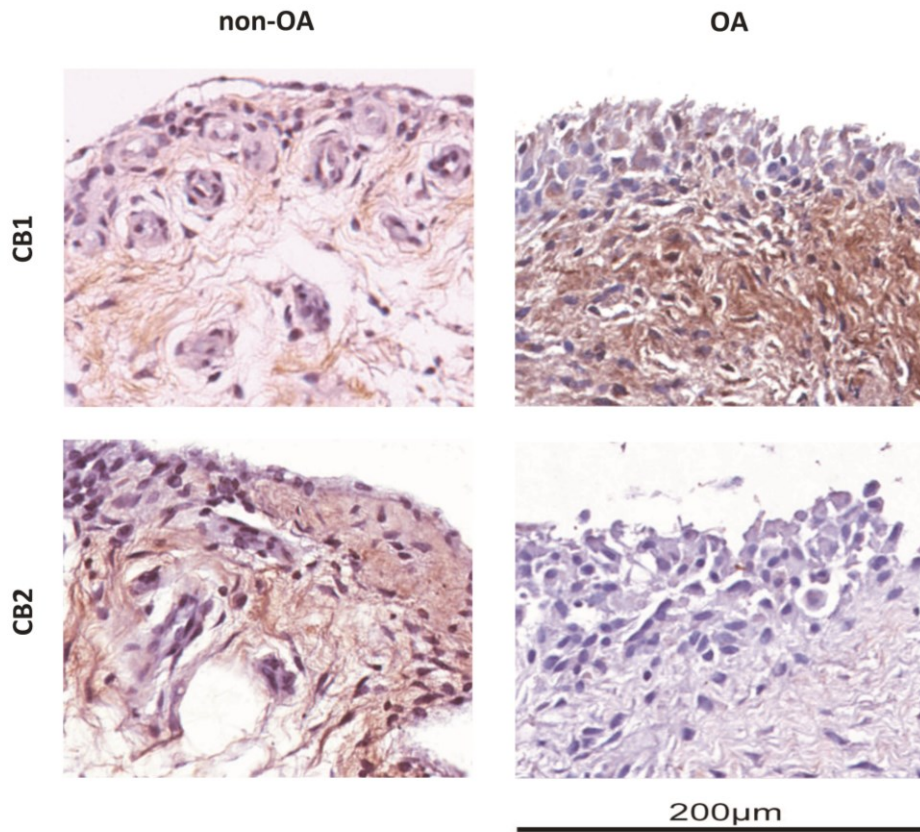

Figure 9. Immunohistochemical sections of synovial membranes from non-OA and OA patients. Slides were stained with haematoxylin and eosin and mounted with permanent mounting media. This figure shows representative images of different experiments (n = 5 non-OA and n = 5 OA). The yellow arrow indicates the hyperplastic lining cell layer, while the blue one the dense cell infiltrate composed largely of lymphocytes and monocytes.

Pain is the most common symptom of both acute and chronic inflammation that affects the quality of life of patients by prompting them to seek medical attention. Within the joint, there are pain-sensing afferent neurons or nociceptors in many of the anatomic tissues affected by OA including subchondral bone and synovial membrane. While, although cartilage loss is largely involved in OA pathogenesis, it is not innervated and therefore cannot be a direct source of pain [5].

The endocannabinoid system, that participates in the modulation of the nociceptive transmission of pain, has been described as associate to OA inflammation [184]. In particular, CB2 receptor is involved in anti-inflammatory and immunosuppressive actions by modulating the release of cytokines and inflammatory mediators [185]. Considering its participation in OA pain and inflammation, immunohistochemical analyses were performed to investigate the expression of CB1 and CB2 receptors, in non-OA and OA synovial membrane.

CB1 receptors, classically described as localized only in the central nervous system, resulted expressed in both normal and pathological tissues but with different scores based on their intensity and distribution. They were moderately present in non-OA synovial membrane (score 1+), while strongly present in OA ones (score 3+). On the other hand, CB2 receptors were detected only in non-OA tissue (score 2+) (Fig.10). The reduced expression of CB2 receptors is likely to have a role in OA pathogenesis, agrees with the observations of Fukuda and co-workers. They found that CB2 receptors were expressed only in rheumatoid arthritis synovial membranes and not in OA synovial membranes [186].

Figure 10. Immunohistochemical analysis of synovial membranes from non-OA and OA patients. Slices were stained with anti-CB1 and anti-CB2 receptor antibodies and counterstained with haematoxylin and eosin and mounted with permanent mounting media. This figure shows representative images of different experiments (n = 5 non-OA and n = 5 OA).

4.2 *Harpagophytum procumbens* phytochemical characterization

Harpagophytum procumbens, commonly known as Devil's claw, is a plant used worldwide as a traditional remedy for joint pain associated with mild OA. Its activity is caused and started by the secondary root chemical constituents like iridoid glycosides (mainly harpagoside, harpagide and procumbide), triterpenoids, phytosterols and flavonoids. Harpagoside, that is the most abundant molecule among these components, show anti-inflammatory and analgesic effects and for this reason is considered to be the active substance of the plant [187]. However, although *H. procumbens* is a remedy used since the time of traditional medicine, still little is known about the biochemical mechanisms underlying its pharmacological effect. Recently, studies aimed at understanding the *H. procumbens* root extract individual components activity have highlighted the analgesic role of some of its phytochemical constituents. Among them, β-caryophyllene and eugenol has been described to mitigate pain through an agonism on CB2 receptors and, at the same time, to reduce inflammation acting on NF-κB pathway [188–191].

In light of these findings, considering the absence of CB2 receptors in OA samples, thus suggesting their involvement in pathology, it was decided to analyse the effect of *H. procumbens* root extract on human primary synoviocytes from OA synovial membranes. Preliminarly, HPE dissolved in different solvents, DMSO, 100% v/v EtOH, 50% v/v EtOH, and H_2O, chosen basing on their ability to dissolve different classes of molecules, was phytochemically characterized. Spectrophotometric analyses of the four extracts, HPE_{DMSO}, $HPE_{EtOH100}$, HPE_{EtOH50} and HPE_{H2O}, revealed that the

highest amount of total polyphenols were extracted by DMSO and 50% v/v EtOH, followed by deionized water and pure ethanol. Indeed, their levels in HPE_{DMSO} and HPE_{EtOH50} were 1.2- to 1.4-fold higher than in HPE_{H2O} and $HPE_{EtOH100}$. Among polyphenols, tannins were mainly recovered by H_2O and DMSO, their amount in HPE_{H2O} and HPE_{DMSO} being 1.5- to 1.9-fold higher than that found in $HPE_{EtOH100}$ and HPE_{EtOH50}. Regarding flavonoids and their subclass flavonols, the highest extraction power was exhibited by DMSO; HPE_{DMSO} exhibited about 1.5- to 3-fold and 1.5- to 1.7-fold higher concentrations of total flavonoids and flavonols than HPE_{EtOH50} or $HPE_{EtOH100}$ and HPE_{H2O}, respectively (Table 4).

Table 4. Amounts of total polyphenols, tannins, flavonoids, and flavonols in HPE_{DMSO}, $HPE_{EtOH100}$, HPE_{EtOH50}, and HPE_{H2O}. Data are the mean ± SEM of at least three independent experiments with three replicates for each experiment (n = 9).

COMPOUNDS	HPE_{DMSO}	$HPE_{EtOH100}$	HPE_{EtOH50}	HPE_{H2O}
	μg/mg of dry extract (mean ± SEM)			
Polyphenols (TAE)	99.6 ± 0.05[***§]	69.6 ± 0.05	97.9 ± 0.01[***§]	84.2 ± 0.04[**]
Tannins (TAE)	14.2 ± 0.02[**]	9.2 ± 0.04	9.2 ± 0.02	17.9 ± 0.03[***]
Flavonoids (QE)	113.0± 5.1[***§§]	71.3 ± 6.6[§§]	75.1 ± 6.1[§§]	37.6 ± 4.3
Flavonols (QE)	43.8 ± 2.4[***§§]	27.6 ± 3.2	30.1 ± 2.0[§]	25.1 ± 2.0

TAE-tannic acid equivalent. QE-quercetin equivalent. ** $p < 0.01$ and *** $p < 0.01$ significantly higher than $HPE_{EtOH100}$ (ANOVA followed by Bonferroni's multiple comparison post hoc test). § $p < 0.05$ and §§ $p < 0.01$ significantly higher than HPE_{H2O} (ANOVA followed by Bonferroni's multiple comparison post hoc test).

Altogether, these results revealed that DMSO was the most suitable for recovering total polyphenols, including tannins, flavonoids, and flavonols, followed by 50% v/v EtOH, especially for total flavonoids and flavonols. Pure ethanol extract retained similar features compared to 50% v/v EtOH regarding total flavonoids and flavonols, with a lower recovery of total polyphenols. Finally, pure deionized water was able to better extract tannins, with significantly lower flavonoid levels.

In order to determine the presence of minor volatile compounds a SPME-GC-MS analysis was performed. This investigation highlighted the presence of different volatile compounds in all the samples except for the aqueous extract. Among them, eight biologically active compounds, listed in Table 5, were identified and their relative percentage amounts were calculated. Eugenol and β-caryophyllene were the main volatile phytochemicals in all extracts. Eugenol achieved a maximum 51.6% amount in HPE_{EtOH50}, while HPE_{DMSO} and $HPE_{EtOH100}$ contained the highest percentages of β-caryophyllene (i.e., 77.4% and 77.1%, respectively). Moreover, β-pinene (5.1%) and isoeugenol (1.0%) were found in HPE_{EtOH50}, while thymol (0.8%) was found in HPE_{DMSO}. α-copaene was also identified in ethanolic extracts $HPE_{EtOH100}$ and HPE_{EtOH50} (6.3% and 3.7%, respectively). On the other hand, α-humulene (10.0%; 0.8%) and δ-cadinene (5.8%; 1.3%) were detected in HPE_{DMSO} and $HPE_{EtOH100}$, respectively.

Table 5. Volatile compounds (relative percentage in the volatile fraction) detected in HPE_{DMSO}, $HPE_{EtOH100}$, HPE_{EtOH50}, and HPE_{H2O}.

No.[1]	Compound[2]	LRI[3]	RI[4]	MS[5]	HPE_{DMSO} (%)	$HPE_{EtOH100}$ (%)	HPE_{EtOH50} (%)	HPE_{H2O} (%)
1	β-pinene	978	974	+	-	-	5.1	-
2	thymol	1308	1310	+	0.8	-	-	-
3	eugenol	1339	1344	+	6.0	14.6	51.6	-
4	α-copaene	1381	1387	+	-	6.3	3.7	-
5	β-caryophyllene	1412	1416	+	77.4	77.1	38.6	-
6	isoeugenol	1432	1439	+	-	-	1.0	-
7	α-humulene	1450	1454	+	10.0	0.8	-	-
8	δ-cadinene	1528	1530[+]	+	5.8	1.3	-	-
	Total (%)				100.0	100.0	100.0	

[1] Compound identification number; [2] compounds are reported according to their elution order on column; [3] linear retention indices measured on apolar columns; [4] linear retention indices from literature; [+] normal alkane RI; [5] identification by MS spectra, tr < 0.1%.

4.3 Effects of HPE on FLS Cell Viability

The effect of each HPE was analysed on synoviocytes isolated from OA synovial membranes. Considering the presence of several different cell populations in the synovial membrane, isolated primary human cells were first characterized by the presence of vimentin protein. Vimentin is a cell cytoskeleton protein typically expressed in mesenchymal origin cells such as Fibroblast-like synoviocytes (FLSs). In addition to the different morphology, the presence of this protein allows to distinguish them from Macrophage-like synoviocytes (MLSs), the second most abundant cell population of the synovial membrane.

Human primary cells stained with primary anti-vimentin antibody are characterized by an elongated shape and expressed vimentin in their cytoskeleton (Fig.11). These features suggest a uniform isolated cell population characterized by FLSs.
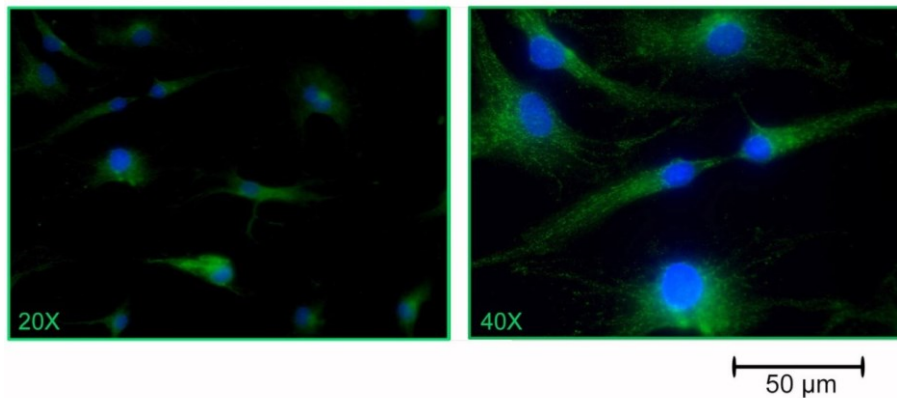
Figure 11. Human primary FLSs, isolated by synovial membranes and cultured in vitro, were stained with anti-vimentin primary antibody and with Alexa Fluor 488 (green) secondary antibody. Nuclei were stained with DAPI.

73

The effects of the four HPE, HPE$_{DMSO}$, HPE$_{EtOH100}$, HPE$_{EtOH50}$ and HPE$_{H2O}$, on FLS cell viability were determined by the MTS colorimetric method. The extracts, tested at 1 mg/mL, 0.5 mg/mL, and 0.1 mg/mL for 24, 48, and 72 h, did not show detrimental effects at any analysed concentration or time point (Fig.12). It was decided to use 0.1 mg/mL as final concentration for further experiments.
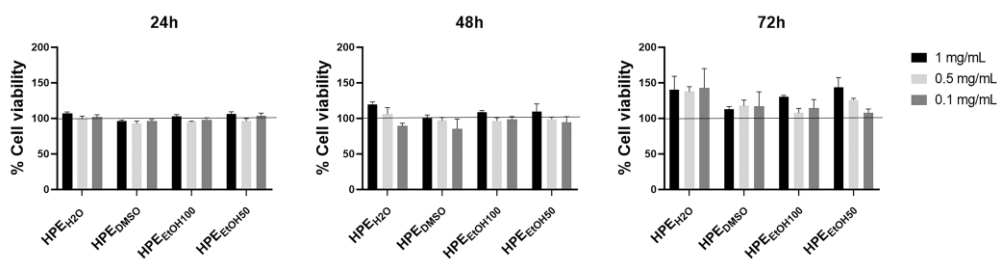
Figure 12. Cell viability was assessed by the MTS colorimetric method, and FLSs were treated with three concentrations, 1 mg/mL, 0.5 mg/mL, and 0.1 mg/mL of HPE$_{H2O}$, HPE$_{DMSO}$, HPE$_{EtOH100}$, and HPE$_{EtOH50}$, for 24, 48, and 72 h. Cell viability of treated samples was normalized to the untreated cells, which is reported as 100% and represented by a horizontal line.

4.4 HPE mechanism of action on FLSs: CB2 receptors

The four extracts previously characterised by the presence of bioactive compounds were tested on human primary FLSs to assess the effect on the endocannabinoid system. They were added to cell culture medium at a concentration of 0.1 mg/mL for 24 h, then, the mRNA expression level of CB1 and CB2 receptors was analysed. Although CB1 receptors are typically described as associated with the central nervous system, our previously conducted immunohistochemistry experiments have detected their presence in the synovial membranes. For this reason, they have been objects of this analysis. The HPE_{H2O} and HPE_{DMSO} and to a lesser extent, HPE_{EtOH50}, were able to increase the CB2 mRNA expression level, whereas $HPE_{EtOH100}$ did not show any effect. On the other hand, CB1 receptor mRNA expression level was increased by HPE_{H2O} and HPE_{DMSO} and to a lesser extent by $HPE_{EtOH100}$, whereas it was decreased by HPE_{EtOH50} (Fig.13).
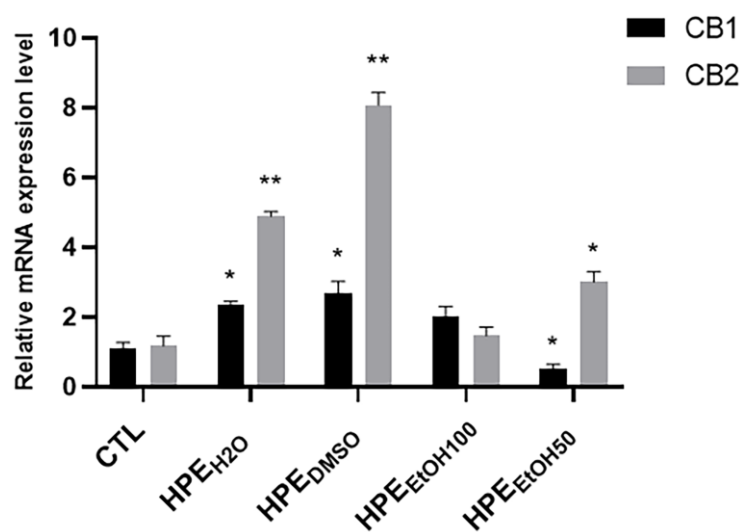
Figure 13. Effects of all HPE extracts on CB1 and CB2 mRNA expression level in human primary FLSs. After 24 hour-treatment with 0.1 mg/mL of HPE$_{H2O}$, HPE$_{DMSO}$, HPE$_{EtOH100}$, and HPE$_{EtOH50}$, cells were harvested, and mRNA was extracted and analysed by RT-PCR. CB1 and CB2 receptor mRNA levels were reported as relative mRNA expression level with respect to 18S rRNA ($2^{-\Delta\Delta Ct}$ method). Results are expressed as mean ± SEM of data obtained by three different experiments. Statistical significance was * $p < 0.05$; **$p < 0.01$ vs CTL.

In line with these findings, HPE$_{H2O}$ and HPE$_{DMSO}$ have been found to be the best extracts in stimulating CB2 receptor gene expression, although they have been shown to be also effective on CB1 even if to a lesser extent. However, considering that only CB2 receptors are associated with the modulation of inflammation and nociceptive transmission in OA disease, it was decided to focus the study exclusively on CB2 signalling pathways. Consequently, an immunofluorescence analysis was performed in order to evaluate whether the effect of HPEs on CB2 expression was confirmed also at protein level. FLSs were treated with 0.1 mg/mL of the four extracts for 24 and 48 h, then the

cells were stained with antibody anti-CB2. At protein level, HPE_{H2O} and HPE_{DMSO} extracts were able to stimulate the exposure in membrane of CB2 receptors, both at 24 and 48 h, whereas HPE_{EtOH50} and $HPE_{EtOH100}$ did not stimulate CB2 receptor expression at any analysed time (Fig.14 and 15).
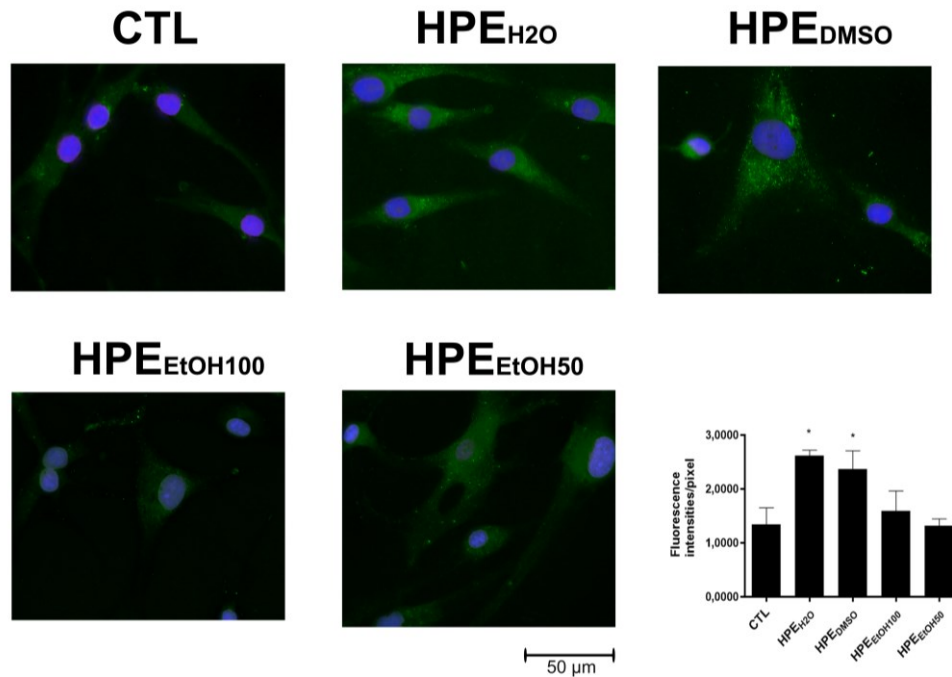
Figure 14. Effects of all HPE extracts on CB2 receptor protein production. Cells were treated with 0.1 mg/mL of HPE_{H2O}, HPE_{DMSO}, $HPE_{EtOH100}$, and HPE_{EtOH50}, for 24 h and then, analysed by immunofluorescence using anti-CB2 primary antibody and Alexa Fluor 488 (green) secondary antibody. Nuclei were stained with DAPI (original magnification 40X). The pixel intensities in the region of interest were obtained by ImageJ. $*p < 0.05$ vs CTL. In this figure representative images from three different experiments are reported.

77
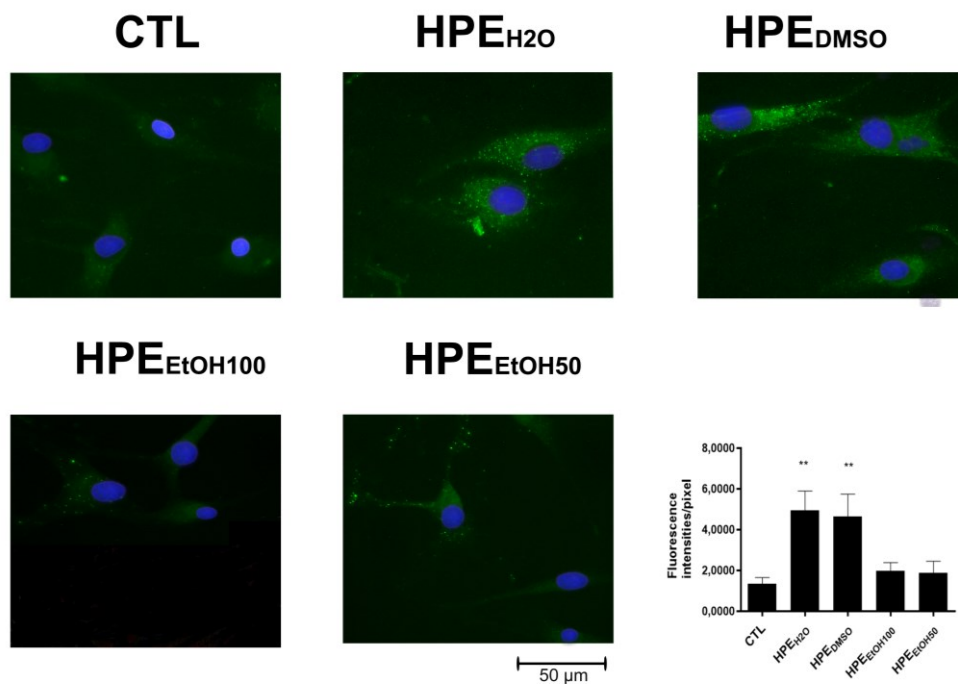
Figure 15. Effects of all HPE extracts on CB2 receptor protein production. Cells were treated with 0.1 mg/mL of HPE$_{H2O}$, HPE$_{DMSO}$, HPE$_{EtOH100}$, and HPE$_{EtOH50}$, for 48 h and then, analysed by immunofluorescence using anti-CB2 primary antibody and Alexa Fluor 488 (green) secondary antibody. Nuclei were stained with DAPI (original magnification 40X). The pixel intensities in the region of interest were obtained by ImageJ. **p < 0.01 vs CTL. In this figure representative images from three different experiments are reported.

In light of these results, HPE_{H2O} and HPE_{DMSO} showed a similar activity at both mRNA and CB2 receptor protein expression. This same effect can be partially explained by their similar composition in terms of bioactive compounds as emerged from our preliminary analysis. HPE_{H2O} and HPE_{DMSO}, indeed, showed a comparable content of polyphenols and tannins. This hypothesis is supported by several studies where the polyphenol cannabimimetic action on endocannabinoid receptors has been highlighted, suggesting an anti-inflammatory and anti-nociceptive role of these compounds [192,193]. However, it is actually clear that even the minor components, such as the volatile compounds, have a fundamental role in the phytocomplex therapeutic effect [194–196]. Contrary to the similar polyphenol and tannin content, the two extracts had an extremely different amount of volatile compounds. While water was unable to recover volatile compounds, eight biologically active volatile molecules were identified in the DMSO extract. Among these, β-caryophyllene (77.4%), eugenol (6.0%) and α-humulene (10.0%) were the most recovered. For this reason, it was decided to continue with subsequent experiments by analysing the antiarthritic effect of HPE_{DMSO} only. This extract has been proved to be the one with the highest amount of bioactive compounds and effective in stimulating CB2 receptors.

To confirm the HPE_{DMSO} effect on CB2 receptors, FLSs were cultured for 21 days in 3D by performing spheroid culture and treated with 0.1 mg/mL extract. Compared to monolayer, the use of 3D cell cultures allows to have an *in vitro* model with a cell arrangement comparable to that taken in the tissue, maintaining cell intrinsic phenotypic properties by cell-extracellular matrix interactions [197]. After 21 days of treatment, spheroid sections were stained with anti-CB2 antibody. Immunohistochemical analysis proved that

HPE$_{DMSO}$ was able to stimulate the CB2 receptor protein expression also in 3D cell culture. In particular, the receptor expression was more increased in FLSs arranged in the central area of the spheroid, suggesting the ability of phytocompounds to penetrate deep into the tissue (Fig. 16).
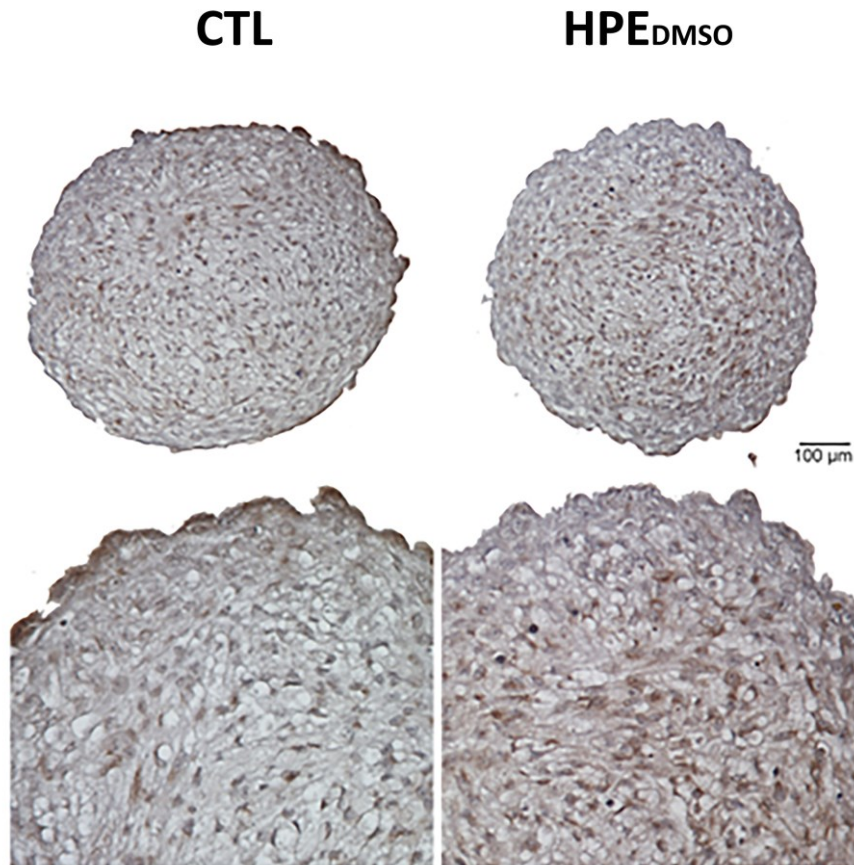
Figure 16. Effects of HPE$_{DMSO}$ extracts on CB2 receptor protein production in 3D-cultured FLSs. Cells were treated with 0.1 mg/mL of HPE$_{DMSO}$ for 21 days and then, analysed by immunohistochemistry using anti-CB2 antibody. In this figure representative images from three different experiments are reported.

4.5 HPE effects on FAAH enzyme

In addition to CB1 and CB2 receptors, the other elements of the endocannabinoid system involved in modulating nociceptive stimulus are the endogenous endocannabinoids and the enzymes involved in their synthesis and degradation. Arachidonoyl ethanolamide, also called Anandamide, (AEA) is the first identified and best characterized endogenous ligand of cannabinoid receptors that was found involved in OA disease [198,199]. Its participation in the nociceptive process in chronic pain has been shown in several studies that have found its presence in both synovial fluid and synovial membrane of OA patients [199–201]. However, AEA is also characterized by a short half-life particularly due to an effective enzymatic degradation catalysed by Fatty Acid Amide Hydrolase (FAAH) enzyme generating arachidonic acid and ethanolamine. AEA degradation has a dual effect: on one side, the decrease of analgesic impact on CB receptors, on the other one, the release of arachidonic acid, a polyunsaturated fatty acid which involved in the synthesis of eicosanoids, a class of inflammatory mediators. Therefore, targeting FAAH degrading enzyme can be a promising strategy to treat the pain stimulus and inflammation.

Considering the effect of *H. procumbens* on CB receptors, its action on the FAAH enzyme has also been evaluated as a possible additional target for antiarthritic activity. Despite the HPE_{DMSO} improved efficacy in the previous experiments, for this analysis it was decided to test all four extracts to evaluate their effect both on FAAH mRNA expression level in FLSs and on the enzymatic activity. All HPEs were added to FLS culture medium at a concentration of 0.1 mg/mL for 24 h, then, the mRNA expression level was analysed. HPE_{H2O} was able to decrease the FAAH mRNA level even if the

81

downregulation was not statistically significant, whereas all other extracts were ineffective (Fig.17A). While on the other hand, under our experimental conditions, all the extracts were able to interfere with the FAAH activity in an *in vitro* assay, although with different efficacy and potency. Particularly, HPE_{H2O} was the least effective sample, achieving a maximum 58.5% enzyme inhibition at the highest concentration of 2500 μg/mL. Conversely, the other extracts could almost completely inhibit the FAAH enzyme, $HPE_{EtOH100}$ being slightly more potent than HPE_{DMSO} and HPE_{EtOH50}, which displayed similar potencies (Fig.16B). Indeed, the IC_{50} value of $HPE_{EtOH100}$ was about 1.2- to 1.5-fold lower than those of HPE_{EtOH50} and HPE_{DMSO}. Under the same experimental conditions, 100 μg/mL harpagoside (corresponding to 200 μM) was found to be ineffective in inhibition of the FAAH enzyme (about 9% inhibition compared the control). Conversely, the positive control JZL 195 (20 μM corresponding to 8.7 μg/mL) produced a maximum 90% enzyme inhibition. As expected, the positive control was significantly more potent than the HPE extracts (Table 6).

Table 6. IC_{50} values of HPE_{DMSO}, $HPE_{EtOH100}$, HPE_{EtOH50}, HPE_{H2O} and the positive control JZL 195 in the FAAH inhibition assay.

Compound	IC_{50} (CL) μg/mL
HPE_{DMSO}	94.7 (23.8–97.5)
$HPE_{EtOH100}$	65.5 (19.2–87.9) [*]
HPE_{EtOH50}	73.8 (24.5–94.3)
HPE_{H2O}	-
JZL 195	0.03 (0.01–0.06) [*]

- Not evaluable being lower than 80% inhibition achieved. [*]$p < 0.05$ significantly lower than HPE_{DMSO} (ANOVA followed by Bonferroni's multiple comparison post-hoc test).
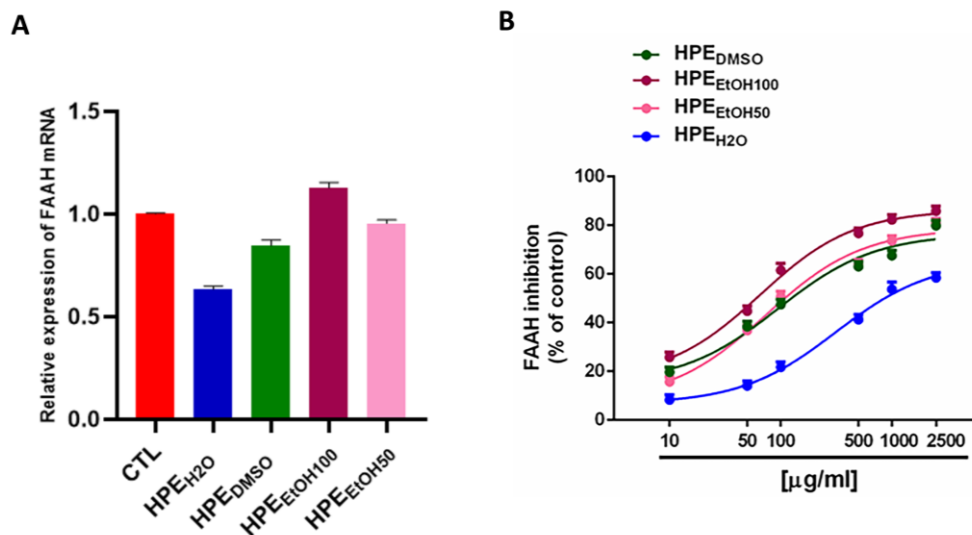
Figure 17. Effects of HPEs on FAAH expression and enzymatic activity. **A:** Cells were treated with 0.1 mg/mL of HPE$_{H2O}$, HPE$_{DMSO}$, HPE$_{EtOH100}$, and HPE$_{EtOH50}$, for 24 h. Cells were then harvested, and mRNA was extracted and analysed by RT-PCR. FAAH mRNA levels were reported as relative mRNA expression level with respect to 18S rRNA ($2^{-\Delta\Delta Ct}$ method). Results are expressed as mean ± SEM of data obtained by three different experiments. **B:** Concentration-response curves showing the inhibitory effects on FAAH from HPE$_{DMSO}$, HPE$_{EtOH100}$, HPE$_{EtOH50}$, and HPE$_{H2O}$. Data are the mean ± SEM of at least three independent experiments with two replicates for each experiment (n = 6).

4.6 Effect of HPE$_{DMSO}$ on CB2 receptor signalling coupled to G$_i$ protein

The pharmacological effect of molecules targeting CB2 receptors is caused by activation of downstream signalling pathways. These receptors are integral membrane proteins coupled with heterotrimeric G proteins (G$_{\alpha\beta\gamma}$) that are activated following ligand binding at the extracellular level. In particular, they are mainly associated with the G$_i$ class of G proteins, therefore involved in the modulation of the adenylate cyclase enzyme catalytic activity [202]. As a result, the enzyme inhibition leads to the modulation of some signalling pathways responsible for the interaction with nuclear transcription factors involved in gene expression. One of the most affected pathways in the activation of CB2 receptors is the MAPK cascade, a complex transduction pathway that involves several proteins through subsequent phosphorylations. MAPK are considered central regulators to control cell proliferation, survival, matrix synthesis, and production of pain mediators; and for this reason, deemed to be potential therapeutic targets for several diseases including OA [72].

From our previous analyses, HPE$_{DMSO}$ has shown to be the extract with multiple bioactive compounds capable of stimulating CB2 receptor gene and protein expression in FLSs. Therefore, in order to deepen its antiarthritic effect, it was decided to investigate its ability to interfere with the CB2 receptor downstream signalling pathway.

4.6.1 Effect of HPE$_{DMSO}$ on cAMP production

Adenylate cyclase is the enzyme directly involved in the activation of G$_i$ protein coupled to CB2 receptors. Therefore, in the first place to clarify the HPE$_{DMSO}$ effect in treated FLSs, the cAMP production was assessed. Cells were treated with 0.1 mg/mL of HPE$_{DMSO}$ for 5 min, 10 min, 20 min, 1 h, 24 h and 48 h, and the amount of cAMP was determined by cAMP ELISA kit. Our experiments revealed that the decrease in cAMP could be observed even after only 5 min of incubation, followed by a slight increase between 10 and 20 min. Finally, cAMP intracellular concentration reached a statistically significant reduction after 24 h up to 48 h of treatment, indicating a long-lasting effect of HPE$_{DMSO}$ on G$_i$ protein (Fig.18A).

To confirm this result, the effects of HPE$_{DMSO}$ were also studied under the stimulation of Forskolin, a powerful, rapid, and reversible stimulator of adenylate cyclase activity and consequently an agent responsible of the cAMP increase [183]. Cells were treated with Forskolin for 20 min or pre-treated with the HPE$_{DMSO}$ for 1 h and then stimulated with Forskolin for 20 min. It was found that, despite Forskolin mediated the increase of cAMP concentration, HPE$_{DMSO}$ was able to significantly reduce the cAMP level even compared to untreated FLSs (Fig.18B).
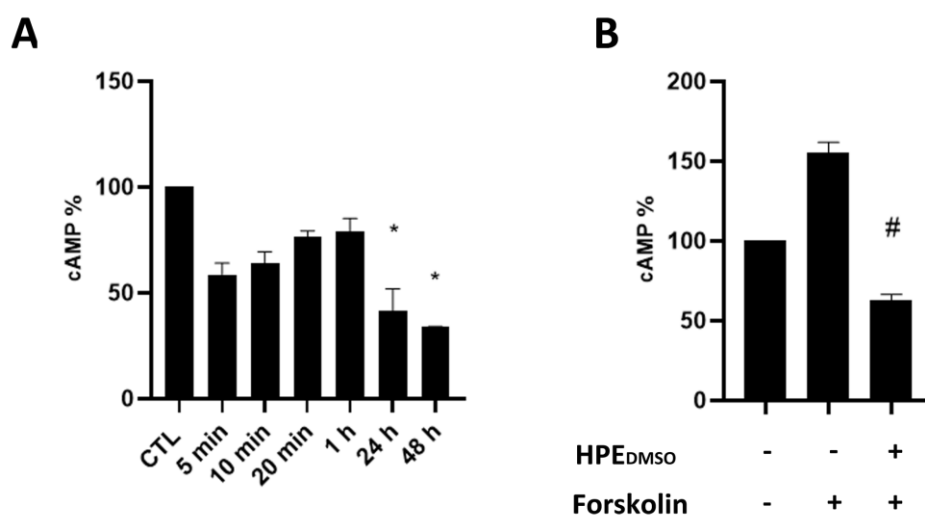
Figure 18. Determination of cAMP in cells treated with HPE_{DMSO}. **A:** FLSs were treated with 0.1 mg/mL of HPE_{DMSO}, and after the indicated times, the amount of cAMP was determined by cAMP ELISA kit. **B:** The amount of cAMP was determined in cells with pre-treated with HPE_{DMSO} for 1 h and then stimulated with Forskolin for 20 min. * $p < 0.05$ vs CTL; # $p < 0.05$ vs Forskolin.

4.6.2 Effect of HPE_{DMSO} on PKA activation

At the intracellular level, the change in cAMP concentration affects the activation of many effectors, among which the most studied is the protein kinase cAMP dependent, commonly known as PKA. Downstream of GPCR signalling, cAMP activates PKA by cooperatively binding to the regulatory subunits, allowing their phosphorylation, and leading to release and activation of the catalytic subunits. When PKA is activated, it phosphorylates a variety of substrates contributing to the signal transmission [203].

86

Considering the HPE$_{DMSO}$ inhibitory effect on cAMP production, and in order to further study the signalling pathway associated with endocannabinoid receptors, the PKA activation was analysed in treated FLSs. The PKA phosphorylation, as mechanism of activation, was evaluated by performing immunofluorescence experiments. Cells were treated with 0.1 mg/mL of HPE$_{DMSO}$ for 20 min, 1 h, 24 h and 48 h, and then stained with anti-p-PKA primary antibody. Experiments revealed that the amount of p-PKA was decreased after 20 min of treatment and to a greater extent after 1 h, 24 h, and 48 h. The confirmation that the extract acts on the pathway associated with the G$_i$ protein is the temporal course of p-PKA expression. The trend indeed agrees with the modulation of the cAMP intracellular levels at the corresponding times observed. It can be assumed that the lower PKA phosphorylation, statistically significant at 24 h and 48 h, is due to the reduction of cAMP level at the same time, while the decrease of p-PKA expression at 1 h probably reflects the one of cAMP after 5 min of treatment (Fig.19).
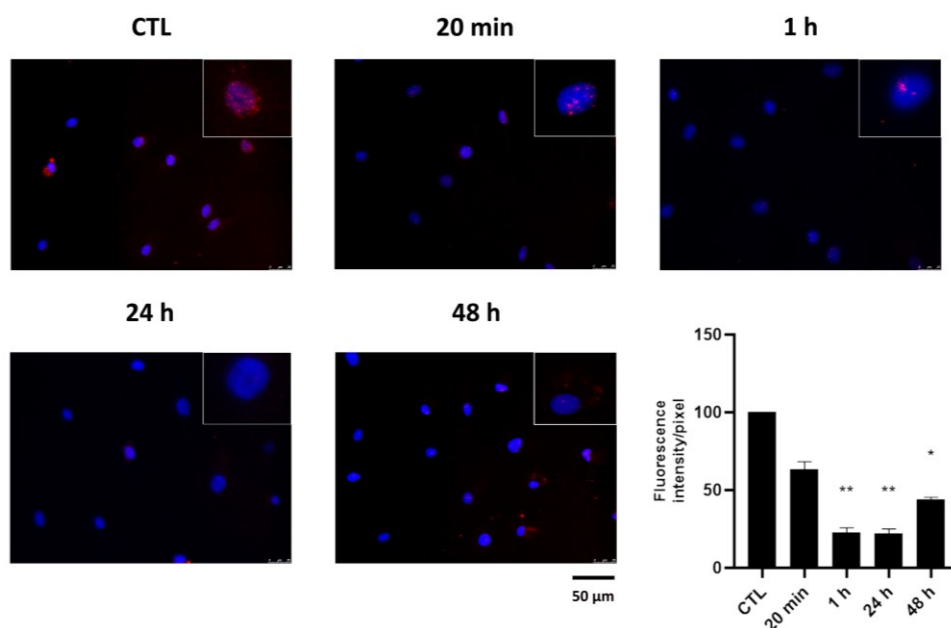
Figure 19. Effects of HPE$_{DMSO}$ extract on PKA phosphorylation. Cells were treated with 0.1 mg/mL HPE$_{DMSO}$ for the reported times and then analysed by immunofluorescence using anti-p-PKA primary antibody and Alexa Fluor 594 (red) secondary antibody. Nuclei were stained with DAPI (original magnification 40X). The bar graph represents the pixel intensities in the region of interest, obtained by ImageJ. * $p < 0.05$; ** $p < 0.01$ vs. CTL. In this figure representative images from three different experiments are reported.

Given the HPE$_{DMSO}$ effect on both cAMP and p-PKA, which are closely related, the activation of PKA was also evaluated under Forskolin stimulation, a cAMP activator. Cells were treated with Forskolin for 30 min or pre-treated with the HPE$_{DMSO}$ for 1 h and then stimulated with Forskolin for 30 min. Comparably with the results of previous experiments on cAMP levels, HPE$_{DMSO}$ was able to counteract the increase in p-PKA expression due to treatment with Forskolin (Fig.20). These data confirm that the inhibition of PKA activation was a consequence of cAMP decrease.

88
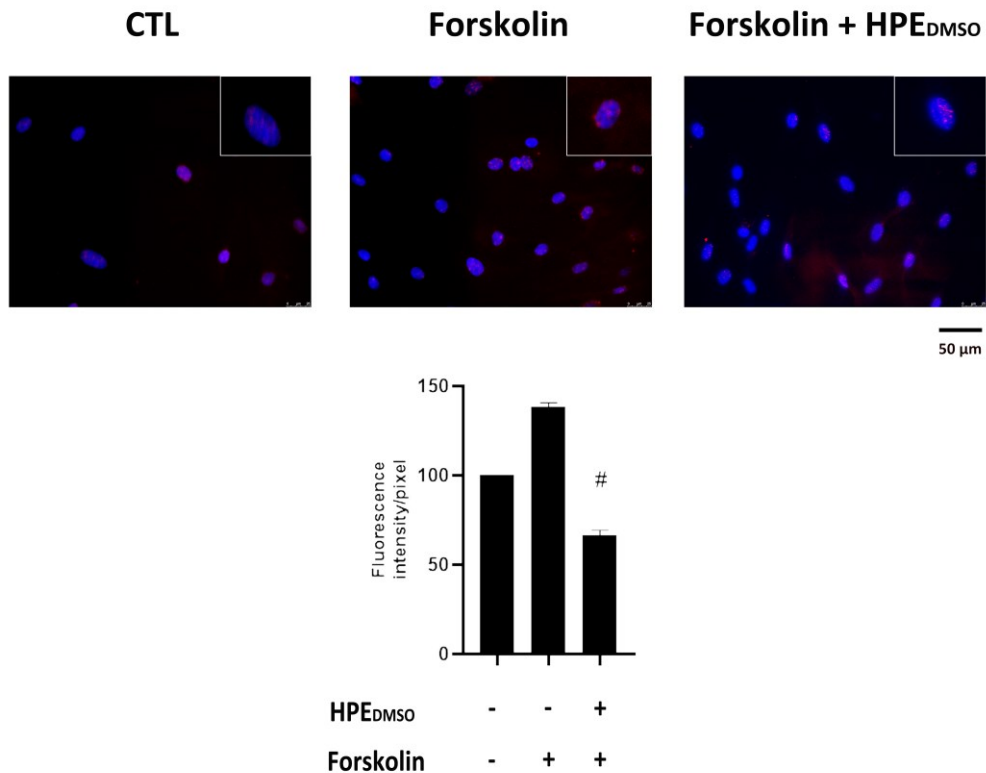
Figure 20. Effects of HPE$_{DMSO}$ extract on PKA phosphorylation after Forskolin stimulation. Cells were treated with Forskolin for 30 min or pre-treated with HPE$_{DMSO}$ for 1 h and then stimulated with Forskolin for 30 min. Cells were analysed by immunofluorescence using anti-p-PKA primary antibody and Alexa Fluor 594 (red) secondary antibody. Nuclei were stained with DAPI (original magnification 40X). The graph represents the pixel intensities in the region of interest, obtained by ImageJ. # $p < 0.05$ vs. Forskolin. In this figure representative images from three different experiments are reported.

To assess the effect of phosphorylation reduction due to HPE$_{DMSO}$ treatment, the modulation of target downstream of PKA was evaluated. Regulation of transcription by PKA is mainly achieved by direct phosphorylation of the

transcription factors as cAMP-response element-binding protein (CREB). Its phosphorylation is a crucial event because it allows this protein to interact with the transcriptional coactivators CREB-binding protein and when bound to cAMP-response elements (CRE) in target genes, increasing or decreasing their transcription.

Performing a RT-PCR experiment, the gene modulation of CREB was analysed in FLSs treated for 24 h with 0.1 mg/mL HPE$_{DMSO}$. After treatment with the extract, CREB gene expression decreased, although the reduction was not statistically significant (Fig.21). In light of this mild effect of HPE$_{DMSO}$ on CREB expression, it was decided to focus on other pathways downstream PKA.
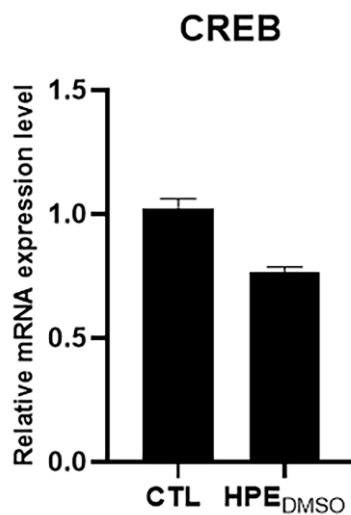
Figure 21. Effects of HPE$_{DMSO}$ on CREB mRNA expression level in human primary FLSs. After 24 hours-treatment with 0.1 mg/mL of HPE$_{DMSO}$, cells were harvested, and mRNA was extracted and analysed by RT-PCR. CREB mRNA level was reported as relative mRNA expression level with respect to 18S rRNA ($2^{-\Delta\Delta Ct}$ method). Results are expressed as mean ± SEM of data obtained by three different experiments.

4.6.3 Effect of HPE$_{DMSO}$ on ERK activation

In addition to CREB phosphorylation, p-PKA targets also the MAPK cascade, mainly by modulating the activation of ERK protein and its nuclear translocation. This cascade transmits signals through sequential activation of protein kinases consisting of an upstream activator, a MAPKKK, a MAPKK and a MAPK. In ERK pathway, Ras acts as an upstream activating protein, Raf acts as MAPKKK, MEK as MAPKK and ERK is the MAPK, forming the Ras-Raf-MEK-ERK pathway [75]. In G_i protein-associated pathway, p-PKA has been described as able to act on the protein Ras, antagonizing its inhibitory activity on Raf. Once phosphorylated by p-PKA, Ras can release Raf protein in its active form, marking the start of ERK signalling cascade [204].

The HPE$_{DMSO}$ effect on cAMP levels and PKA activation demonstrated in our previous experiments, led us to assume that also the MAPK phosphorylation could be modulated. Given the importance of the MAPK cascade activation in many cellular processes including inflammation and nociceptive transmission, a Western Blot analysis was carried out to assess the phosphorylation levels of proteins involved in the signalling pathway. Protein extracts from FLSs treated for 5 min, 1 h, 4 h and then 24 h were analysed using anti-p-ERK1/2, ERK1/2, and Actin primary antibodies. The decrease in ERK1/2 phosphorylation was observed both at short times, after 1 h and 4 h of treatment, and more at longer times, after 24 h of treatment (Fig.22). In contrast, HPE$_{DMSO}$ was shown to be ineffective in modulating JNK and p38 phosphorylation under the same experimental conditions (data not shown).
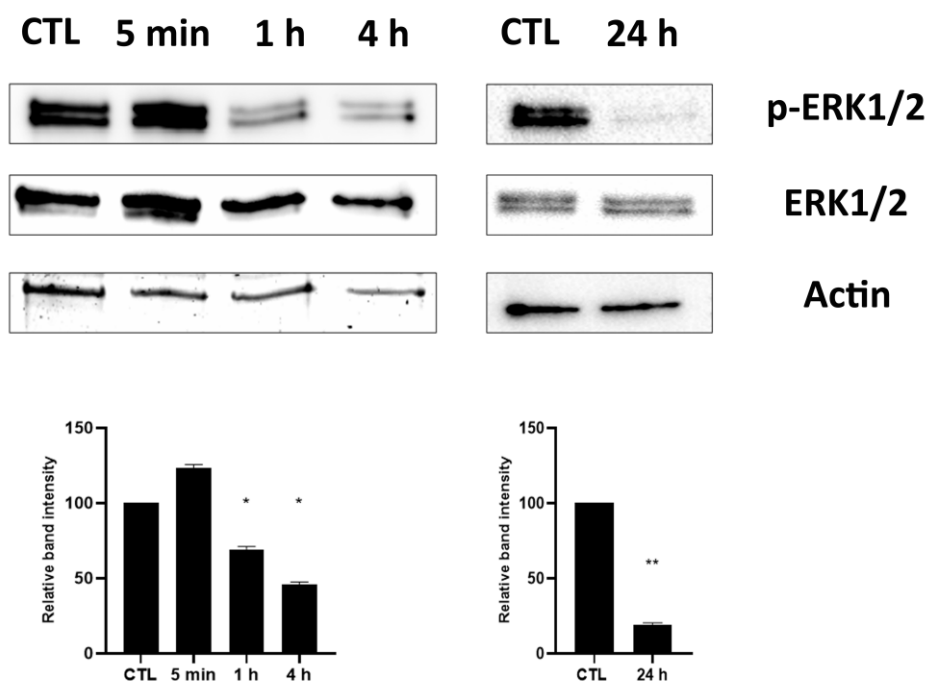
Figure 22. Effects of HPE$_{DMSO}$ on ERK phosphorylation. Cells were left untreated (CTL) or treated with 0.1 mg/mL of HPE$_{DMSO}$. Cell extracts were analysed at 5 min, 1 h, 4 h and 24 h after treatment by Western Blot, using anti-ERK1/2, anti-p-ERK1/2 and anti-Actin antibodies (upper side). The densitometric analysis (bottom side) was performed by ImageJ. Results are expressed as mean ± SEM of data obtained by three independent experiments. * p < 0.05; ** p < 0.01 vs. CTL.

Although the data obtained on ERK1/2 phosphorylation were very interesting, surprisingly they disagreed with the inhibition of PKA activation. Thus, if on one hand it was clear that in our case the modulation of ERK1/2 phosphorylation was not dependent on CB2 activation, on the other hand it was difficult to understand the cellular pathway affected upstream of MAPK.

92

The MAPK signalling pathway, indeed, is activated by different stimuli including cytokines, growth factors, and matrix proteins that bind to tyrosine kinase receptors, G protein coupled receptors, cytokine receptors, or integrins on cell membrane, indicating a complex and multiple involvement of these kinases in the cellular metabolism.

In 2019, while evaluating alternative mechanisms to explain the activation of the MAPK cascade, Saroz and colleagues demonstrated the involvement of $G_{\beta\gamma}$ subunits in the modulation of ERK1/2 phosphorylation. They found that the two subunits, traditionally described as regulatory, performed catalytic functions by activating the MAPK pathway in the presence of CB2 receptor antagonists [205]. However, the complete signalling mechanism is not fully known yet.

Moreover, taking into account that CB2 receptor is also described as associated with G_q proteins, it is possible to consider the MAPK pathway regulation by PI-PLC β enzymes. In this instance, PKC phosphorylation on target proteins triggers kinase cascade activation [206].

Therefore, considering the complexity and the multiplicity of the activation mechanisms of the MAPK pathway, on the base of the data obtained following HPE$_{DMSO}$ treatment it was difficult to uniquely identify the affected mechanism. However, for the purpose of this study it was decided not to focus on the mechanisms regulating this signalling pathway, but to analyse the downstream effects following the inhibition of ERK1/2 phosphorylation.

4.6.3.1 Effect of HPE$_{DMSO}$ on c-Fos expression and activation

The activation of the AP-1 family of transcription factors, including c-Fos and c-Jun family members, is one of the earliest nuclear events induced by molecules that stimulate ERK. More specifically, a dual control mechanism by MAPK operates over these transcription factors. In the case of c-Fos, ERK activation leads to the modulation of *c-fos* mRNA expression by acting on transcription factors bound at the *c-fos* promoter, and the c-Fos post-translational modification by the direct phosphorylation of its activation domain, thereby enhancing c-Fos transcriptional activity [207]. However, the precise mechanism by which phosphorylation by MAPKs alters the function of this transcription factor remains not fully understood [208].

Considering the observed effect on ERK1/2 phosphorylation after treatment with HPE$_{DMSO}$, it was decided to analyse its impact on c-Fos. Given the double control mechanism operated by ERK, both the modulation of the *c-fos* gene and its activation by phosphorylation have been evaluated. Therefore, FLSs were treated for 24 h with 0.1 mg/mL HPE$_{DMSO}$ and then mRNA and proteins were extracted for RT-PCR and Western Blot analyses, respectively. The treatment induced a statistically significant down-regulation of *c-fos* mRNA expression level (Fig. 23A) and the decrease in total c-Fos protein level but was unable to inhibit c-Fos phosphorylation (Fig.23B and C). From the densitometric analysis carried out on the protein bands, in fact, by analysing the expression of p-c-Fos compared to its total protein, it is not possible to appreciate a statistically significant decrease in the phosphorylated protein. However, by looking at the p-c-Fos and c-Fos protein bands, it seemed that a decrease in both phosphorylated and not phosphorylated protein expression, in the treated sample, could be observed.

94

In order to clarify this observation, a second densitometric analysis was carried out by comparing both the phosphorylated and the total protein expression in relation to Actin. From this analysis, it emerged that treatment with HPE_DMSO was able to reduce the total c-Fos protein expression, recalling its effect on gene modulation. This allowed us to affirm that the decrease of p-c-Fos expression, which was visible observing the bands and obtained also putting in relation this protein to Actin (data not shown), showed no real inhibition of phosphorylation since it has an effect on the total protein expression.
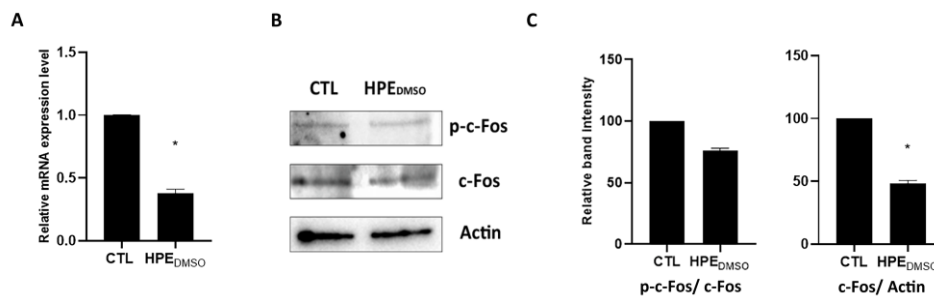
Figure 23. Effects of HPE_DMSO on c-Fos production and activation. **A:** Cells were treated with 0.1 mg/mL HPE_DMSO for 24 h and then the mRNA was extracted and analysed by RT-PCR. *c-Fos* mRNA level was reported as relative mRNA expression level with respect to 18S rRNA ($2^{-\Delta\Delta Ct}$ method). **B:** Cells were treated as described in **A** and then proteins were extracted and analysed by Western Blot using anti-c-Fos, anti-p-c-Fos and anti-Actin antibodies. **C:** Densitometric analysis of bands obtained in Western Blot experiment, performed by ImageJ. Results are expressed as mean ± SEM of data obtained by three independent experiments. * $p < 0.05$ vs. CTL.

4.6.3.2 Effect of HPE$_{DMSO}$ on MMP and ADAMTS expression

Activation or suppression of intracellular signalling via the MAPK family has been linked to expression of MMPs, ADAMTSs and degrading enzymes by several studies [72,209–211]. Most of the genes encoding matrix-degrading MMPs, but also inflammatory cytokines, are indeed under the control of c-Fos that activates such genes by binding directly their promoter AP-1 motifs [212]. Consequently, this pathway plays a key role in OA pathogenesis. The extracellular matrix degrading enzymes are considered the main contributors to the joint degenerative process causing progressive cartilage destruction and, finally, complete loss of chondrocytes [213].

The MMPs family includes many enzymes with different functions and targets [214]. Among them, collagenase MMP-13, mainly released from chondrocytes and synoviocytes, has a predominant role in OA pathogenesis in collagen II degradation. Moreover, it also degrades the aggrecan, a proteoglycan molecule, giving it a dual role in matrix destruction. The expression of other MMPs such as MMP-2, MMP-3, MMP-9, and MMP-10, is also elevated in OA. These enzymes degrade non-collagen matrix components of the joints [215].

However, in addition to the well-characterised MMPs, ADAMTS-4 and ADAMTS-5, and many other ADAMTSs are expressed in cartilage and show significantly altered expression in OA [216]. Similar to MMP-13, these ADAMTSs are responsible for the aggrecan degradation in the extracellular matrix, generating irreversible collagen loss [217].

Considering the role played by these enzymes in OA progression, following c-Fos modulation it was decided to evaluate the HPE$_{DMSO}$ effect on their gene expression in order to establish a possible chondroprotective effect of the

phytocomplex. Performing a RT-PCR experiment, the gene modulation of extracellular matrix degrading enzymes was analysed in FLSs treated for 24 h with 0.1 mg/mL HPE$_{DMSO}$. In line with the expected result, a statistically significant down-regulation of MMP-3, MMP-13 and ADAMTS-5 at the transcriptional level has been demonstrated (Fig. 24A, left graph and B), while surprisingly, HPE$_{DMSO}$ was ineffective in modulating the MMP-10 and ADAMTS-4 gene expression (data not shown).

Moreover, since MMP-13 is the crucial enzyme for the aggressive degradation of type II collagen and an attractive target for the OA treatment, the role of our extract on the enzyme release in the cell culture medium has also been evaluated. The amount of produced MMP-13 was measured in the culture supernatant of cells cultured under the same experimental conditions of the previous experiment and analysed by ELISA. The obtained results confirmed the HPE$_{DMSO}$ inhibitory effect on the release of MMP-13 by FLSs (Fig. 24A, right graph).
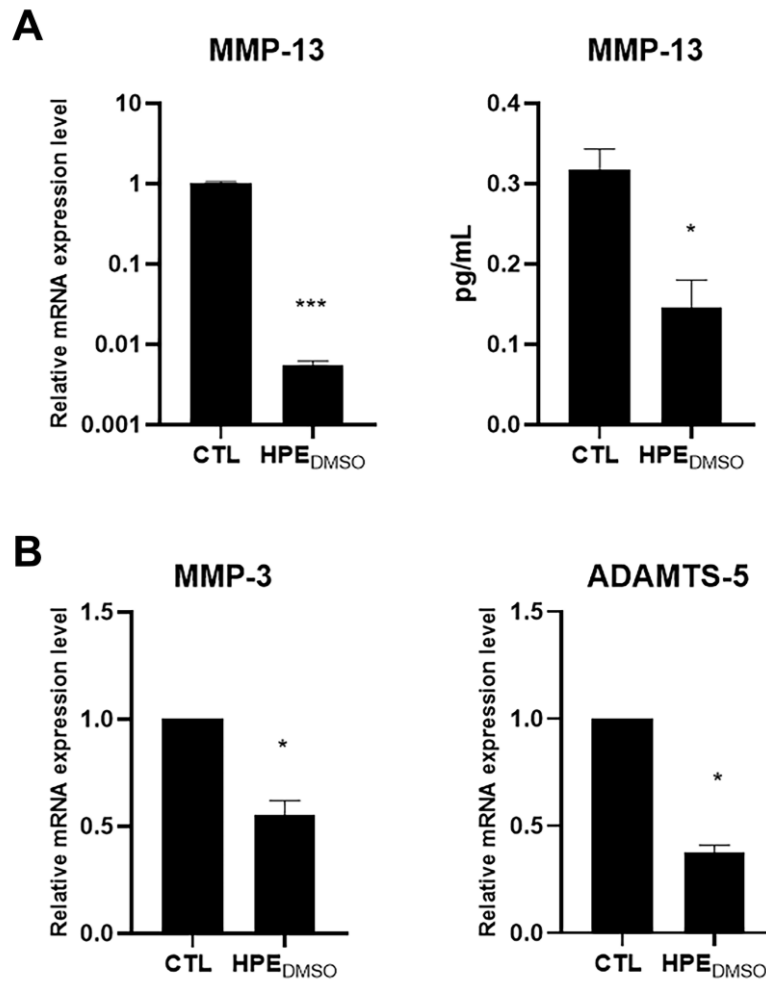
Figure 24. Effects of HPE$_{DMSO}$ on the production of degrading enzymes. Cells were treated with 0.1 mg/mL HPE$_{DMSO}$ for 24 h and then the mRNA was extracted and analysed by RT-PCR. **A, left graph:** MMP-13 mRNA level was reported as relative mRNA expression level with respect to 18S rRNA ($2^{-\Delta\Delta Ct}$ method). **B:** MMP-3 and ADAMTS-5 mRNA level was reported as relative mRNA expression level with respect to 18S rRNA ($2^{-\Delta\Delta Ct}$ method). **A, right graph:** The amount of MMP-13 produced was measured in the culture medium of cells and analysed by ELISA. The results are reported as pg/mL. Results are expressed as mean $\pm$ SEM of data obtained by three independent experiments. * $p < 0.05$ *** $p < 0.005$ vs. CTL.

4.6.4 Effect of HPE$_{DMSO}$ on NF-κB pathway

The effect of MMP-10 and ADAMTS-4 is described in literature as mediated by several pathways, including NF-κB. Considering that in our cellular system these two genes were not modulated by HPE$_{DMSO}$ as result of downstream effect on ERK1/2 inhibition, it was decided to evaluate the effect of the extract on NF-κB signalling pathway in order to give a possible explanation to the lack of modulation of the two enzymes. NF-κB represents a family of inducible transcription factors which regulates a large array of genes involved in inflammatory responses [61]. Moreover, the role of NF-κB is prominent in the inflammation as well as in the cartilage degradation, synovial cell proliferation, angiogenesis, and pannus formation. Consequently, targeted strategies that interfere with NF-κB signalling could offer novel potential therapeutic options for OA treatment [62,218].

For the assessment of the HPE$_{DMSO}$ effect on NF-κB, FLSs were treated with 0.1 mg/mL HPE$_{DMSO}$ for 1 h and then stimulated with 10 ng/mL TNF-α for 30 min, or only stimulated with 10 ng/mL TNF-α for 30 min. The expression of intercellular adhesion molecule-1 (ICAM-1), monocyte chemoattractant protein-1 (MCP-1) and IκBα genes modulated by the NF-κB pathway were evaluated using RT-PCR. However, under these experimental conditions HPE$_{DMSO}$ was proved to be unable to modulate the expression of these genes that were up-regulated by TNF-α, suggesting a failure effect on this pathway (data not shown). Furthermore, this result led us to confirm a correlation between the lack of modulation of MMP-10 and ADAMTS-4 and the ineffectiveness of the extract on the NF-κB pathway. In light of this HPE$_{DMSO}$ effect on the NF-κB gene expression, it has been decided not to continue with the analysis of this pathway.

99

4.6.5 Anti-inflammatory effect of HPE$_{DMSO}$ in TNF-α-stimulated FLSs

As is well known, MAPK and NF-κB pathways are widely involved in the inflammatory response in OA. While HPE$_{DMSO}$ has been shown to be unable of modulating the genes involved in the NF-κB pathway, it has been proved to significantly reduce ERK protein activation.

Consequently, in order to assess its anti-inflammatory effect, it was decided to focus again on the MAPK pathway and the molecules involved in the downstream inflammatory response. Preliminary, the modulation of p-ERK1/2 protein expression by HPE$_{DMSO}$ following cytokine pro-inflammatory stimulus was evaluated. Cytokines, such as TNF-α used in this experiment, are among the many different stimuli capable of activating the ERK1/2 pathway and able to simulate *in vitro* the inflammatory environment typical of OA. Protein extracts from FLSs treated with 0.1 mg/mL HPE$_{DMSO}$ for 1 h and stimulated with 10 ng/mL TNF-α for 30 min or only stimulated with 10 ng/mL TNF-α for 30 min were analysed performing a Western Blot analysis using anti-p-ERK1/2, anti-ERK1/2, and anti-Actin primary antibodies. As expected, HPE$_{DMSO}$ was able to counteract the mild p-ERK1/2 increased protein expression due to stimulation with TNF-α cytokine, bringing the ERK1/2 phosphorylation below that related to untreated cells (Fig.25). This result is comparable to the effect observed in the absence of inflammatory stimulus, confirming its ability to act on the MAPK pathway.
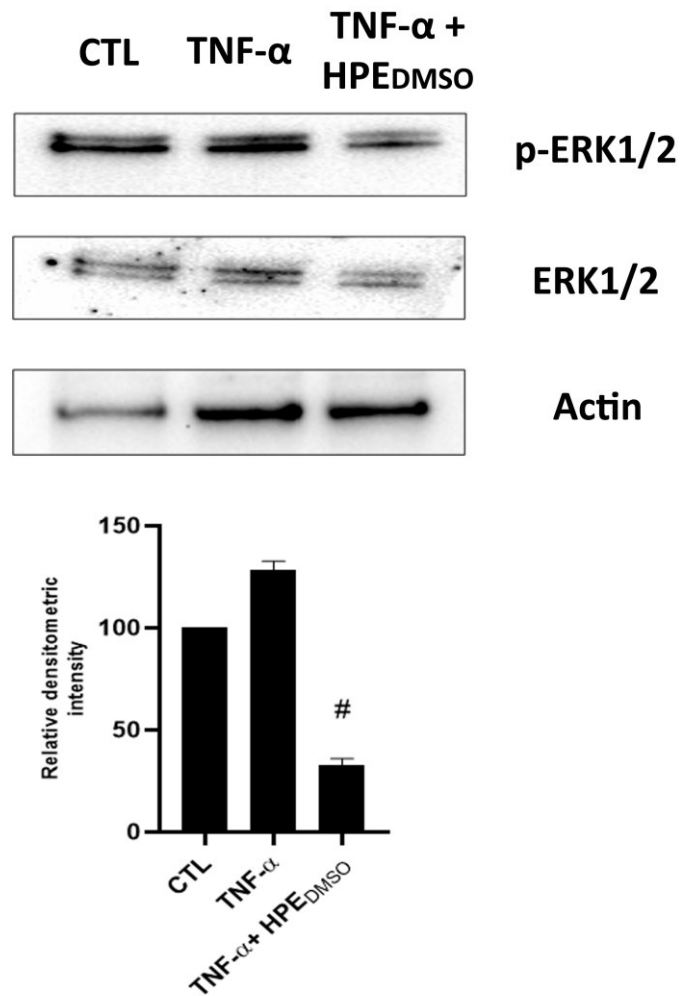
Figure 25. Effects of HPE$_{DMSO}$ on ERK phosphorylation under TNF-α stimulus. Cells were left untreated (CTL) or treated with 0.1 mg/mL HPE$_{DMSO}$ for 1 h and stimulated with 10 ng/mL TNF-α for 30 min or only stimulated with 10 ng/mL TNF-α for 30 min. Cell extracts were analysed after treatment by Western Blot, using anti-ERK1/2, anti-p-ERK1/2 and anti-Actin antibodies (upper side). The densitometric analysis (bottom side) was performed by ImageJ. Results are expressed as mean ± SEM of data obtained by three independent experiments. # $p < 0.05$ vs. TNF-α.

101

Among the various effects on intracellular metabolism, ERK1/2, through transcription factors of the AP-1 complex, is responsible for the transcription of pro-inflammatory genes, such as interleukins and TNF-α [219], in addition to the MMP and ADAMTS degrading enzymes, as our previous experiments have shown.

Performing a RT-PCR experiment, the gene modulation of IL-1β, IL-6 and IL-8 was analysed in FLSs treated with 0.1 mg/mL HPE$_{DMSO}$ for 1 h and stimulated with 10 ng/mL TNF-α for 30 min or only stimulated with 10 ng/mL TNF-α for 30 min, to assess the extract anti-inflammatory effect. HPE$_{DMSO}$ resulted able to reduce the gene expression of the three analysed interleukins, overexpressed following TNF-α stimulation. For IL-6, however, this decrease was not statistically significant (Fig.26).

All together these results allowed to consider HPE a phytocomplex with antiarthritic properties able to counteract both the nociceptive stimulus, through agonism on CB2 receptors, and the inflammation and extracellular matrix degenerative effects, by acting on the pathways associated with these receptors.
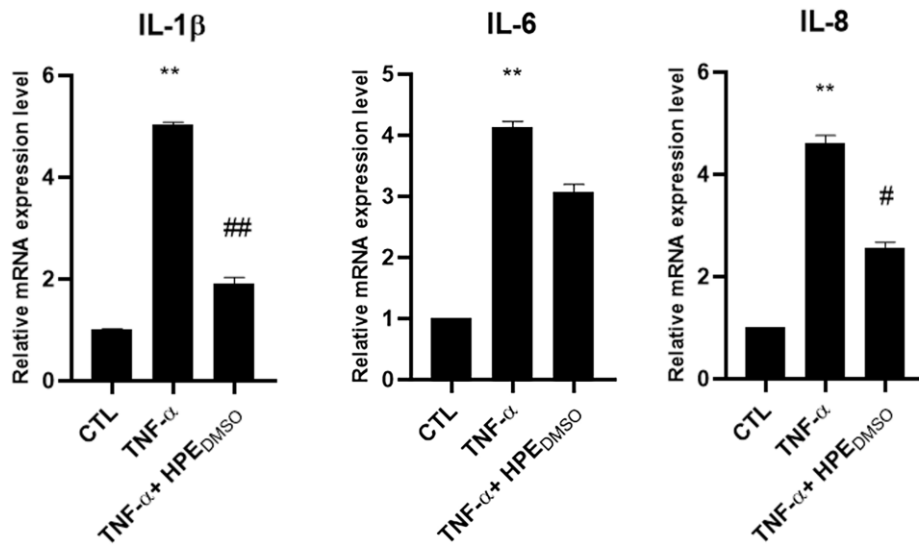
Figure 26. Effects of HPE$_{DMSO}$ on interleukin expressions under TNF-α stimulus. Cells were left untreated (CTL) or treated with 0.1 mg/mL HPE$_{DMSO}$ for 1 h and stimulated with 10 ng/mL TNF-α for 30 min or only stimulated with 10 ng/mL TNF-α for 30 min and then the mRNA was extracted and analysed by RT-PCR. IL-1β, IL-6 and IL-8 mRNA level was reported as relative mRNA expression level with respect to 18S rRNA ($2^{-\Delta\Delta Ct}$ method). Results are expressed as mean ± SEM of data obtained by three independent experiments. ** p< 0.01 vs. CTL; # p < 0.05; ## p< 0.01 vs. TNF-α

4.6.6 Activity of pure compounds contained in HPE$_{DMSO}$ alone and in combination compared to HPE$_{DMSO}$

From experiments carried out so far, the whole extract of *H. procumbens* solubilized in DMSO has been shown to act on the signalling pathway associated with CB2 receptors as an agonist. This extract, in addition to stimulating the endocannabinoid receptor expression, through action on the G$_i$ protein was able to modulate the signalling downstream cAMP, and also to inhibit the ERK enzyme activation and correlated transcription factors, although with a mechanism not clarified yet. Preliminary experiments showed that HPE$_{EtOH100}$, HPE$_{EtOH50}$ and in particular HPE$_{H2O}$ were also able to increase the CB2 receptor expression, but with a lower effect than HPE$_{DMSO}$. This greater effect may be linked with the results obtained from our phytochemical characterization analyses. Among the four extracts, HPE$_{DMSO}$ was found to contain the largest number of bioactive compounds, and in the highest concentration. For instance, compared to HPE$_{H2O}$, with which it shared a similar *in vitro* effect, it contained a higher amount of volatile compounds to which a therapeutic function is attributed. For this reason, in order to clarify the role of some of the bioactive molecules contained in the HPE$_{DMSO}$ in its effect on the observed biochemical pathways, it was decided to individually analyse those most abundant on primary FLSs.

Taking into account the previously conducted GC-MS analyses, the three more represented volatile compounds in the HPE$_{DMSO}$, β-caryophyllene, α-humulene, eugenol, and in the end the harpagoside, which is considered the HPE active substance, were tested. Preliminary, the concentration of each compound was measured in 0.1 mg/mL of the HPE$_{DMSO}$. GC-MS analysis

was performed to quantify the three volatile compounds, whereas, to determine the harpagoside amount the UHPLC-MS analysis was used (Table 7).

Table 7. Absolute concentration of major single volatile compounds and harpagoside, the main component of HPE$_{DMSO}$. The concentrations were determined in 0.1 mg/mL HPE$_{DMSO}$. Data are expressed as mean (μg) ± SEM per mg of extract (n =3).

Compound	HPE$_{DMSO}$ Mean (μg) ± SEM in 1 mg extract
β-Caryophyllene	0.082 ± 0.0002
α-Humulene	0.024 ± 0.0004
Eugenol	0.004 ± 0.0002
Harpagoside	4 ± 0.0049

It was then decided to evaluate the effect of these single molecules on some key points of the signalling pathway: the CB2 receptor expression and the related intracellular cAMP amount, the ERK1/2 phosphorylation and finally the expression of MMP-13 extracellular matrix degrading enzyme. The effect of a mixture (Mix) containing β-caryophyllene, α-humulene, eugenol and harpagoside at the same concentration found in 0.1 mg/mL HPE$_{DMSO}$ has also been tested and compared to the whole extract activity. FLSs were treated with 0.1 mg/mL HPE$_{DMSO}$, 8 ng/mL β-caryophyllene, 2 ng/mL α-humulene, 0.4 ng/mL eugenol and 0.4 μg/mL harpagoside and with Mix at same concentration, for 24 h, when performing these analyses.

Initially, the effect of single compounds on the mRNA expression level of CB2 gene was determined. The RT-PCR experiment revealed that the CB2 expression was increased by all compounds except for β-caryophyllene, even

105

if the α-humulene, eugenol and harpagoside were found to be less effective than the Mix of all four compounds, and particularly when compared to HPE$_{DMSO}$ (Fig.27A). As consequence of the effect on CB2 receptors, the effect of single compound on modulation of intracellular cAMP levels was evaluated. According to the results obtained on the CB2 mRNA expression level, all compounds as well as the mixture were able to decrease the cAMP production, even though β-caryophyllene decreased the cAMP in a non-statistically significant manner (Fig.27B). This result was very surprising in terms of β-caryophyllene effects. This bioactive compound, indeed, although it is described in several research as a CB2 receptor agonist, has been shown to be unable to up-regulate the expression of endocannabinoid receptors and consequently to interfere with their signalling pathway.

Considering the significative HPE$_{DMSO}$ inhibition on ERK1/2 phosphorylation and the multiple involvement of this pathway in OA disease, the effect of single substances and Mix was tested by carrying out an immunofluorescence analysis. Among the four analysed substances, α-humulene and harpagoside were totally inactive on the ERK1/2 activation, while β-caryophyllene, the Mix and more than all the eugenol inhibited the phosphorylation. However, β-caryophyllene and Mix inhibition was not statistically significant, while eugenol had even a higher inhibitory effect than HPE$_{DMSO}$. This result clearly suggested that the whole extract effect on the MAPK pathway is mainly due to the presence of eugenol (Fig.28).

Finally, in order to evaluate the effect of the treatments on the MMP-13 production, the mRNA expression level of this metalloprotease was analysed. It was found that only the harpagoside and the Mix of the four components were able to decrease its production even if to a lower extent compared to

HPE_DMSO. Thus, although eugenol has been shown to be very effective in reducing ERK1/2 phosphorylation, it has not been able to modulate the MMP-13 expression, which on the contrary was affected by harpagoside treatment (Fig.27C). Hence, in both cases, the MMP-13 modulation was probably not correlated with the MAPK pathway.
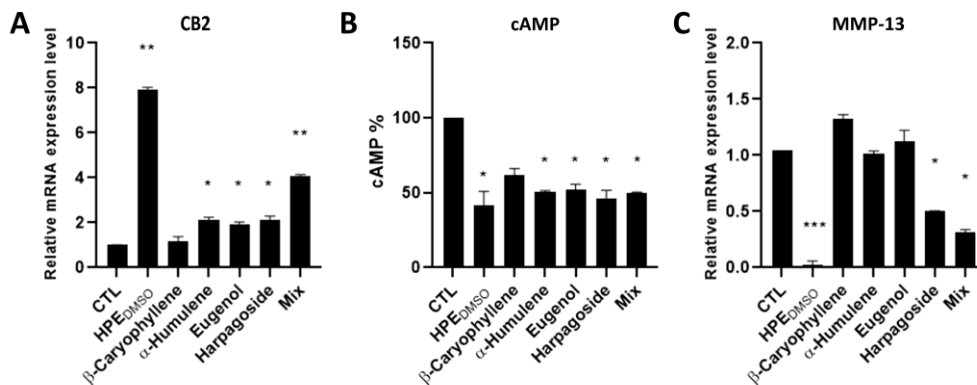
Figure 27. Effects of HPE_DMSO on CB2, cAMP and MMP-13 production. Cells were treated with 0.1 mg/mL HPE_DMSO, 8 ng/mL β-caryophyllene, 2 ng/mL α-humulene, 0.4 ng/mL eugenol and 0.4 μg/mL harpagoside and with the mixture of all four compounds (Mix) at same concentration, for 24 h. After treatment, the mRNA was extracted and analysed by RT-PCR. **A and C, respectively:** CB2 and MMP-13 mRNA level was reported as relative mRNA expression level with respect to 18S rRNA ($2^{-\Delta\Delta Ct}$ method). **B:** The cAMP amount was measured by cAMP ELISA kit. Results are expressed as mean ± SEM of data obtained by three independent experiments. *p<0.05; **p<0.01; *** p<0.005 vs. CTL
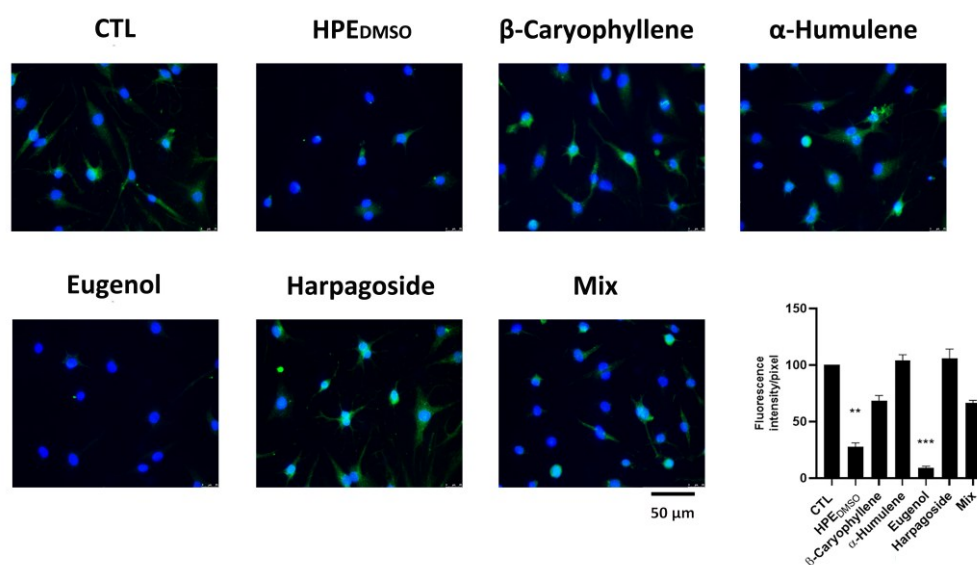
Figure 28. Effects of HPE$_{DMSO}$ on ERK1/2 phosphorylation. Cells were treated with 0.1 mg/mL HPE$_{DMSO}$, 8 ng/mL β-caryophyllene, 2 ng/mL α-humulene, 0.4 ng/mL eugenol and 0.4 μg/mL harpagoside and with the mixture of all four compounds (Mix) at same concentration, for 24 h. Cells were analysed by immunofluorescence using anti-p-ERK1/2 primary antibody and Alexa Fluor 488 (green) secondary antibody. Nuclei were stained with DAPI (original magnification 40X). The graph represents the pixel intensities in the region of interest, obtained by ImageJ. **p<0.01; *** p<0.005 vs. CTL. In this figure representative images from three different experiments are reported.

In conclusion, performing these experiments, it was observed that the single compounds were always less effective than the *H. procumbens* whole extract and the Mix, suggesting a synergistic action between the analysed molecules. However, the surprising result was that the mixture was less effective than HPE$_{DMSO}$ whole extract, although containing individual compounds in the same concentrations. This evidence suggested the existence of synergistic

interactions between the individual compounds analysed and other molecules not identified in phytochemical analyses or contained in smaller quantities that contribute to the bioactivity of the entire extract.

Finally, it was possible to undoubtedly affirm the existence of a phytocomplex, characterized by the cooperation between several molecules, to which the antiarthritic effect can be attributed.

4.7 Effect of HPE$_{DMSO}$ on CB2 receptor signalling coupled to G$_q$ protein

The investigation of the *H. procumbens* effects on G$_i$ protein coupled CB2 receptors has made it possible to fully understand the extract antiarthritic role attributable to the modulation of this signal pathway.

Historically, endocannabinoid receptors have been described exclusively as being associated with the cAMP and PKA pathway for nociceptive transmission at the intracellular level. However, in recent years there is an increasing amount of data showing other alternative regulatory pathways which are modulated by this receptor activation, depending on the cell type involved [220]. In the nervous system, for example, the involvement of CB1 receptors in decreasing Ca^{2+} entry into cells through calcium channels has been demonstrated to be critical for the neuronal signal integration [221]. These findings are supported by more recent evidence also demonstrating the CB2 receptors involvement in Ca^{2+} signalling in several cell types [222]. CB2, in contrast to CB1, regulates the Ca^{2+} release at the peripheral level, but it is now clear that both act with the same mechanism through the modulation of the PI-PLC/DAG/IP$_3$ pathway [223]. Although researches are still ongoing, the effect on the PI-PLC pathway following endocannabinoid receptor activation appears to be mediated either by the involvement of the G$_i$ protein βγ subunit catalytic activity, or by a switch from G$_i$ to G$_q$ protein coupled receptors [224]. To continue our study on the HPE agonism on CB2 receptors, it was decided to analyse its effect on PI-PLC enzymes and their downstream mediators, in order to deepen the knowledge of HPE antiarthritic activity through less explored signalling pathways.

4.7.1 Effect of HPE$_{DMSO}$ on PI-PLC expression

Members of the PI-PLC β family are among the most well studied PI-PLC isoforms involved in a myriad of biological functions downstream of GPCR activation including inflammation and pain. There are four isoforms of the PI-PLC β family that show different tissue expression and G protein regulation. All PI-PLC β isoforms are activated by the G_α subunits of the G_q class: PI-PLC β1 and PI-PLC β3 bind G_α with larger affinity compared to PI-PLC β2 or PI-PLC β 4. $G_{\beta\gamma}$ subunits have a good effect on PI-PLC β3 and PI-PLC β2, a small effect on PI-PLC β1 and do not bind PI-PLC β4 [100]. Moreover, PI-PLC β1 and β4 are mostly expressed, although not exclusively, in the nervous system. PI-PLC β2 can be found in the hematopoietic lineage, while PI-PLC β3 is more widely distributed [100,225].

To evaluate the HPE$_{DMSO}$ effect on the signalling pathway downstream of the activation of G_q or $G_{i\beta\gamma}$ protein coupled CB2 receptor, a gene modulation experiment performing a semi-quantitative-PCR was carried out. Although only the PI-PLC β isoforms are described as directly coupled to GPCR signalling, it was decided to preliminarily analyse all the primary and secondary PI-PLC isoforms. From this explorative analysis only the PI-PLC ζ was excluded because it has been described as a sperm-specific protein [99].

FLSs were treated for 24 h with 0.1 mg/mL HPE$_{DMSO}$, then the mRNA was extracted, and PCR reactions were performed. After treatment with the extract, a modulation of PI-PLC β gene expression was observed. In particular, HPE$_{DMSO}$ was able to reduce the expression of PI-PLC β2 isoform and to increase that of β3 and β4 isoforms. However, in addition to the mild effect on PI-PLC β gene expression, a very interesting modulation of the γ1 isoform, which deserves to be deepened with further experiments within this

study, has also emerged. On the other hand, HPE_{DMSO} has been shown to be irrelevant in gene modulation of all other PI-PLC enzymes and therefore they will not be further analysed in this study (Fig.29).
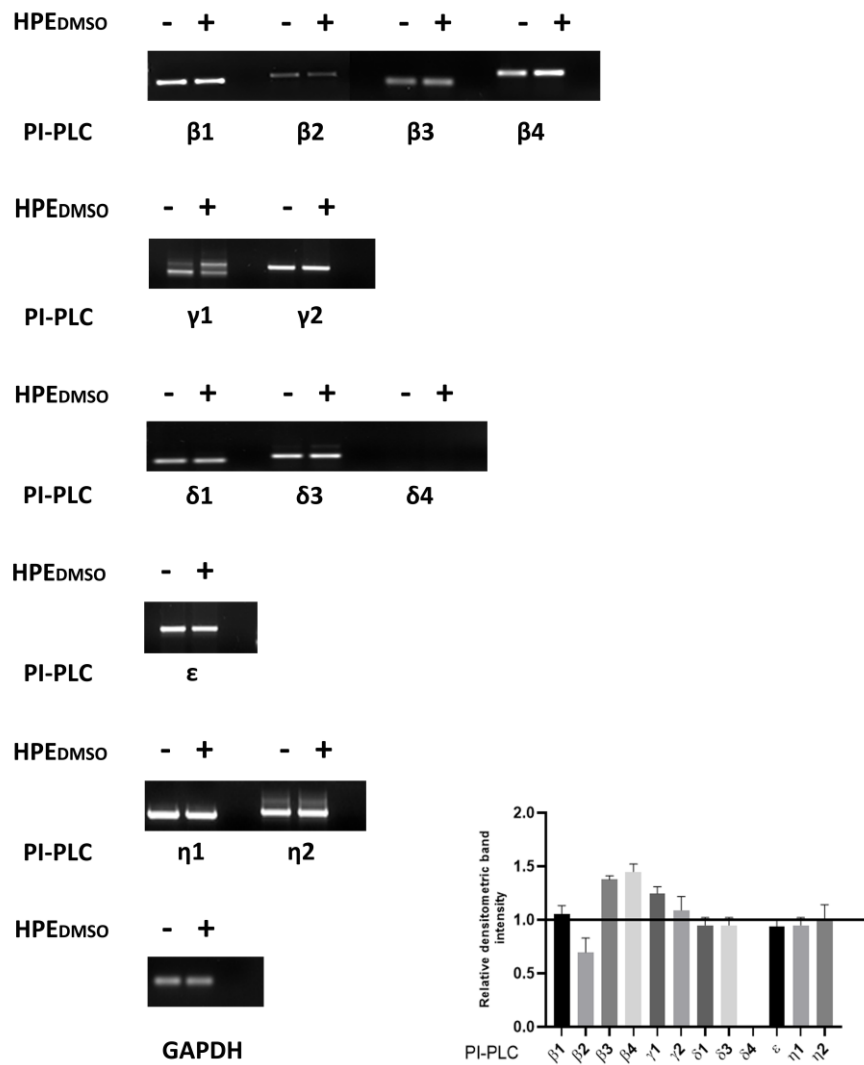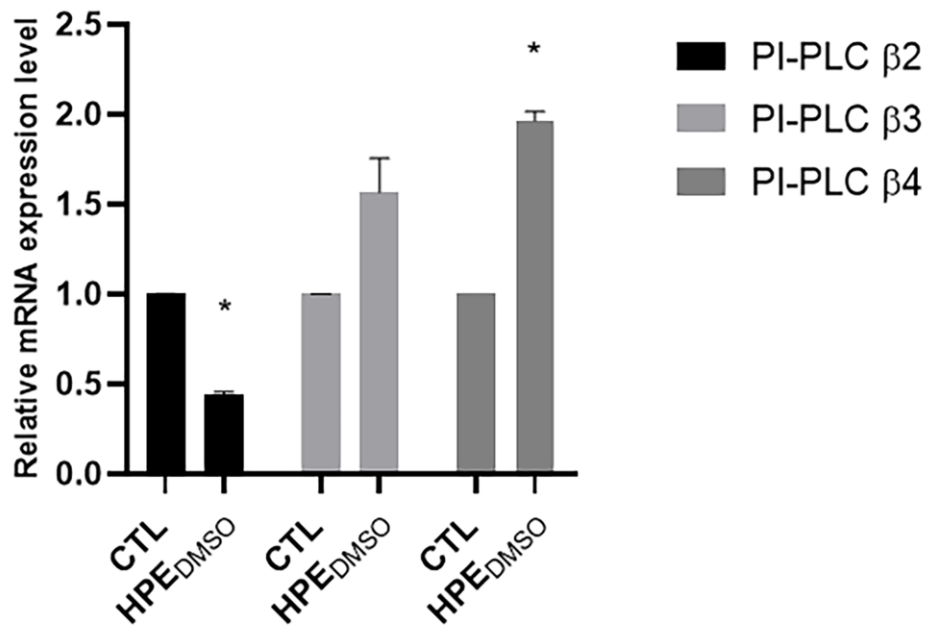
Figure 29. Effects of HPE$_{DMSO}$ on PI-PLC expressions. Cells were left untreated (-) or treated with 0.1 mg/mL HPE$_{DMSO}$ for 24 h (+), then the mRNA was extracted and analysed by semi-quantitative-PCR. All PI-PLC mRNA levels were reported as relative mRNA expression level with respect to GAPDH, as housekeeping gene. PI-PLC expression of treated samples was normalized to the untreated cells, reported as 1 and represented by a horizontal line. The densitometric analysis (bottom right) was performed by ImageJ. Results are expressed as mean ± SEM of data obtained by three independent experiments.

4.7.2 Effect of HPE$_{DMSO}$ on PI-PLC β expression

Considering our preliminary analysis results on PI-PLC β, it was decided to explore the HPE$_{DMSO}$ treatment effect on this enzyme expression, in more detailed way. At first, the extract effect on PI-PLC β2, β3 and β4 gene modulation, highlighted by the semi-quantitative-PCR experiment, was confirmed by performing a RT-PCR analysis to obtain a more accurate result. Through this experiment, it was possible to observe a statistically significant modulation of PI-PLC β2 and β4 gene expression, and a more moderate modulation of PI-PLC β3 mRNA levels (Fig.30).

Then, the HPE$_{DMSO}$ effect on PI-PLC β2, β3 and β4 was also tested at protein level by culturing FLSs in 3D performing spheroid culture for 21 days, in the presence of 0.1 mg/mL of the extract. HPE$_{DMSO}$ was able to decrease PI-PLC β2 protein level and to increase those of PI-PLC β3 and β4, as shown by immunofluorescence experiments using anti-PI-PLC β2, β3 and β4 antibodies (Fig.31). Therefore, all these results were in line with those previously obtained by PCR analysis.

Figure 30. Effects of HPE$_{DMSO}$ on PI-PLC β expressions. Cells were left untreated (CTL) or treated with 0.1 mg/mL HPE$_{DMSO}$ for 24 h and then mRNA was extracted and analysed by RT-PCR. PI-PLC β2, β3 and β4 mRNA levels were reported as relative mRNA expression level with respect to 18S rRNA ($2^{-\Delta\Delta Ct}$ method). Results are expressed as mean ± SEM of data obtained by three independent experiments. * p<0.05 vs. CTL
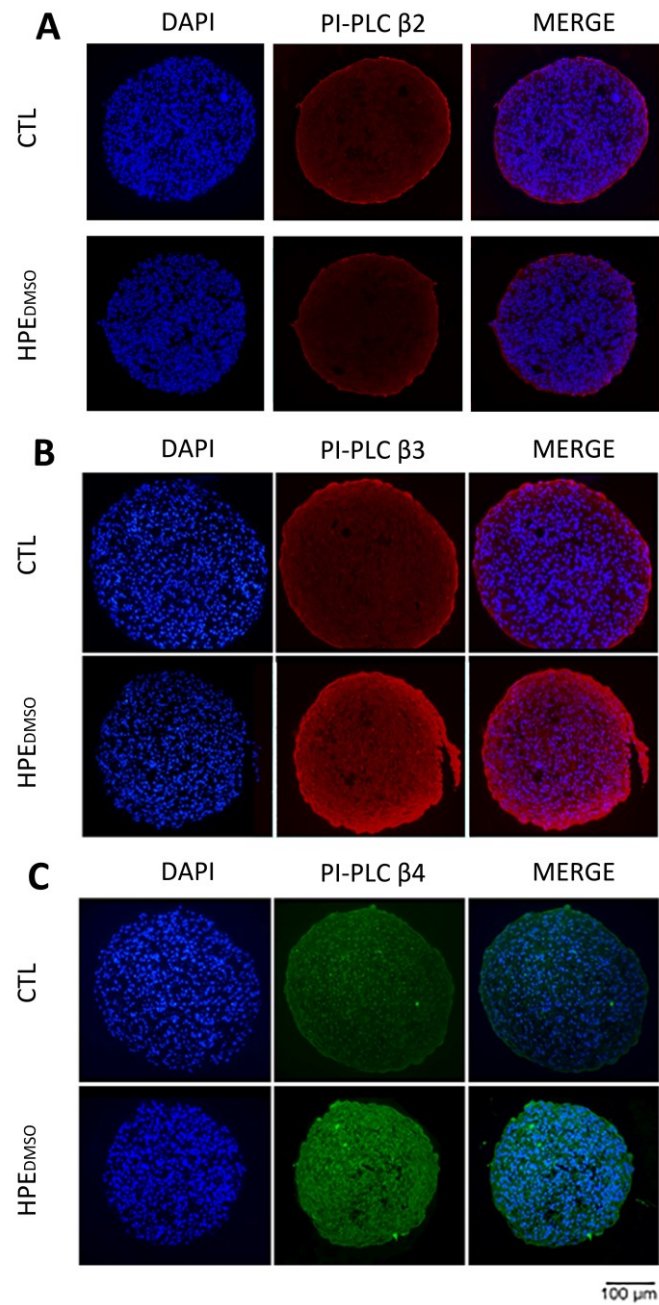
Figure 31. Effects of HPE$_{DMSO}$ extracts on PI-PLC β2, β3 and β4 protein production in 3D-cultured FLSs. Cells were treated with 0.1 mg/mL of HPE$_{DMSO}$ for 21 days and then,

116

analysed by immunofluorescence using anti-PI-PLC β2 **(A)** and β3 **(B)** primary antibody and Alexa Fluor 594 (red) secondary antibody and anti-PI-PLC β4 **(C)** primary antibody and Alexa Fluor 488 (green) secondary antibody. Nuclei were stained with DAPI (original magnification 40X). In this figure representative images from three different experiments are reported.

4.7.2.1   Effect of HPE$_{DMSO}$ on Ca^{2+} intracellular level

At the intracellular level, the change in the PI-PLC β activation affects the IP$_3$ and DAG release following the PIP$_2$ cleavage catalysed by these enzymes. DAG, which remains bound to membrane, activates the PKC, modulating a signalling pathway like that modulated by PKA. IP$_3$, a small water-soluble molecule, diffuses from the membrane through the cytosol to bind its receptor on the endoplasmic reticulum inducing the release of Ca^{2+}. Ca^{2+}, as a second messenger, activates downstream transcription factors responsible of gene modulation [92,93].

Accordingly, to further explore the HPE$_{DMSO}$ downstream effect on the PI-PLC β pathway coupled to CB2 receptors, the intracellular Ca^{2+} amount in FLSs treated was measured. Cells were treated for 20 min, 1 h and 24 h with 0.1 mg/mL HPE$_{DMSO}$ and then the fluorescence intensity was determined. The assay revealed that after 20 min HPE$_{DMSO}$ treatment was able to drastically decrease the Ca^{2+} amount. Then, it increased to nearly untreated cell level after 1 h and was stable over time (Fig.32).
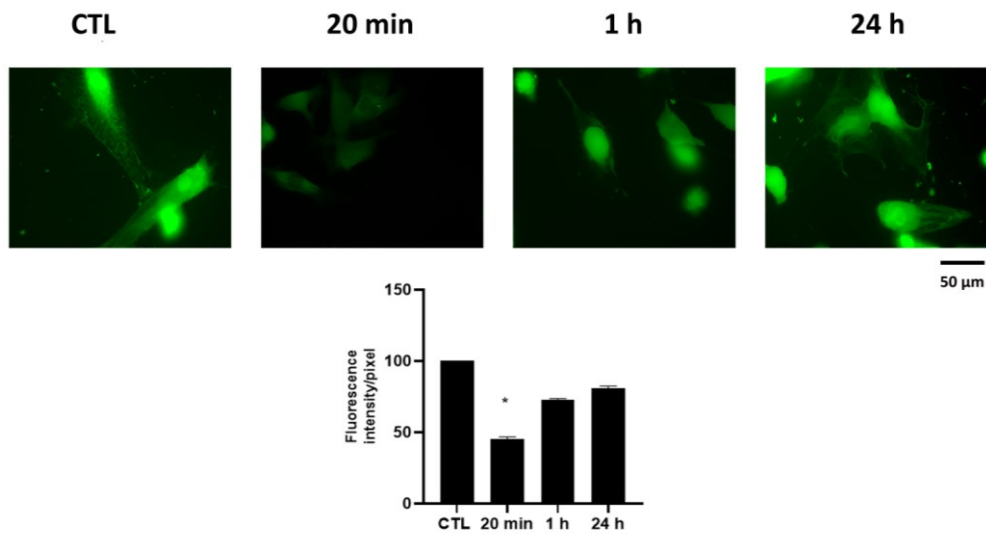
Figure 32. Effects of HPE$_{DMSO}$ on intracellular Ca^{2+} concentration. Cells were treated with 0.1 mg/mL HPE$_{DMSO}$ for 20 min, 1 h and 24 h, then the amount of intracellular Ca^{2+} concentration was measured by Calcium Green-1 AM (original magnification 40X). The densitometric analysis (bottom) was performed by ImageJ. Results are expressed as mean ± SEM of data obtained by three independent experiments. * p<0.05 vs. CTL

Although the effect on the intracellular Ca^{2+} amount was very evident, it is also difficult to explain and to correlate this decrease with the observed PI-PLC β modulation. Firstly, HPE$_{DMSO}$ was able to modulate three of the four PI-PLCs β, causing the decrease in β2 and the increase in β3 and β4 expression. Since it is not well described which of the four PI-PLC isoforms β is involved in the activation of the signalling pathway downstream CB2 receptors in synoviocytes, or alternatively if there is a cooperation between the four isoforms, it is not possible to attribute the effect precisely to one of these PI-PLCs. Secondly, while the HPE$_{DMSO}$ effect on PI-PLC β was

118

observed after 24 h of treatment, the intracellular Ca^{2+} variation was already detected after 20 min in the presence of HPE_{DMSO}. Therefore, to give an explanation to what was observed, we have made the hypothesis that the cell compensates for the ion decrease, which could be due to the rapid Ca^{2+} channel opening, restoring its concentration to almost the untreated cell level. Indeed, it is essential to consider the importance of intracellular Ca^{2+} level for both for cell metabolism and cell itself survival. However, although the HPE_{DMSO} activity on the PI-PLC β signalling pathway was evident, it was difficult to further explore each isoform involvement in the intracellular transmission and antiarthritic activity, as little is known about this from scientific literature.

Therefore, to continue the study of the phytocomplex effect on FLSs, we decided to shift the focus to the very interesting PI-PLC γ1 modulation emerged from our preliminary PCR experiment.

4.7.3 Effect of HPE_{DMSO} on PI-PLC γ expression

While the PI-PLC β isoforms are activated following the stimulation of GPCR receptors, PI-PLC γ1 and γ2 are coupled with RTK receptors. Consequently, they are directly activated by tyrosine phosphorylation in response to a wide variety of extracellular stimuli. Once phosphorylated, PI-PLC γ1 and γ2 control numerous aspects of cell metabolism including the development of the vascular, neuronal, and immune systems during the embryogenesis, adaptive immune responses, neuronal transmission, bone homeostasis, chemotaxis, and platelet aggregation, playing a fundamental role in several human diseases [226].

As a result, whereas they are linked to RTK receptors, the HPE_{DMSO} effect on these enzymes should not be described as a consequence of the extract agonism on CB2 receptors. However, although not attributable to this pathway, our preliminary gene modulation experiment showed an HPE_{DMSO} effect on PI-PLC γ1 expression. Interestingly, by analysing both untreated and treated cDNA samples in PCR reactions with a pair of forward-reverse primers, specific for the PI-PLC γ1 gene, two different bands in each sample were obtained (Fig.29 and 33).
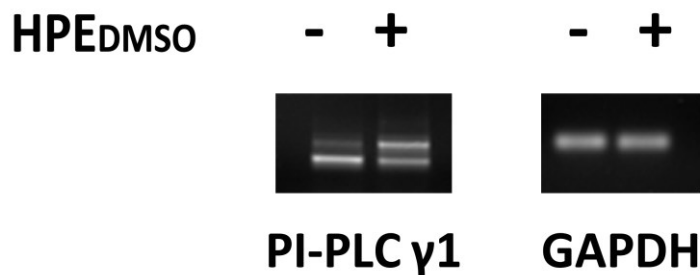
Figure 33. Effects of HPE_{DMSO} on PI-PLC γ1 expression. Cells were left untreated (-) or treated with 0.1 mg/mL HPE_{DMSO} for 24 h (+) and then the mRNA was extracted and analysed by semi-quantitative-PCR. PI-PLC γ1 mRNA level was reported as relative mRNA expression level with respect to GAPDH, as housekeeping gene.

The primer pair was designed in our laboratory by placing them on different exons of the PI-PLC γ1 gene sequence to obtain a PCR product of about 300 bp. However, the electrophoresis gel, in addition to this expected PCR product, revealed an additional band of about 500 bp in both samples. The surprising result emerged from this experiment concerned the HPE_{DMSO}

120

ability to modulate the expression of the two PCR products. While in the untreated sample the 300 bp product was the most expressed, the HPE$_{DMSO}$ treatment induced a decrease in this product expression, increasing that of the product with more base pairs.

Excluding possible contamination by genomic DNA, in order to investigate this unexpected product formation, the PCR product was purified from the agarose gel and sequenced by Sanger method at Bio-Fab research laboratories. The gene sequencing analysis provided a 500 bp sequence perfectly overlapping with a Homo sapiens PI-PLC γ1 complete coding sequence (NCBI accession number: DQ297143.1) region. This region consisted of both protein encoding exons and non-coding introns. Surprisingly, by removing the introns from this analysed region, a fragment 300 bp long corresponding to our smaller PCR product was obtained (Fig.34). In light of these findings, HPE$_{DMSO}$ treatment was able to reduce, but not to completely inhibit, the splicing process in this analysed region of the PI-PLC γ1 gene.

Figure 34. Schematic representation of the two PCR products obtained from PI-PLC γ1 analysis.

However, studies describing the *H. procumbens* ability to interfere with the splicing process were not available in scientific literature. Moreover, also considering that many enzymes and factors are involved in the process, it was very difficult to understand the inhibition mechanism of the extract.

An accurate analysis of the PI-PLC γ1 gene has been carried out by the Human and Vertebrate Analysis and Annotation (HAVANA) group at the Wellcome Trust Sanger Institute (Cambridge, UK) and published on the Ensembl database [227]. Performing the gene sequence analysis, they identified some intron complete retention, which were not eliminated during mRNA maturation. More specifically, their analyses showed that not all the introns were retained, but those retained were only 16, located in 5 different regions of the gene sequence. The 5 alternative transcripts obtained from intron retention were respectively named by the HAVANA group as PLCG1-212, PLCG1-207, PLCG1-205, PLCG1-208 and PLCG1-204 (Fig.35). For this reason, in our study we decided to use these names to indicate the gene sequence regions where the intron retention phenomenon was described.
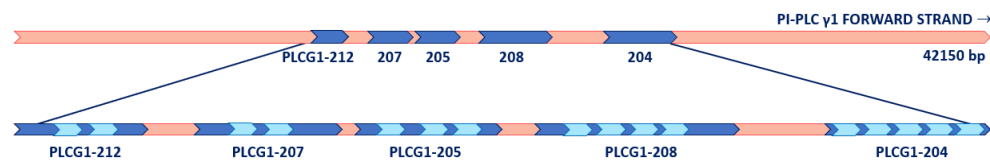
Figure 35. Schematic representation of the 5 different regions (in blue) of the PI-PLC γ1 gene sequence where introns (in light blue) are retained [227].

By comparing these analyses to our previous PCR and Sanger sequencing results, we verified that the introns that were retained in our experimental

conditions were also described by the HAVANA group as corresponding to the PLCG1-207 region.

Taking these findings into account, it was decided to deepen the the investigation of the HPE_{DMSO} effect on intron retention in PI-PLC γ1 gene. Therefore, its ability to interfere with the splicing process of the other retained introns described by the HAVANA group was evaluated. To perform these analyses, primer pairs with the primer forward on the intron and the primer reverse on the adjacent exon were designed in our laboratory. Then, RT-PCR experiments were performed on cDNA samples of both untreated and 0.1 mg/mL HPE_{DMSO} treated FLSs. These experiments revealed that HPE_{DMSO} was able to interfere with PI-PLC γ1 splicing process by increasing the retention of introns described on Ensembl database (Fig.36). In contrast, splicing was not inhibited in other regions of the gene sequence where the intron retention phenomenon was not detected by the HAVANA group (data not shown).
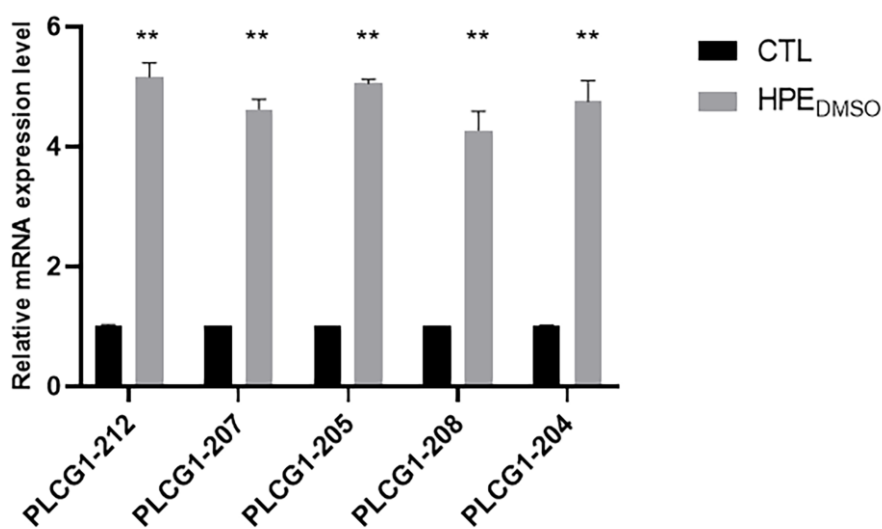
Figure 36. Effects of HPE$_{DMSO}$ on PI-PLC γ1 intron retention. Cells were left untreated (CTL) or treated with 0.1 mg/mL HPE$_{DMSO}$ for 24 h and then mRNA was extracted and analysed by RT-PCR. PLCG1-212, 207, 205, 208 and 204 mRNA levels were reported as relative mRNA expression level with respect to 18S mRNA (2$^{-\Delta\Delta Ct}$ method). Results are expressed as mean ± SEM of data obtained by three independent experiments. ** $p < 0.01$ vs CTL.

As described in the Ensembl database, the splicing process inhibition in PI-PLC γ1 ultimately results in protein not being translated, due to stop codons insertion inside the mRNA sequence. By analysing the PI-PLC γ1 gene sequence, indeed, a stop codon was found within an intron in the PLCG1-212 region. Consequently, to confirm the intron retention effect on protein translation, an immunofluorescence experiment was carried out. FLSs were treated for 24 h with 0.1 mg/mL HPE$_{DMSO}$ and then stained with anti-PI-PLC γ1 primary antibody. As expected, in HPE$_{DMSO}$ treated sample the PI-PLC γ1 protein expression was significantly reduced (Fig.37).
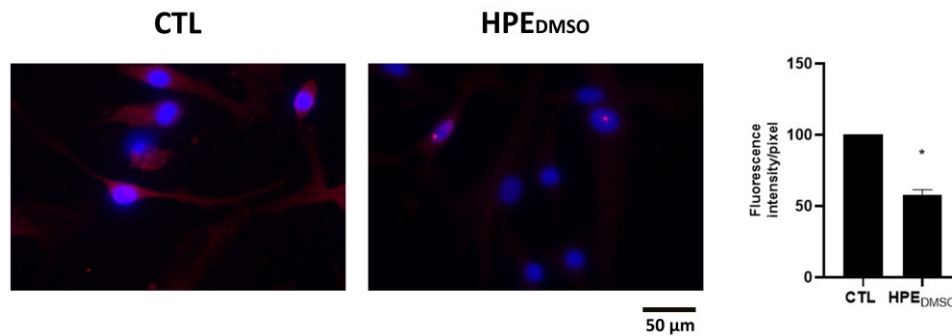
Figure 37. Effects of HPE$_{DMSO}$ on PI-PLC γ1 expression. Cells were treated with 0.1 mg/mL HPE$_{DMSO}$ for 24 h and then analysed by immunofluorescence using anti-PI-PLC γ1 primary antibody and Alexa Fluor 594 (red) secondary antibody. Nuclei were stained with DAPI (original magnification 40X). The graph represents the pixel intensities in the region of interest, obtained by ImageJ. * $p < 0.05$ vs CTL. In this figure representative images from three different experiments are reported.

4.7.4 The inter-individual variability of HPE$_{DMSO}$ effect on PI-PLC γ1 expression

During these analyses on PI-PLC γ1 gene, several human primary FLSs samples isolated from different OA patients were treated, in order to better understand the HPE$_{DMSO}$ effects. This allowed to demonstrate that samples from different patients had diverse treatment responses with regard to the phenomenon of intron retention. Indeed, it has been observed that only in approximately 37% of the HPE$_{DMSO}$ treated samples the intron retention phenomenon occurred, while in the remaining part of the samples no modulation was observed. However, as the mechanism by which the extract inhibited the splicing process was not clear enough, similarly we have not

125

been able to understand what mentioned inter-individual variability depends on. Interestingly, the PCR analyses showed that although PI-PLC γ1 intron retention was markedly evidenced in some FLS samples after HPE$_{DMSO}$ treatment, the same FLS samples showed intron retention also in the untreated condition, even if to a lesser extent. This was evidenced by the presence of two bands in the electrophoresis gel both in the untreated and in the HPE$_{DMSO}$ treated sample. In the latter, however, as a result of stimulated intron retention, an increase in 500 bp band expression was observed. Conversely, in samples where only a single band of about 300 bp was obtained, intron retention phenomenon was not stimulated following HPE$_{DMSO}$ treatment (Fig.38A). This result, obtained by both PCR and RT-PCR experiments, was in line with the lack of modulation of PI-PLC γ1 protein expression observed by immunofluorescence analysis (Fig.38B).
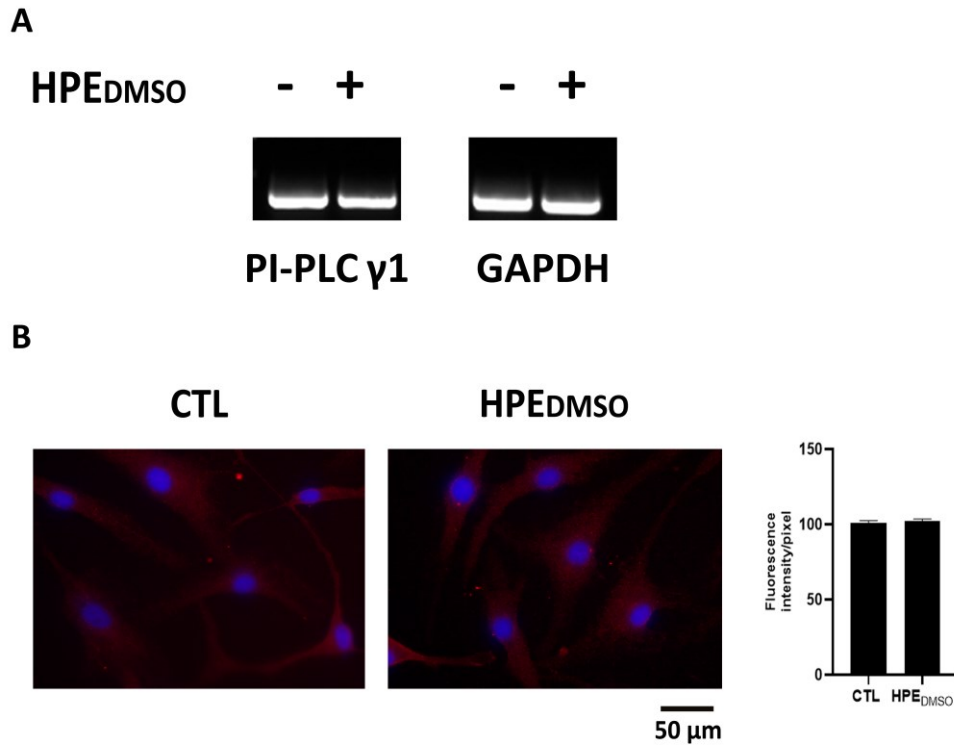
Figure 38. Effects of HPE$_{DMSO}$ on PI-PLC γ1 expression. **A:** Cells were left untreated (-) or treated with 0.1 mg/mL HPE$_{DMSO}$ for 24 h (+) and then the mRNA was extracted and analysed by semi-quantitative-PCR. PI-PLC γ1 mRNA level was reported as relative mRNA expression level with respect to GAPDH, as housekeeping gene **B:** Cells were treated as described in **A** and then analysed by immunofluorescence using anti-PI-PLC γ1 primary antibody and Alexa Fluor 594 (red) secondary antibody. Nuclei were stained with DAPI (original magnification 40X). The graph represents the pixel intensities in the region of interest, obtained by ImageJ. In this figure representative images from three different experiments are reported.

4.7.4.1 The inter-individual variability effect on MMP and ADAMTS expression following HPE$_{DMSO}$ treatment

Although the mechanism by which HPE$_{DMSO}$ stimulates the intron retention in the PI-PLC γ1 gene has not been understood, the effect on the protein expression decrease is very interesting at the metabolic level.

Many studies have analysed the PI-PLC γ1 role in OA pathogenesis for its involvement in the synthesis and release of extracellular matrix degrading enzymes. Among these, particular attention was paid to the MMP enzymes, whose gene expression and extracellular release is modulated by the PI-PLC γ1 through a mechanism involving PKC [228–232].

This evidence led us to consider more carefully some data obtained in our previous experiments on MMP and ADAMTS production. By analysing the HPE$_{DMSO}$ effect on several human primary FLS samples from OA patients as a result of ERK1/2 inhibition, a different response to the treatment was highlighted depending on the cell sample. While, as described above, in some samples HPE$_{DMSO}$ was able to inhibit MMP-3, MMP-13 and ADAMTS-5 gene expression and MMP-13 release, in other samples it was quite totally ineffective. Considering the PI-PLC γ1 downstream effect on MMPs described in literature, we speculated a link on the inter-individual variability of PI-PLC γ1 gene modulation and the lack of effect on these degrading enzymes in some FLS samples. Surprisingly, comparing the FLS samples analysed for these different experiments, it was shown that HPE$_{DMSO}$ was ineffective in inhibiting the MMP-3, MMP-13 and ADAMTS-5 gene expression and MMP-13 release precisely in those samples where the PI-PLC γ1 protein expression was not reduced for the absence of the intron retention phenomenon. Only a slight modulation in MMP-13 protein release was

observed in treated FLSs for 48 h and 72 h in presence of 0.1 mg/mL HPE$_{DMSO}$, but still not statistically significant (Fig.39). These results strongly suggested that the reduction of PI-PLC γ1 protein level was responsible for the MMP and ADAMTS-5 gene expression decrease, described above (Fig.24).
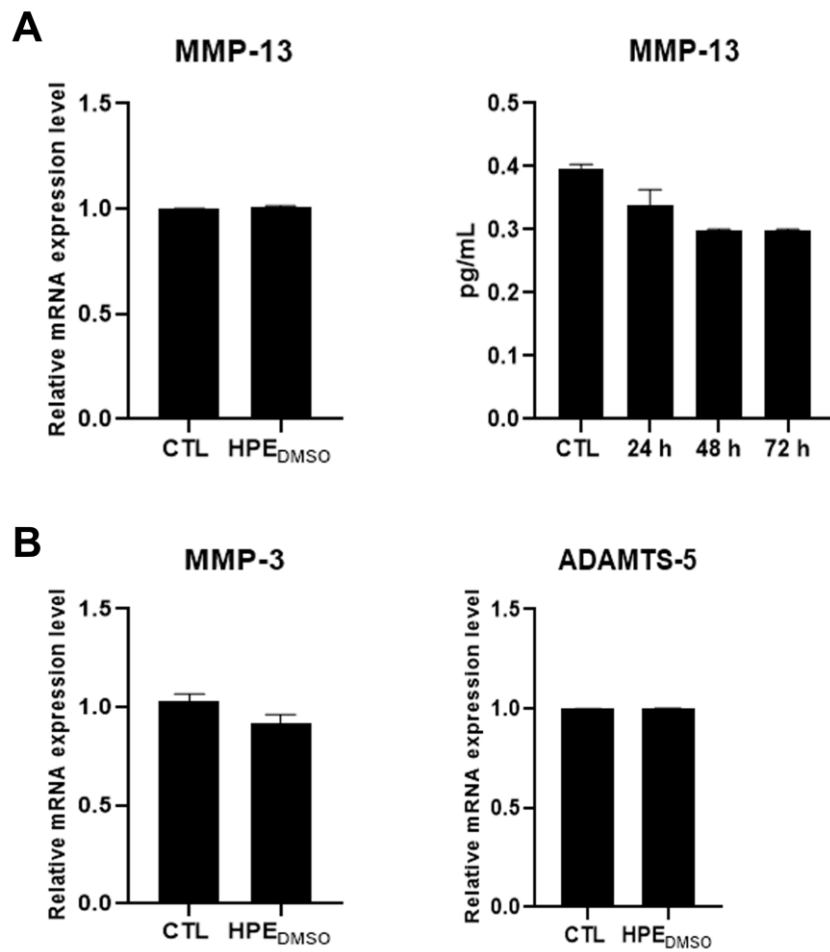
Figure 39. Effects of HPE$_{DMSO}$ on the production of degrading enzymes. Cells were treated with 0.1 mg/mL HPE$_{DMSO}$ for 24 h and then the mRNA was extracted and analysed by RT-PCR. **A, left graph:** MMP-13 mRNA level was reported as relative mRNA expression level with respect to 18S mRNA ($2^{-\Delta\Delta Ct}$ method). **B:** MMP-3 and ADAMTS-5 mRNA level was reported as relative mRNA expression level with respect to 18S mRNA ($2^{-\Delta\Delta Ct}$ method). **A, right graph:** The amount of MMP-13 produced was measured in the culture medium of cells treated with 0.1 mg/mL HPE$_{DMSO}$ for 24 h, 48 h and 72 h and analysed by ELISA. The results are reported as pg/mL. Results are expressed as mean ± SEM of data obtained by three independent experiments.

130

5. Conclusions
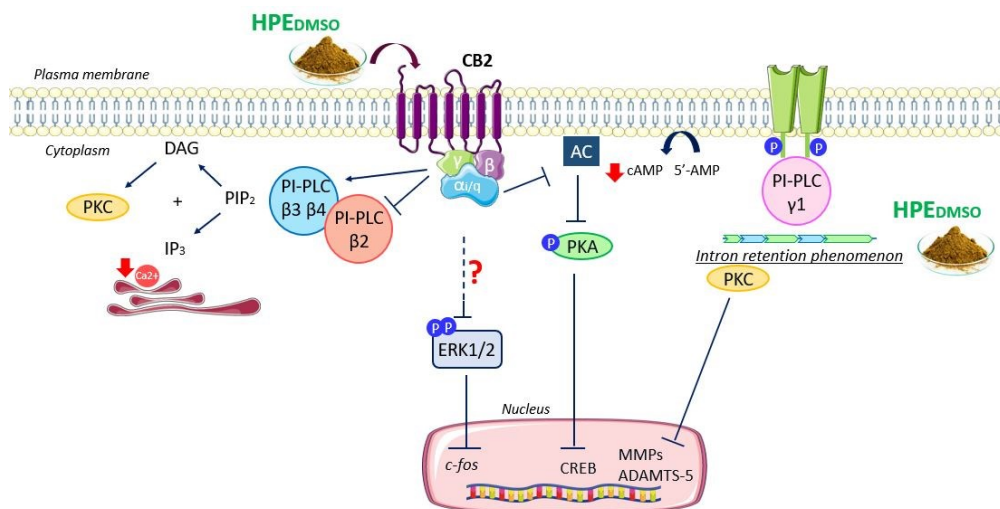
Figure 40. Schematic representation of metabolic pathways modulated by HPE$_{DMSO}$ in FLSs resulting from this study.

During the last decades, *Harpagophytum procumbens* has been one of the most used herbal drugs as a natural remedy for joint diseases. However, although its therapeutic properties were well known, the biochemical mechanisms at the cellular level responsible for its pharmacological effects had not been described yet. For this reason, the purpose of this study was to explore the HPE activity on metabolic pathways involved in inflammation and nociceptive transmission, in order to understand the biochemical processes downstream of the known therapeutic effects.

Summarizing, our analysis showed a triple HPE antiarthritic effect. Firstly, this extract has been able to modulate the pathway downstream of CB2

receptors involved in the nociceptive stimulus. Secondly, it has proven to counteract the pro-inflammatory process acting on ERK1/2 activation and on interleukin expression. Lastly, it has established a possible chondroprotective role reducing the production of extracellular matrix degrading enzymes (Fig.40). Besides, the results obtained from experiments with single bioactive molecules also highlighted the phytocomplex role in these antiarthritic effects. Indeed, the synergistic and cooperative interactions between several molecules in the whole extract contributed to the demonstrated therapeutic effect [233,234].

However, the most surprising result obtained, which deserves to be deepen investigated in the coming months, concerns the HPE_{DMSO} effect on the intron retention phenomenon in PI-PLC γ1 gene. This phenomenon, although subject to an inter-individual variability, was found to be responsible for the downstream effect on the modulation of extracellular matrix degrading enzymes (Fig.40), confirming once again the *H. procumbens* antiarthritic activity.

References

1.   Robinson, W.H.; Lepus, C.M.; Wang, Q.; Raghu, H.; Mao, R.; Lindstrom, T.M.; Sokolove, J. Low-grade inflammation as a key mediator of the pathogenesis of osteoarthritis. *Nat. Rev. Rheumatol.* **2016**, *12*, 580–592, doi:10.1038/nrrheum.2016.136.

2.   Miehle, W. Arthrosis or osteoarthritis: Do these terms imply therapy with pure analgesics or non-steroidal antirheumatic agents? *Scand. J. Rheumatol.* **1987**, *16*, 123–130, doi:10.3109/03009748709102190.

3.   Chen, L.; Yu, Y. Exercise and Osteoarthritis. In *Advances in Experimental Medicine and Biology*; 2020; Vol. 1228, pp. 219–231.

4.   Hame, S.L.; Alexander, R.A. Knee osteoarthritis in women. *Curr. Rev. Musculoskelet. Med.* **2013**, *6*, 182–187, doi:10.1007/s12178-013-9164-0.

5.   O'Neill, T.W.; Felson, D.T. Mechanisms of Osteoarthritis (OA) Pain. *Curr. Osteoporos. Rep.* **2018**, *16*, 611–616, doi:10.1007/s11914-018-0477-1.

6.   Puig-Junoy, J.; Ruiz Zamora, A. Socio-economic costs of osteoarthritis: A systematic review of cost-of-illness studies. *Semin. Arthritis Rheum.* **2015**, *44*, 531–541, doi:10.1016/j.semarthrit.2014.10.012.

7.   He, Y.; Li, Z.; Alexander, P.G.; Ocasio-Nieves, B.D.; Yocum, L.; Lin, H.; Tuan, R.S. Pathogenesis of Osteoarthritis: Risk Factors, Regulatory Pathways in Chondrocytes, and Experimental Models. *Biology (Basel).* **2020**, *9*, 194, doi:10.3390/biology9080194.

8.   Man, G.S.; Mologhianu, G. Osteoarthritis pathogenesis - a complex

process that involves the entire joint. *J. Med. Life* **2014**, *7*, 37–41.

9. Xia, B.; Di Chen; Zhang, J.; Hu, S.; Jin, H.; Tong, P. Osteoarthritis Pathogenesis: A Review of Molecular Mechanisms. *Calcif. Tissue Int.* **2014**, *95*, 495–505, doi:10.1007/s00223-014-9917-9.

10. Standring, S. *Gray's Anatomy 40th edition*; 2008; ISBN ISBN: 9780443066849.

11. Baker, G.F.; Tortora, G.J.; Nostakos, N.P.A. Principles of Anatomy and Physiology. *Am. J. Nurs.* **1976**, *76*, 477, doi:10.2307/3423898.

12. GOSS, C.M. GARY'S ANATOMY OF THE HUMAN BODY. *Am. J. Med. Sci.* **1967**, *253*, 510, doi:10.1097/00000441-196704000-00048.

13. Osburn, W.D.G.A. Anatomy of the Human Body. *South. Med. J.* **1925**, *18*, 485, doi:10.1097/00007611-192506000-00042.

14. Tarafder, S.; Lee, C.H. Synovial Joint. In *In Situ Tissue Regeneration*; Elsevier, 2016; pp. 253–273.

15. Lawry, G. V.; Bewyer, D. Anatomy of joints, general considerations, and principles of joint examination. In *Fam's Musculoskeletal Examination and Joint Injection Techniques: Second Edition*; 2010.

16. Firestein S, G. et al. *FIRESTEIN & KELLEY'S TEXTBOOK OF RHEUMATOLOGY, ELEVENTH EDITION*; 2021;

17. Carballo, C.B.; Nakagawa, Y.; Sekiya, I.; Rodeo, S.A. Basic Science of Articular Cartilage. *Clin. Sports Med.* **2017**, *36*, 413–425, doi:10.1016/j.csm.2017.02.001.

18. Khajehsaeid, H.; Abdollahpour, Z.; Farahmandpour, H. Effect of Degradation and Osteoarthritis on the Viscoelastic Properties of Human Knee Articular Cartilage: An Experimental Study and Constitutive Modeling. *Biomechanics* **2021**, *1*, 225–238,

doi:10.3390/biomechanics1020019.

19.   Armiento, A.R.; Stoddart, M.J.; Alini, M.; Eglin, D. Biomaterials for articular cartilage tissue engineering: Learning from biology. *Acta Biomater.* **2018**, *65*, 1–20, doi:10.1016/j.actbio.2017.11.021.

20.   Chaumel, J.; Schotte, M.; Bizzarro, J.J.; Zaslansky, P.; Fratzl, P.; Baum, D.; Dean, M.N. Co-aligned chondrocytes: Zonal morphological variation and structured arrangement of cell lacunae in tessellated cartilage. *Bone* **2020**, *134*, 115264, doi:10.1016/j.bone.2020.115264.

21.   Akkiraju, H.; Nohe, A. Role of Chondrocytes in Cartilage Formation, Progression of Osteoarthritis and Cartilage Regeneration. *J. Dev. Biol.* **2015**, *3*, 177–192, doi:10.3390/jdb3040177.

22.   Aigner, T.; Söder, S.; Gebhard, P.M.; McAlinden, A.; Haag, J. Mechanisms of Disease: role of chondrocytes in the pathogenesis of osteoarthritis—structure, chaos and senescence. *Nat. Clin. Pract. Rheumatol.* **2007**, *3*, 391–399, doi:10.1038/ncprheum0534.

23.   Westacott, C.I.; Webb, G.R.; Warnock, M.G.; Sims, J. V.; Elson, C.J. Alteration of cartilage metabolism by cells from osteoarthritic bone. *Arthritis Rheum.* **1997**, *40*, 1282–1291, doi:10.1002/1529-0131(199707)40:7<1282::AID-ART13>3.0.CO;2-E.

24.   Goldring, M.B.; Otero, M.; Tsuchimochi, K.; Ijiri, K.; Li, Y. Defining the roles of inflammatory and anabolic cytokines in cartilage metabolism. *Ann. Rheum. Dis.* **2008**, *67*, iii75–iii82, doi:10.1136/ard.2008.098764.

25.   D. Smith, M. The Normal Synovium. *Open Rheumatol. J.* **2011**, *5*, 100–106, doi:10.2174/1874312901105010100.

26.   Macchi, V.; Stocco, E.; Stecco, C.; Belluzzi, E.; Favero, M.;

Porzionato, A.; De Caro, R. The infrapatellar fat pad and the synovial membrane: an anatomo-functional unit. *J. Anat.* **2018**, *233*, 146–154, doi:10.1111/joa.12820.

27. Iwanaga, T.; Shikichi, M.; Kitamura, H.; Yanase, H.; Nozawa-Inoue, K. Morphology and Functional Roles of Synoviocytes in the Joint. *Arch. Histol. Cytol.* **2005**, doi:10.1679/aohc.63.17.

28. Kleine, S.A.; Budsberg, S.C. Synovial membrane receptors as therapeutic targets: A review of receptor localization, structure, and function. *J. Orthop. Res.* **2017**, *35*, 1589–1605, doi:10.1002/jor.23568.

29. Barland, P.; Novikoff, A.B.; Hamerman, D. Electron microscopy of the human synovial membrane. *J. Cell Biol.* **1962**, *14*, 207–220, doi:10.1083/jcb.14.2.207.

30. Graabı̆k, P.M. Ultrastructural evidence for two distinct types of synoviocytes in rat synovial membrane. *J. Ultrastruct. Res.* **1982**, *78*, 321–339, doi:10.1016/S0022-5320(82)80006-3.

31. Graabaek, P.M. Characteristics of the two types of synoviocytes in rat synovial membrane. An ultrastructural study. *Lab. Investig.* **1984**, *50*.

32. Kennedy, A.; Fearon, U.; Veale, D.J.; Godson, C. Macrophages in Synovial Inflammation. *Front. Immunol.* **2011**, *2*, doi:10.3389/fimmu.2011.00052.

33. Kurowska-Stolarska, M.; Alivernini, S. Synovial tissue macrophages: Friend or foe? *RMD Open* 2017, *3*.

34. Zvaifler, N.J. Macrophages and the Synovial Lining. *Scand. J. Rheumatol.* **1995**, *24*, 67–75, doi:10.3109/03009749509100904.

35. Li, F.; Tang, Y.; Song, B.; Yu, M.; Li, Q.; Zhang, C.; Hou, J.; Yang, R. Nomenclature clarification: Synovial fibroblasts and synovial

mesenchymal stem cells. *Stem Cell Res. Ther.* **2019**, *10*, 260, doi:10.1186/s13287-019-1359-x.

36.   Bartok, B.; Firestein, G.S. Fibroblast-like synoviocytes: key effector cells in rheumatoid arthritis. *Immunol. Rev.* **2010**, *233*, 233–255, doi:10.1111/j.0105-2896.2009.00859.x.

37.   Frisbie, D.D.; Johnson, S.A. Synovial Joint Biology and Pathobiology. In *Equine Surgery*; Elsevier, 2019; pp. 1326–1348.

38.   Wang, X.; Hunter, D.J.; Jin, X.; Ding, C. The importance of synovial inflammation in osteoarthritis: current evidence from imaging assessments and clinical trials. *Osteoarthr. Cartil.* **2018**, *26*, 165–174, doi:10.1016/j.joca.2017.11.015.

39.   Van Der Helm-Van Mil, A.H.M.; Huizinga, T.W.J. Early Synovitis and Early Undifferentiated Arthritis. In *Kelley and Firestein's Textbook of Rheumatology*; Elsevier, 2017; pp. 1213–1220.

40.   Mathiessen, A.; Conaghan, P.G. Synovitis in osteoarthritis: current understanding with therapeutic implications. *Arthritis Res. Ther.* **2017**, *19*, 18, doi:10.1186/s13075-017-1229-9.

41.   Prieto-Potin, I.; Largo, R.; Roman-Blas, J.A.; Herrero-Beaumont, G.; Walsh, D.A. Characterization of multinucleated giant cells in synovium and subchondral bone in knee osteoarthritis and rheumatoid arthritis. *BMC Musculoskelet. Disord.* **2015**, *16*, 226, doi:10.1186/s12891-015-0664-5.

42.   Farinelli, L.; Aquili, A.; Mattioli-Belmonte, M.; Manzotti, S.; D'Angelo, F.; Ciccullo, C.; Gigante, A. Synovial mast cells from knee and hip osteoarthritis: histological study and clinical correlations. *J. Exp. Orthop.* **2022**, *9*, 13, doi:10.1186/s40634-022-00446-2.

43. Tsuneyoshi, Y.; Tanaka, M.; Nagai, T.; Sunahara, N.; Matsuda, T.; Sonoda, T.; Ijiri, K.; Komiya, S.; Matsuyama, T. Functional folate receptor beta-expressing macrophages in osteoarthritis synovium and their M1/M2 expression profiles. *Scand. J. Rheumatol.* **2012**, *41*, 132–140, doi:10.3109/03009742.2011.605391.

44. Bondeson, J.; Wainwright, S.D.; Lauder, S.; Amos, N.; Hughes, C.E. The role of synovial macrophages and macrophage-produced cytokines in driving aggrecanases, matrix metalloproteinases, and other destructive and inflammatory responses in osteoarthritis. *Arthritis Res. Ther.* **2006**, *8*, doi:10.1186/ar2099.

45. Wu, C.-L.; Harasymowicz, N.S.; Klimak, M.A.; Collins, K.H.; Guilak, F. The role of macrophages in osteoarthritis and cartilage repair. *Osteoarthr. Cartil.* **2020**, *28*, 544–554, doi:10.1016/j.joca.2019.12.007.

46. Thomson, A.; Hilkens, C.M.U. Synovial Macrophages in Osteoarthritis: The Key to Understanding Pathogenesis? *Front. Immunol.* **2021**, *12*, doi:10.3389/fimmu.2021.678757.

47. Blom, A.B.; van Lent, P.L.; Libregts, S.; Holthuysen, A.E.; van der Kraan, P.M.; van Rooijen, N.; van den Berg, W.B. Crucial role of macrophages in matrix metalloproteinase–mediated cartilage destruction during experimental osteoarthritis : Involvement of matrix metalloproteinase 3. *Arthritis Rheum.* **2007**, *56*, 147–157, doi:10.1002/art.22337.

48. Han, D.; Fang, Y.; Tan, X.; Jiang, H.; Gong, X.; Wang, X.; Hong, W.; Tu, J.; Wei, W. The emerging role of fibroblast-like synoviocytes-mediated synovitis in osteoarthritis: An update. *J. Cell.*

Mol. Med. **2020**, *24*, 9518–9532, doi:10.1111/jcmm.15669.

49. Hu, Q.; Ecker, M. Overview of MMP-13 as a Promising Target for the Treatment of Osteoarthritis. *Int. J. Mol. Sci.* **2021**, *22*, 1742, doi:10.3390/ijms22041742.

50. Monemdjou, R.; Fahmi, H.; Kapoor, M. Synovium in the pathophysiology of osteoarthritis. *Therapy* 2010, *7*.

51. Mobasheri, A.; Batt, M. An update on the pathophysiology of osteoarthritis. *Ann. Phys. Rehabil. Med.* **2016**, *59*, 333–339, doi:10.1016/j.rehab.2016.07.004.

52. Murphy, G. What are the roles of metalloproteinases in cartilage and bone damage? *Ann. Rheum. Dis.* **2005**, *64*, iv44–iv47, doi:10.1136/ard.2005.042465.

53. Carlson, A.K.; Rawle, R.A.; Wallace, C.W.; Brooks, E.G.; Adams, E.; Greenwood, M.C.; Olmer, M.; Lotz, M.K.; Bothner, B.; June, R.K. Characterization of synovial fluid metabolomic phenotypes of cartilage morphological changes associated with osteoarthritis. *Osteoarthr. Cartil.* **2019**, *27*, 1174–1184, doi:10.1016/j.joca.2019.04.007.

54. Timur, U.T.; Jahr, H.; Anderson, J.; Green, D.C.; Emans, P.J.; Smagul, A.; van Rhijn, L.W.; Peffers, M.J.; Welting, T.J.M. Identification of tissue-dependent proteins in knee OA synovial fluid. *Osteoarthr. Cartil.* **2021**, *29*, doi:10.1016/j.joca.2020.09.005.

55. Rezende, M.U. de; Campos, G.C. de Is osteoarthritis a mechanical or inflammatory disease? *Rev. Bras. Ortop.* **2013**, *48*, 471–474, doi:10.1016/j.rbo.2013.03.003.

56. Scanzello, C.R. Role of low-grade inflammation in osteoarthritis.

Curr. Opin. Rheumatol. **2017**, *29*, 79–85, doi:10.1097/BOR.0000000000000353.

57. Barreto, G.; Manninen, M.; K. Eklund, K. Osteoarthritis and Toll-Like Receptors: When Innate Immunity Meets Chondrocyte Apoptosis. *Biology (Basel).* **2020**, *9*, 65, doi:10.3390/biology9040065.

58. Foell, D.; Wittkowski, H.; Roth, J. Mechanisms of Disease: a "DAMP" view of inflammatory arthritis. *Nat. Clin. Pract. Rheumatol.* **2007**, *3*, 382–390, doi:10.1038/ncprheum0531.

59. Miller, R.J.; Malfait, A.-M.; Miller, R.E. The innate immune response as a mediator of osteoarthritis pain. *Osteoarthr. Cartil.* **2020**, *28*, 562–571, doi:10.1016/j.joca.2019.11.006.

60. Sen, R.; Baltimore, D. Inducibility of κ immunoglobulin enhancer-binding protein NF-κB by a posttranslational mechanism. *Cell* **1986**, doi:10.1016/0092-8674(86)90807-X.

61. Liu, T.; Zhang, L.; Joo, D.; Sun, S.-C. NF-κB signaling in inflammation. *Signal Transduct. Target. Ther.* **2017**, *2*, 17023, doi:10.1038/sigtrans.2017.23.

62. Rigoglou, S.; Papavassiliou, A.G. The NF-κB signalling pathway in osteoarthritis. *Int. J. Biochem. Cell Biol.* **2013**, *45*, 2580–2584, doi:10.1016/j.biocel.2013.08.018.

63. Choi; Jo; Park; Kang; Park NF-kB Signaling Pathways in Osteoarthritic Cartilage Destruction. *Cells* **2019**, *8*, 734, doi:10.3390/cells8070734.

64. Bonizzi, G.; Karin, M. The two NF-κB activation pathways and their role in innate and adaptive immunity. *Trends Immunol.* **2004**, *25*, 280–288, doi:10.1016/j.it.2004.03.008.

65. Israel, A. The IKK Complex, a Central Regulator of NF-kB Activation. *Cold Spring Harb. Perspect. Biol.* **2010**, *2*, a000158–a000158, doi:10.1101/cshperspect.a000158.

66. Karin, M. How NF-κB is activated: the role of the IκB kinase (IKK) complex. *Oncogene* **1999**, *18*, 6867–6874, doi:10.1038/sj.onc.1203219.

67. Nelson, D.E.; Ihekwaba, A.E.C.; Elliott, M.; Johnson, J.R.; Gibney, C.A.; Foreman, B.E.; Nelson, G.; See, V.; Horton, C.A.; Spiller, D.G.; et al. Oscillations in NF-κB Signaling Control the Dynamics of Gene Expression. *Science (80-.).* **2004**, *306*, 704–708, doi:10.1126/science.1099962.

68. Yamamoto, Y.; Gaynor, R. Role of the NF-kB Pathway in the Pathogenesis of Human Disease States. *Curr. Mol. Med.* **2001**, *1*, 287–296, doi:10.2174/1566524013363816.

69. Hoesel, B.; Schmid, J.A. The complexity of NF-κB signaling in inflammation and cancer. *Mol. Cancer* **2013**, *12*, 86, doi:10.1186/1476-4598-12-86.

70. Soares-Silva, M.; Diniz, F.F.; Gomes, G.N.; Bahia, D. The Mitogen-Activated Protein Kinase (MAPK) Pathway: Role in Immune Evasion by Trypanosomatids. *Front. Microbiol.* **2016**, *7*, doi:10.3389/fmicb.2016.00183.

71. Morrison, D.K. MAP Kinase Pathways. *Cold Spring Harb. Perspect. Biol.* **2012**, *4*, a011254–a011254, doi:10.1101/cshperspect.a011254.

72. Loeser, R.F.; Erickson, E.A.; Long, D.L. Mitogen-activated protein kinases as therapeutic targets in osteoarthritis. *Curr. Opin. Rheumatol.* **2008**, *20*, 581–586, doi:10.1097/BOR.0b013e3283090463.

73.	Kyriakis, J.M.; Avruch, J. Mammalian MAPK Signal Transduction Pathways Activated by Stress and Inflammation: A 10-Year Update. *Physiol. Rev.* **2012**, *92*, 689–737, doi:10.1152/physrev.00028.2011.

74.	Dinev, D.; Jordan, B.W.M.; Neufeld, B.; Lee, J.; Lindemann, D.; Rapp, U.R.; Ludwig, S. Extracellular signal regulated kinase 5 (ERK5) is required for the differentiation of muscle cells. *EMBO Rep.* **2001**, *2*, 829–834, doi:10.1093/embo-reports/kve177.

75.	Guo, Y.; Pan, W.; Liu, S.; Shen, Z.; Xu, Y.; Hu, L. ERK/MAPK signalling pathway and tumorigenesis (Review). *Exp. Ther. Med.* **2020**, doi:10.3892/etm.2020.8454.

76.	Wortzel, I.; Seger, R. The ERK Cascade: Distinct Functions within Various Subcellular Organelles. *Genes Cancer* **2011**, *2*, 195–209, doi:10.1177/1947601911407328.

77.	ZHANG, W.; LIU, H.T. MAPK signal pathways in the regulation of cell proliferation in mammalian cells. *Cell Res.* **2002**, *12*, 9–18, doi:10.1038/sj.cr.7290105.

78.	Kong, T.; Liu, M.; Ji, B.; Bai, B.; Cheng, B.; Wang, C. Role of the Extracellular Signal-Regulated Kinase 1/2 Signaling Pathway in Ischemia-Reperfusion Injury. *Front. Physiol.* **2019**, *10*, doi:10.3389/fphys.2019.01038.

79.	de los Reyes Corrales, T.; Losada-Pérez, M.; Casas-Tintó, S. JNK Pathway in CNS Pathologies. *Int. J. Mol. Sci.* **2021**, *22*, 3883, doi:10.3390/ijms22083883.

80.	Ip, Y.T.; Davis, R.J. Signal transduction by the c-Jun N-terminal kinase (JNK) — from inflammation to development. *Curr. Opin. Cell Biol.* **1998**, *10*, 205–219, doi:10.1016/S0955-0674(98)80143-9.

81.   ZHAO, H.-F.; WANG, J.; TO, S.-S.T. The phosphatidylinositol 3-kinase/Akt and c-Jun N-terminal kinase signaling in cancer: Alliance or contradiction? (Review). *Int. J. Oncol.* **2015**, *47*, 429–436, doi:10.3892/ijo.2015.3052.

82.   Zechner, D.; Thuerauf, D.J.; Hanford, D.S.; McDonough, P.M.; Glembotski, C.C. A Role for the p38 Mitogen-activated Protein Kinase Pathway in Myocardial Cell Growth, Sarcomeric Organization, and Cardiac-specific Gene Expression. *J. Cell Biol.* **1997**, *139*, 115–127, doi:10.1083/jcb.139.1.115.

83.   Pua, L.J.W.; Mai, C.-W.; Chung, F.F.-L.; Khoo, A.S.-B.; Leong, C.-O.; Lim, W.-M.; Hii, L.-W. Functional Roles of JNK and p38 MAPK Signaling in Nasopharyngeal Carcinoma. *Int. J. Mol. Sci.* **2022**, *23*, 1108, doi:10.3390/ijms23031108.

84.   Martínez-Limón, A.; Joaquin, M.; Caballero, M.; Posas, F.; de Nadal, E. The p38 Pathway: From Biology to Cancer Therapy. *Int. J. Mol. Sci.* **2020**, *21*, 1913, doi:10.3390/ijms21061913.

85.   Wagner, E.F.; Nebreda, Á.R. Signal integration by JNK and p38 MAPK pathways in cancer development. *Nat. Rev. Cancer* **2009**, *9*, 537–549, doi:10.1038/nrc2694.

86.   Im, H.-J.; Muddasani, P.; Natarajan, V.; Schmid, T.M.; Block, J.A.; Davis, F.; van Wijnen, A.J.; Loeser, R.F. Basic Fibroblast Growth Factor Stimulates Matrix Metalloproteinase-13 via the Molecular Cross-talk between the Mitogen-activated Protein Kinases and Protein Kinase Cδ Pathways in Human Adult Articular Chondrocytes. *J. Biol. Chem.* **2007**, *282*, 11110–11121, doi:10.1074/jbc.M609040200.

87.   Ma, W.; Quirion, R. The ERK/MAPK pathway, as a target for the

treatment of neuropathic pain. *Expert Opin. Ther. Targets* **2005**, *9*, 699–713, doi:10.1517/14728222.9.4.699.

88. Wilton, D.C.; Waite, M. Chapter 11 Phospholipases. In *New Comprehensive Biochemistry*; 2002; Vol. 36, pp. 291–314.

89. Zhu, L.; Jones, C.; Zhang, G. The Role of Phospholipase C Signaling in Macrophage-Mediated Inflammatory Response. *J. Immunol. Res.* **2018**, *2018*, 1–9, doi:10.1155/2018/5201759.

90. Wang, L.; Zhou, Y.; Chen, Z.; Sun, L.; Wu, J.; Li, H.; Liu, F.; Wang, F.; Yang, C.; Yang, J.; et al. PLCβ2 negatively regulates the inflammatory response to virus infection by inhibiting phosphoinositide-mediated activation of TAK1. *Nat. Commun.* **2019**, *10*, 746, doi:10.1038/s41467-019-08524-3.

91. Liao, H.-J.; Carpenter, G. Phospholipase C. In *Handbook of Cell Signaling*; Elsevier, 2010; Vol. 2, pp. 887–891.

92. Fukami, K.; Inanobe, S.; Kanemaru, K.; Nakamura, Y. Phospholipase C is a key enzyme regulating intracellular calcium and modulating the phosphoinositide balance. *Prog. Lipid Res.* **2010**, *49*, 429–437, doi:10.1016/j.plipres.2010.06.001.

93. Rebecchi, M.J.; Pentyala, S.N. Structure, Function, and Control of Phosphoinositide-Specific Phospholipase C. *Physiol. Rev.* **2000**, *80*, 1291–1335, doi:10.1152/physrev.2000.80.4.1291.

94. Haas, E.; Stanley, D.W. Phospholipase C. In *xPharm: The Comprehensive Pharmacology Reference*; Elsevier, 2007; pp. 1–7.

95. Charnock-Jones, D.S.; Day, K.; Smith, S.K. Cloning, expression and genomic organization of human placental protein disulfide isomerase (previously identified as phospholipase C alpha). *Int. J. Biochem. Cell*

Biol. **1996**, *28*, 81–89, doi:10.1016/1357-2725(95)00120-4.

96. Yelumalai, S.; Yeste, M.; Jones, C.; Amdani, S.N.; Kashir, J.; Mounce, G.; Da Silva, S.J.M.; Barratt, C.L.; McVeigh, E.; Coward, K. Total levels, localization patterns, and proportions of sperm exhibiting phospholipase C zeta are significantly correlated with fertilization rates after intracytoplasmic sperm injection. *Fertil. Steril.* **2015**, *104*, 561-568.e4, doi:10.1016/j.fertnstert.2015.05.018.

97. Béziau, D.M.; Toussaint, F.; Blanchette, A.; Dayeh, N.R.; Charbel, C.; Tardif, J.-C.; Dupuis, J.; Ledoux, J. Expression of Phosphoinositide-Specific Phospholipase C Isoforms in Native Endothelial Cells. *PLoS One* **2015**, *10*, e0123769, doi:10.1371/journal.pone.0123769.

98. Gresset, A.; Sondek, J.; Harden, T.K. The Phospholipase C Isozymes and Their Regulation. In *Subcellular Biochemistry*; 2012; Vol. 58, pp. 61–94.

99. Cocco, L.; Follo, M.Y.; Manzoli, L.; Suh, P.-G. Phosphoinositide-specific phospholipase C in health and disease. *J. Lipid Res.* **2015**, doi:10.1194/jlr.r057984.

100. Sandal, M.; Paltrinieri, D.; Carloni, P.; Musiani, F.; Giorgetti, A. Structure/Function Relationships of Phospholipases C Beta. *Curr. Protein Pept. Sci.* **2013**, *14*, 650–657, doi:10.2174/13892037113146660085.

101. Lyon, A.M.; Tesmer, J.J.G. Structural Insights into Phospholipase C-β Function. *Mol. Pharmacol.* **2013**, *84*, 488–500, doi:10.1124/mol.113.087403.

102. Raimondi, C.; Falasca, M. Phosphoinositides signalling in cancer: Focus on PI3K and PLC. *Adv. Biol. Regul.* **2012**, *52*, 166–182,

doi:10.1016/j.advenzreg.2011.09.016.

103. Nakamura, Y.; Fukami, K. Regulation and physiological functions of mammalian phospholipase C. *J. Biochem.* **2017**, *161*, mvw094, doi:10.1093/jb/mvw094.

104. Breivik, H. International Association for the Study of Pain. *J. Pain Symptom Manage.* **2002**, *24*, 97–101, doi:10.1016/S0885-3924(02)00465-7.

105. Neogi, T. The epidemiology and impact of pain in osteoarthritis. *Osteoarthr. Cartil.* **2013**, *21*, 1145–1153, doi:10.1016/j.joca.2013.03.018.

106. Fu, K.; Robbins, S.R.; McDougall, J.J. Osteoarthritis: the genesis of pain. *Rheumatology* **2018**, *57*, iv43–iv50, doi:10.1093/rheumatology/kex419.

107. Perrot, S. Targeting Pain or Osteoarthritis? Implications Implications for Optimal Management of Osteoarthritis Pain. *PAIN Clin. Updat.* **2016**, *XXIV*.

108. Wang, K.; Kim, H.A.; Felson, D.T.; Xu, L.; Kim, D.H.; Nevitt, M.C.; Yoshimura, N.; Kawaguchi, H.; Lin, J.; Kang, X.; et al. Radiographic Knee Osteoarthritis and Knee Pain: Cross-sectional study from Five Different Racial/Ethnic Populations. *Sci. Rep.* **2018**, *8*, 1364, doi:10.1038/s41598-018-19470-3.

109. Dieppe, P.A.; Lohmander, L.S. Pathogenesis and management of pain in osteoarthritis. *Lancet* **2005**, *365*, 965–973, doi:10.1016/S0140-6736(05)71086-2.

110. Lafeber, F.P.J.G.; Besselink, N.J.; Mastbergen, S.C. Oxford Textbook of Osteoarthritis and Crystal Arthropathy (3 ed.). *Oxford Textb.*

Osteoarthr. Cryst. Arthropathy **2016**, *1*.

111. Abulhasan, J.; Grey, M. Anatomy and Physiology of Knee Stability. *J. Funct. Morphol. Kinesiol.* **2017**, *2*, 34, doi:10.3390/jfmk2040034.

112. Grässel, S.; Muschter, D. Peripheral Nerve Fibers and Their Neurotransmitters in Osteoarthritis Pathology. *Int. J. Mol. Sci.* **2017**, *18*, 931, doi:10.3390/ijms18050931.

113. McDougall, J.J. Arthritis and pain. Neurogenic origin of joint pain. *Arthritis Res. Ther.* 2006, *8*, 220.

114. Miller, R.E.; Miller, R.J.; Malfait, A.-M. Osteoarthritis joint pain: The cytokine connection. *Cytokine* **2014**, *70*, 185–193, doi:10.1016/j.cyto.2014.06.019.

115. Lu, H.-C.; Mackie, K. An Introduction to the Endogenous Cannabinoid System. *Biol. Psychiatry* **2016**, *79*, 516–525, doi:10.1016/j.biopsych.2015.07.028.

116. Zou, S.; Kumar, U. Cannabinoid Receptors and the Endocannabinoid System: Signaling and Function in the Central Nervous System. *Int. J. Mol. Sci.* **2018**, *19*, 833, doi:10.3390/ijms19030833.

117. Pacher, P.; Bátkai, S.; Kunos, G. The Endocannabinoid System as an Emerging Target of Pharmacotherapy. *Pharmacol. Rev.* **2006**, *58*, 389–462, doi:10.1124/pr.58.3.2.

118. Battista, N.; Di Tommaso, M.; Bari, M.; Maccarrone, M. The endocannabinoid system: an overview. *Front. Behav. Neurosci.* **2012**, *6*, doi:10.3389/fnbeh.2012.00009.

119. Mechoulam, R.; Parker, L.A. The Endocannabinoid System and the Brain. *Annu. Rev. Psychol.* **2013**, *64*, 21–47, doi:10.1146/annurev-psych-113011-143739.

120. Liu, J.; Wang, L.; Harvey-White, J.; Osei-Hyiaman, D.; Razdan, R.; Gong, Q.; Chan, A.C.; Zhou, Z.; Huang, B.X.; Kim, H.-Y.; et al. A biosynthetic pathway for anandamide. *Proc. Natl. Acad. Sci.* **2006**, *103*, 13345–13350, doi:10.1073/pnas.0601832103.

121. Lu, H.-C.; Mackie, K. Review of the Endocannabinoid System. *Biol. Psychiatry Cogn. Neurosci. Neuroimaging* **2021**, *6*, 607–615, doi:10.1016/j.bpsc.2020.07.016.

122. Murataeva, N.; Straiker, A.; Mackie, K. Parsing the players: 2-arachidonoylglycerol synthesis and degradation in the CNS. *Br. J. Pharmacol.* **2014**, *171*, 1379–1391, doi:10.1111/bph.12411.

123. Castillo, P.E.; Younts, T.J.; Chávez, A.E.; Hashimotodani, Y. Endocannabinoid Signaling and Synaptic Function. *Neuron* **2012**, *76*, 70–81, doi:10.1016/j.neuron.2012.09.020.

124. Bari, M.; Battista, N.; Fezza, F.; Gasperi, V.; Maccarrone, M. New Insights into Endocannabinoid Degradation and its Therapeutic Potential. *Mini-Reviews Med. Chem.* **2006**, *6*, 257–268, doi:10.2174/138955706776073466.

125. Mackie, K. Cannabinoid Receptors: Where They are and What They do. *J. Neuroendocrinol.* **2008**, *20*, 10–14, doi:10.1111/j.1365-2826.2008.01671.x.

126. Wu, J. Cannabis, cannabinoid receptors, and endocannabinoid system: yesterday, today, and tomorrow. *Acta Pharmacol. Sin.* **2019**, *40*, 297–299, doi:10.1038/s41401-019-0210-3.

127. Bie, B.; Wu, J.; Foss, J.F.; Naguib, M. An overview of the cannabinoid type 2 receptor system and its therapeutic potential. *Curr. Opin. Anaesthesiol.* **2018**, *31*, 407–414,

doi:10.1097/ACO.0000000000000616.

128. Shahbazi, F.; Grandi, V.; Banerjee, A.; Trant, J.F. Cannabinoids and Cannabinoid Receptors: The Story so Far. *iScience* **2020**, *23*, 101301, doi:10.1016/j.isci.2020.101301.

129. Kamato, D.; Thach, L.; Bernard, R.; Chan, V.; Zheng, W.; Kaur, H.; Brimble, M.; Osman, N.; Little, P.J. Structure, Function, Pharmacology, and Therapeutic Potential of the G Protein, Gα/q,11. *Front. Cardiovasc. Med.* 2015, *2*.

130. Neves, S.R.; Ram, P.T.; Iyengar, R. G Protein Pathways. *Science (80-.).* **2002**, *296*, 1636–1639, doi:10.1126/science.1071550.

131. Bhagavan, N. V; Ha, C.-E. Chapter 28 - Endocrine Metabolism I: Introduction and Signal Transduction. In *Essentials of Medical Biochemistry*; 2011.

132. Cho, K.-S.; Guo, C.; Chew, J.; Yuan, J.C.; Zhu, R.; He, Z.; Chen, D.F. The Intrinsic Determinants of Axon Regeneration in the Central Nervous System. In *Neural Regeneration*; Elsevier, 2015; pp. 197–207.

133. Delghandi, M.P.; Johannessen, M.; Moens, U. The cAMP signalling pathway activates CREB through PKA, p38 and MSK1 in NIH 3T3 cells. *Cell. Signal.* **2005**, *17*, 1343–1351, doi:10.1016/j.cellsig.2005.02.003.

134. Melck, D.; Rueda, D.; Galve-Roperh, I.; De Petrocellis, L.; Guzmán, M.; Di Marzo, V. Involvement of the cAMP/protein kinase A pathway and of mitogen-activated protein kinase in the anti-proliferative effects of anandamide in human breast cancer cells. *FEBS Lett.* **1999**, *463*, 235–240, doi:10.1016/S0014-5793(99)01639-7.

149

135. Howlett, A.C. Cannabinoid Receptor Signaling. In *Cannabinoids*; Springer-Verlag: Berlin/Heidelberg, 2005; Vol. 168, pp. 53–79.

136. Brock, C.; Schaefer, M.; Reusch, H.P.; Czupalla, C.; Michalke, M.; Spicher, K.; Schultz, G.; Nürnberg, B. Roles of Gβγ in membrane recruitment and activation of p110γ/p101 phosphoinositide 3-kinase γ. *J. Cell Biol.* **2003**, *160*, 89–99, doi:10.1083/jcb.200210115.

137. Smrcka, A. V. G protein βγ subunits: Central mediators of G protein-coupled receptor signaling. *Cell. Mol. Life Sci.* **2008**, *65*, 2191–2214, doi:10.1007/s00018-008-8006-5.

138. Goldsmith, Z.G.; Dhanasekaran, D.N. G Protein regulation of MAPK networks. *Oncogene* **2007**, *26*, 3122–3142, doi:10.1038/sj.onc.1210407.

139. De Petrocellis, L.; Di Marzo, V. Role of endocannabinoids and endovanilloids in Ca2+ signalling. *Cell Calcium* **2009**, *45*, 611–624, doi:10.1016/j.ceca.2009.03.003.

140. Zhang, L.; Shi, G. Gq-Coupled Receptors in Autoimmunity. *J. Immunol. Res.* **2016**, *2016*, 1–8, doi:10.1155/2016/3969023.

141. Slack, J.M.W. Molecular biology of the cell. In *Principles of Tissue Engineering*; Elsevier, 2020; pp. 65–78.

142. Bruyère, O.; Honvo, G.; Veronese, N.; Arden, N.K.; Branco, J.; Curtis, E.M.; Al-Daghri, N.M.; Herrero-Beaumont, G.; Martel-Pelletier, J.; Pelletier, J.-P.; et al. An updated algorithm recommendation for the management of knee osteoarthritis from the European Society for Clinical and Economic Aspects of Osteoporosis, Osteoarthritis and Musculoskeletal Diseases (ESCEO). *Semin. Arthritis Rheum.* **2019**, *49*, 337–350, doi:10.1016/j.semarthrit.2019.04.008.

143. Jevsevar, D.S. Treatment of Osteoarthritis of the Knee: Evidence-Based Guideline, 2nd Edition. *J. Am. Acad. Orthop. Surg.* **2013**, *21*, 571–576, doi:10.5435/JAAOS-21-09-571.

144. Jüni, P.; Reichenbach, S.; Dieppe, P. Osteoarthritis: rational approach to treating the individual. *Best Pract. Res. Clin. Rheumatol.* 2006, *20*.

145. Majeed, M.H.; Sherazi, S.A.A.; Bacon, D.; Bajwa, Z.H. Pharmacological Treatment of Pain in Osteoarthritis: A Descriptive Review. *Curr. Rheumatol. Rep.* **2018**, *20*, 88, doi:10.1007/s11926-018-0794-5.

146. Rannou, F.; Poiraudeau, S. Non-pharmacological approaches for the treatment of osteoarthritis. *Best Pract. Res. Clin. Rheumatol.* **2010**, *24*, 93–106, doi:10.1016/j.berh.2009.08.013.

147. Steinmeyer, J.; Bock, F.; Stöve, J.; Jerosch, J.; Flechtenmacher, J. Pharmacological treatment of knee osteoarthritis: Special considerations of the new German guideline. *Orthop. Rev. (Pavia).* **2018**, *10*, doi:10.4081/or.2018.7782.

148. Da Costa, B.R.; Pereira, T. V.; Saadat, P.; Rudnicki, M.; Iskander, S.M.; Bodmer, N.S.; Bobos, P.; Gao, L.; Kiyomoto, H.D.; Montezuma, T.; et al. Effectiveness and safety of non-steroidal anti-inflammatory drugs and opioid treatment for knee and hip osteoarthritis: Network meta-analysis. *BMJ* **2021**, *375*, doi:10.1136/bmj.n2321.

149. Lee, C.; Straus, W.L.; Balshaw, R.; Barlas, S.; Vogel, S.; Schnitzer, T.J. A comparison of the efficacy and safety of nonsteroidal antiinflammatory agents versus acetaminophen in the treatment of osteoarthritis: A meta-analysis. *Arthritis Rheum.* **2004**, *51*, 746–754, doi:10.1002/art.20698.

150. Rannou, F.; Pelletier, J.P.; Martel-Pelletier, J. Efficacy and safety of topical NSAIDs in the management of osteoarthritis: Evidence from real-life setting trials and surveys. *Semin. Arthritis Rheum.* **2016**, doi:10.1016/j.semarthrit.2015.11.007.

151. Bannuru, R.R.; Osani, M.C.; Vaysbrot, E.E.; Arden, N.K.; Bennell, K.; Bierma-Zeinstra, S.M.A.; Kraus, V.B.; Lohmander, L.S.; Abbott, J.H.; Bhandari, M.; et al. OARSI guidelines for the non-surgical management of knee, hip, and polyarticular osteoarthritis. *Osteoarthr. Cartil.* **2019**, *27*, 1578–1589, doi:10.1016/j.joca.2019.06.011.

152. McAlindon, T.E.; Bannuru, R.R.; Sullivan, M.C.; Arden, N.K.; Berenbaum, F.; Bierma-Zeinstra, S.M.; Hawker, G.A.; Henrotin, Y.; Hunter, D.J.; Kawaguchi, H.; et al. OARSI guidelines for the non-surgical management of knee osteoarthritis. *Osteoarthr. Cartil.* **2014**, *22*, 363–388, doi:10.1016/j.joca.2014.01.003.

153. Rosenblum, A.; Marsch, L.A.; Joseph, H.; Portenoy, R.K. Opioids and the treatment of chronic pain: Controversies, current status, and future directions. *Exp. Clin. Psychopharmacol.* **2008**, *16*, 405–416, doi:10.1037/a0013628.

154. Browne, J.A.; Nho, S.J.; Goodman, S.B.; Della Valle, C.J. American Association of Hip and Knee Surgeons, Hip Society, and Knee Society Position Statement on Biologics for Advanced Hip and Knee Arthritis. *J. Arthroplasty* **2019**, *34*, 1051–1052, doi:10.1016/j.arth.2019.03.068.

155. Zhang, S.; Kong, X.; Chai, W. Opioids in primary total joint arthroplasty: Interpretation of 2020 AAHKS/ASRA/AAOS/THS/TKS clinical practice guidelines. *Zhongguo Xiu Fu Chong Jian Wai Ke Za Zhi* **2021**, *35*, doi:10.7507/1002-1892.202103090.

156. Ghouri, A.; Conaghan, P.G. Prospects for Therapies in Osteoarthritis. *Calcif. Tissue Int.* **2021**, *109*, 339–350, doi:10.1007/s00223-020-00672-9.

157. Reginster, J.Y.; Neuprez, A.; Lecart, M.P.; Sarlet, N.; Bruyere, O. Role of glucosamine in the treatment for osteoarthritis. *Rheumatol. Int.* 2012, *32*, 2959–2967.

158. Honvo, G.; Reginster, J.Y.; Rabenda, V.; Geerinck, A.; Mkinsi, O.; Charles, A.; Rizzoli, R.; Cooper, C.; Avouac, B.; Bruyère, O. Safety of Symptomatic Slow-Acting Drugs for Osteoarthritis: Outcomes of a Systematic Review and Meta-Analysis. *Drugs and Aging* **2019**, *36*, 65–99, doi:10.1007/s40266-019-00662-z.

159. Jerosch, J. Effects of glucosamine and chondroitin sulfate on cartilage metabolism in OA: Outlook on other nutrient partners especially omega-3 fatty acids. *Int. J. Rheumatol.* **2011**, *2011*, 969012, doi:10.1155/2011/969012.

160. Scotto d'Abusco, A.; Corsi, A.; Grillo, M.G.; Cicione, C.; Calamia, V.; Panzini, G.; Sansone, A.; Giordano, C.; Politi, L.; Scandurra, R. Effects of intra-articular administration of glucosamine and a peptidyl-glucosamine derivative in a rabbit model of experimental osteoarthritis: A pilot study. *Rheumatol. Int.* **2008**, *28*, 437–443, doi:10.1007/s00296-007-0463-x.

161. The European Medicines Agency Guideline on clinical investigation of medicinal products used in the treatment of osteoarthritis. *Eur. Med. agency* 2010.

162. Uitterlinden, E.; Koevoet, J.; Verkoelen, C.; Bierma-Zeinstra, S.; Jahr, H.; Weinans, H.; Verhaar, J.; van Osch, G. Glucosamine increases

hyaluronic acid production in human osteoarthritic synovium explants. *BMC Musculoskelet. Disord.* **2008**, *9*, 120, doi:10.1186/1471-2474-9-120.

163. Yamagishi, Y.; Someya, A.; Imai, K.; Nagao, J.; Nagaoka, I. Evaluation of the anti-inflammatory actions of various functional food materials including glucosamine on synovial cells. *Mol. Med. Rep.* **2017**, doi:10.3892/mmr.2017.6691.

164. Scotto d'Abusco, A.; Politi, L.; Giordano, C.; Scandurra, R. A peptidyl-glucosamine derivative affects IKKα kinase activity in human chondrocytes. *Arthritis Res. Ther.* **2010**, doi:10.1186/ar2920.

165. Williams, D.H.; Garbuz, D.S.; Masri, B.A. Total knee arthroplasty: Techniques and results. *B. C. Med. J.* **2010**, *52*.

166. Liu, X.W.; Zi, Y.; Xiang, L.B.; Wang, Y. Total hip arthroplasty: A review of advances, advantages and limitations. *Int. J. Clin. Exp. Med.* 2015, *8*.

167. Colitti, M.; Stefanon, B.; Gabai, G.; Gelain, M.; Bonsembiante, F. Oxidative Stress and Nutraceuticals in the Modulation of the Immune Function: Current Knowledge in Animals of Veterinary Interest. *Antioxidants* **2019**, *8*, 28, doi:10.3390/antiox8010028.

168. Halsted, C.H. Dietary supplements and functional foods: 2 sides of a coin? *Am. J. Clin. Nutr.* **2003**, *77*, 1001S-1007S, doi:10.1093/ajcn/77.4.1001S.

169. Committee on Herbal Medicinal Products (HMPC). Assessment report on Harpagophytum procumbens DC. and/or Harpagophytum zeyheri Decne., radix. (EMA/HMPC/627058/2015). *Eur. Med. Agency,* **2015**.

170. Brien, S.; Lewith, G.T.; McGregor, G. Devil's Claw (Harpagophytum

procumbens) as a Treatment for Osteoarthritis: A Review of Efficacy and Safety. *J. Altern. Complement. Med.* **2006**, *12*, 981–993, doi:10.1089/acm.2006.12.981.

171. Qi, J.; Chen, J.-J.; Cheng, Z.-H.; Zhou, J.-H.; Yu, B.-Y.; Qiu, S.X. Iridoid glycosides from Harpagophytum procumbens D.C. (devil's claw). *Phytochemistry* **2006**, *67*, 1372–1377, doi:10.1016/j.phytochem.2006.05.029.

172. Akhtar, N.; Haqqi, T.M. Current nutraceuticals in the management of osteoarthritis: A review. *Ther. Adv. Musculoskelet. Dis.* **2012**, *4*, 181–207, doi:10.1177/1759720X11436238.

173. Mncwangi, N.; Chen, W.; Vermaak, I.; Viljoen, A.M.; Gericke, N. Devil's Claw - A review of the ethnobotany, phytochemistry and biological activity of Harpagophytum procumbens. *J. Ethnopharmacol.* **2012**, *143*, 755–771, doi:10.1016/j.jep.2012.08.013.

174. Ghasemian, M.; Owlia, S.; Owlia, M.B. Review of Anti-Inflammatory Herbal Medicines. *Adv. Pharmacol. Sci.* **2016**, doi:10.1155/2016/9130979.

175. Kriukova, A.; Vladymyrova, I.; Levashova, O.; Tishakova, T. Determination of Amino Acid Composition in the Harpagophytum procumbens Root. *Dhaka Univ. J. Pharm. Sci.* **2019**, *18*, 85–91, doi:10.3329/dujps.v18i1.41895.

176. McGregor, G.; Fiebich, B.; Wartenberg, A.; Brien, S.; Lewith, G.; Wegener, T. Devil's Claw (Harpagophytum procumbens): An Anti-Inflammatory Herb with Therapeutic Potential. *Phytochem. Rev.* **2005**, *4*, 47–53, doi:10.1007/s11101-004-2374-8.

177. Garner-wizard, M.; Henson, S.; Oppel-sutter, M.; Milot, B.; Oliff,

E.H.S.; Ris, M.S.G. Anti-inflammatory Activity of Devil's Claw Reviewed. *Am. Bot. Counc.* **2008**.

178. Hostanska, K.; Melzer, J.; Rostock, M.; Suter, A.; Saller, R. Alteration of anti-inflammatory activity of Harpagophytum procumbens (devil's claw) extract after external metabolic activation with S9 mix. *J. Pharm. Pharmacol.* **2014**, *66*, 1606–1614, doi:10.1111/jphp.12242.

179. Inaba, K.; Murata, K.; Naruto, S.; Matsuda, H. Inhibitory effects of devil's claw (secondary root of Harpagophytum procumbens) extract and harpagoside on cytokine production in mouse macrophages. *J. Nat. Med.* **2010**, *64*, 219–222, doi:10.1007/s11418-010-0395-8.

180. Fiebich, B.L.; Muñoz, E.; Rose, T.; Weiss, G.; McGregor, G.P. Molecular targets of the antiinflammatory Harpagophytum procumbens (Devil's claw): Inhibition of TNFα and COX-2 gene expression by preventing activation of AP-1. *Phyther. Res.* **2012**, *26*, doi:10.1002/ptr.3636.

181. Krenn, V.; Morawietz, L.; Häupl, T.; Neidel, J.; Petersen, I.; König, A. Grading of Chronic Synovitis — A Histopathological Grading System for Molecular and Diagnostic Pathology. *Pathol. - Res. Pract.* **2002**, *198*, 317–325, doi:10.1078/0344-0338-5710261.

182. Schmittgen, T.D.; Livak, K.J. Analyzing real-time PCR data by the comparative CT method. *Nat. Protoc.* **2008**, *3*, 1101–1108, doi:10.1038/nprot.2008.73.

183. Sapio, L.; Gallo, M.; Illiano, M.; Chiosi, E.; Naviglio, D.; Spina, A.; Naviglio, S. The Natural cAMP Elevating Compound Forskolin in Cancer Therapy: Is It Time? *J. Cell. Physiol.* **2017**, *232*, 922–927, doi:10.1002/jcp.25650.

184. Turcotte, C.; Blanchet, M.R.; Laviolette, M.; Flamand, N. The CB2 receptor and its role as a regulator of inflammation. *Cell. Mol. Life Sci.* **2016**, *73*, 4449–4470, doi:10.1007/s00018-016-2300-4.

185. Cassano, T.; Calcagnini, S.; Pace, L.; De Marco, F.; Romano, A.; Gaetani, S. Cannabinoid Receptor 2 Signaling in Neurodegenerative Disorders: From Pathogenesis to a Promising Therapeutic Target. *Front. Neurosci.* **2017**, *11*, doi:10.3389/fnins.2017.00030.

186. Fukuda, S.; Kohsaka, H.; Takayasu, A.; Yokoyama, W.; Miyabe, C.; Miyabe, Y.; Harigai, M.; Miyasaka, N.; Nanki, T. Cannabinoid receptor 2 as a potential therapeutic target in rheumatoid arthritis. *BMC Musculoskelet. Disord.* **2014**, *15*, 275, doi:10.1186/1471-2474-15-275.

187. Kondamudi, N.; Turner, M.W.; McDougal, O.M. Harpagoside Content in Devil's Claw Extracts. *Nat. Prod. Commun.* **2016**, *11*, 1934578X1601100, doi:10.1177/1934578X1601100903.

188. Kamikubo, R.; Kai, K.; Tsuji-Naito, K.; Akagawa, M. β-Caryophyllene attenuates palmitate-induced lipid accumulation through AMPK signaling by activating CB2 receptor in human HepG2 hepatocytes. *Mol. Nutr. Food Res.* **2016**, *60*, 2228–2242, doi:10.1002/mnfr.201600197.

189. Irrera, N.; D'ascola, A.; Pallio, G.; Bitto, A.; Mazzon, E.; Mannino, F.; Squadrito, V.; Arcoraci, V.; Minutoli, L.; Campo, G.M.; et al. β-Caryophyllene Mitigates Collagen Antibody Induced Arthritis (CAIA) in Mice Through a Cross-Talk between CB2 and PPAR-γ Receptors. *Biomolecules* **2019**, *9*, 326, doi:10.3390/biom9080326.

190. Manikandan, P.; Vinothini, G.; Vidya Priyadarsini, R.; Prathiba, D.;

Nagini, S. Eugenol inhibits cell proliferation via NF-κB suppression in a rat model of gastric carcinogenesis induced by MNNG. *Invest. New Drugs* **2011**, *29*, 110–117, doi:10.1007/s10637-009-9345-2.

191. Dal Bó, W.; Luiz, A.P.; Martins, D.F.; Mazzardo-Martins, L.; Santos, A.R.S. Eugenol reduces acute pain in mice by modulating the glutamatergic and tumor necrosis factor alpha (TNF-α) pathways. *Fundam. Clin. Pharmacol.* **2013**, *27*, 517–525, doi:10.1111/j.1472-8206.2012.01052.x.

192. Kumar, A.; Premoli, M.; Aria, F.; Bonini, S.A.; Maccarinelli, G.; Gianoncelli, A.; Memo, M.; Mastinu, A. Cannabimimetic plants: are they new cannabinoidergic modulators? *Planta* **2019**, *249*, 1681–1694, doi:10.1007/s00425-019-03138-x.

193. El-mekkawy, S.; Shahat, A.A.; Alqahtani, A.S.; Alsaid, M.S.; Abdelfattah, M.A.O.; Ullah, R.; Emam, M.; Yasri, A.; Sobeh, M. A Polyphenols-Rich Extract from Moricandia sinaica Boiss. Exhibits Analgesic, Anti-Inflammatory and Antipyretic Activities In Vivo. *Molecules* **2020**, *25*, 5049, doi:10.3390/molecules25215049.

194. Fernandes, E.S.; Passos, G.F.; Medeiros, R.; da Cunha, F.M.; Ferreira, J.; Campos, M.M.; Pianowski, L.F.; Calixto, J.B. Anti-inflammatory effects of compounds alpha-humulene and (−)-trans-caryophyllene isolated from the essential oil of Cordia verbenacea. *Eur. J. Pharmacol.* **2007**, *569*, 228–236, doi:10.1016/j.ejphar.2007.04.059.

195. Barboza, J.N.; da Silva Maia Bezerra Filho, C.; Silva, R.O.; Medeiros, J.V.R.; de Sousa, D.P. An Overview on the Anti-inflammatory Potential and Antioxidant Profile of Eugenol. *Oxid. Med. Cell. Longev.* **2018**, *2018*, 1–9, doi:10.1155/2018/3957262.

196. Ames-Sibin, A.P.; Barizão, C.L.; Castro-Ghizoni, C. V.; Silva, F.M.S.; Sá-Nakanishi, A.B.; Bracht, L.; Bersani-Amado, C.A.; Marçal-Natali, M.R.; Bracht, A.; Comar, J.F. β-Caryophyllene, the major constituent of copaiba oil, reduces systemic inflammation and oxidative stress in arthritic rats. *J. Cell. Biochem.* **2018**, *119*, 10262–10277, doi:10.1002/jcb.27369.

197. Ryu, N.-E.; Lee, S.-H.; Park, H. Spheroid Culture System Methods and Applications for Mesenchymal Stem Cells. *Cells* **2019**, *8*, 1620, doi:10.3390/cells8121620.

198. Devane, W.A.; Hanuš, L.; Breuer, A.; Pertwee, R.G.; Stevenson, L.A.; Griffin, G.; Gibson, D.; Mandelbaum, A.; Etinger, A.; Mechoulam, R. Isolation and Structure of a Brain Constituent That Binds to the Cannabinoid Receptor. *Science (80-.).* **1992**, *258*, 1946–1949, doi:10.1126/science.1470919.

199. Bryk, M.; Chwastek, J.; Kostrzewa, M.; Mlost, J.; Pędracka, A.; Starowicz, K. Alterations in Anandamide Synthesis and Degradation during Osteoarthritis Progression in an Animal Model. *Int. J. Mol. Sci.* **2020**, *21*, 7381, doi:10.3390/ijms21197381.

200. Richardson, D.; Pearson, R.G.; Kurian, N.; Latif, M.L.; Garle, M.J.; Barrett, D.A.; Kendall, D.A.; Scammell, B.E.; Reeve, A.J.; Chapman, V. Characterisation of the cannabinoid receptor system in synovial tissue and fluid in patients with osteoarthritis and rheumatoid arthritis. *Arthritis Res. Ther.* **2008**, *10*, R43, doi:10.1186/ar2401.

201. Valastro, C.; Campanile, D.; Marinaro, M.; Franchini, D.; Piscitelli, F.; Verde, R.; Di Marzo, V.; Di Bello, A. Characterization of endocannabinoids and related acylethanolamides in the synovial fluid

of dogs with osteoarthritis: a pilot study. *BMC Vet. Res.* **2017**, *13*, 309, doi:10.1186/s12917-017-1245-7.

202. Dhopeshwarkar, A.; Mackie, K. CB 2 Cannabinoid Receptors as a Therapeutic Target—What Does the Future Hold? *Mol. Pharmacol.* **2014**, *86*, 430–437, doi:10.1124/mol.114.094649.

203. Sassone-Corsi, P. The Cyclic AMP Pathway. *Cold Spring Harb. Perspect. Biol.* **2012**, *4*, a011148–a011148, doi:10.1101/cshperspect.a011148.

204. Takahashi, M.; Li, Y.; Dillon, T.J.; Stork, P.J.S. Phosphorylation of Rap1 by cAMP-dependent Protein Kinase (PKA) Creates a Binding Site for KSR to Sustain ERK Activation by cAMP. *J. Biol. Chem.* **2017**, *292*, 1449–1461, doi:10.1074/jbc.M116.768986.

205. Saroz, Y.; Kho, D.T.; Glass, M.; Graham, E.S.; Grimsey, N.L. Cannabinoid Receptor 2 (CB2) Signals via G-alpha-s and Induces IL-6 and IL-10 Cytokine Secretion in Human Primary Leukocytes. *ACS Pharmacol. Transl. Sci.* **2019**, *2*, doi:10.1021/acsptsci.9b00049.

206. Amin, A.; Ichigotani, Y.; Oo, M.; Biswas, M.; Yuan, H.; Huang, P.; Mon, N.; Hamaguchi, M. The PLC-PKC cascade is required for IL-1β-dependent Erk and Akt activation: their role in proliferation. *Int. J. Oncol.* **2003**, *23*, doi:10.3892/ijo.23.6.1727.

207. Wang, Y.; Prywes, R. Activation of the c-fos enhancer by the Erk MAP kinase pathway through two sequence elements: the c-fos AP-1 and p62TCF sites. *Oncogene* **2000**, *19*, 1379–1385, doi:10.1038/sj.onc.1203443.

208. Monje, P.; Hernández-Losa, J.; Lyons, R.J.; Castellone, M.D.; Gutkind, J.S. Regulation of the Transcriptional Activity of c-Fos by

ERK. *J. Biol. Chem.* **2005**, *280*, doi:10.1074/jbc.c500353200.

209. Davidson, B.; Givant-Horwitz, V.; Lazarovici, P.; Risberg, B.; Nesland, J.M.; Trope, C.G.; Schaefer, E.; Reich, R. Matrix metalloproteinases (MMP), EMMPRIN (extracellular matrix metalloproteinase inducer) and mitogen-activated protein kinases (MAPK): Co-expression in metastatic serous ovarian carcinoma. *Clin. Exp. Metastasis* **2003**, *20*, doi:10.1023/A:1027347932543.

210. Shin, C.Y.; Lee, W.J.; Choi, J.W.; Choi, M.S.; Park, G.H.; Yoo, B.K.; Han, S.Y.; Ryu, J.R.; Choi, E.Y.; Ko, K.H. Role of p38 mapk on the down-regulation of matrix metallo-proteinase-9 expression in rat astrocytes. *Arch. Pharm. Res.* **2007**, *30*, 624–633, doi:10.1007/BF02977658.

211. Ding, X.; Xiang, W.; Meng, D.; Chao, W.; Fei, H.; Wang, W. Osteoblasts Regulate the Expression of ADAMTS and MMPs in Chondrocytes through ERK Signaling Pathway. *Z. Orthop. Unfall.* **2021**, doi:10.1055/a-1527-7900.

212. Shiozawa, S.; Tsumiyama, K. Pathogenesis of rheumatoid arthritis and c-Fos/AP-1. *Cell Cycle* **2009**, *8*, 1539–1543, doi:10.4161/cc.8.10.8411.

213. Mehana, E.-S.E.; Khafaga, A.F.; El-Blehi, S.S. The role of matrix metalloproteinases in osteoarthritis pathogenesis: An updated review. *Life Sci.* **2019**, *234*, 116786, doi:10.1016/j.lfs.2019.116786.

214. Laronha, H.; Caldeira, J. Structure and Function of Human Matrix Metalloproteinases. *Cells* **2020**, *9*, 1076, doi:10.3390/cells9051076.

215. Burrage, P.S. Matrix Metalloproteinases: Role In Arthritis. *Front. Biosci.* **2006**, *11*, 529, doi:10.2741/1817.

216. Yang, C.-Y.; Chanalaris, A.; Troeberg, L. ADAMTS and ADAM metalloproteinases in osteoarthritis – looking beyond the 'usual suspects.' *Osteoarthr. Cartil.* **2017**, *25*, 1000–1009, doi:10.1016/j.joca.2017.02.791.

217. Bondeson, J.; Wainwright, S.; Hughes, C.; Caterson, B. The regulation of the ADAMTS4 and ADAMTS5 aggrecanases in osteoarthritis: A review. *Clin. Exp. Rheumatol.* 2008, *26*.

218. Roman-Blas, J.A.; Jimenez, S.A. NF-κB as a potential therapeutic target in osteoarthritis and rheumatoid arthritis. *Osteoarthr. Cartil.* **2006**, *14*, 839–848, doi:10.1016/j.joca.2006.04.008.

219. Ray, N.; Kuwahara, M.; Takada, Y.; Maruyama, K.; Kawaguchi, T.; Tsubone, H.; Ishikawa, H.; Matsuo, K. c-Fos suppresses systemic inflammatory response to endotoxin. *Int. Immunol.* **2006**, *18*, 671–677, doi:10.1093/intimm/dxl004.

220. Boczek, T.; Zylinska, L. Receptor-Dependent and Independent Regulation of Voltage-Gated Ca2+ Channels and Ca2+-Permeable Channels by Endocannabinoids in the Brain. *Int. J. Mol. Sci.* **2021**, *22*, 8168, doi:10.3390/ijms22158168.

221. Lauckner, J.E.; Hille, B.; Mackie, K. The cannabinoid agonist WIN55,212-2 increases intracellular calcium via CB 1 receptor coupling to G q/11 G proteins. *Proc. Natl. Acad. Sci.* **2005**, *102*, 19144–19149, doi:10.1073/pnas.0509588102.

222. Sarott, R.C.; Viray, A.E.G.; Pfaff, P.; Sadybekov, A.; Rajic, G.; Katritch, V.; Carreira, E.M.; Frank, J.A. Optical Control of Cannabinoid Receptor 2-Mediated Ca 2+ Release Enabled by Synthesis of Photoswitchable Probes. *J. Am. Chem. Soc.* **2021**, *143*,

736–743, doi:10.1021/jacs.0c08926.

223. Zoratti, C.; Kipmen-Korgun, D.; Osibow, K.; Malli, R.; Graier, W.F. Anandamide initiates Ca2+ signaling via CB2 receptor linked to phospholipase C in calf pulmonary endothelial cells. *Br. J. Pharmacol.* **2003**, *140*, 1351–1362, doi:10.1038/sj.bjp.0705529.

224. Battaglia, A.A. *An Introduction to Pain and its Relation to Nervous System Disorders*; Battaglia, A.A., Ed.; John Wiley & Sons, Ltd: Chichester, UK, 2016; ISBN 9781118455968.

225. Kawakami, T.; Xiao, W. Phospholipase C-β in immune cells. *Adv. Biol. Regul.* 2013.

226. Hajicek, N.; Keith, N.C.; Siraliev-Perez, E.; Temple, B.R.S.; Huang, W.; Zhang, Q.; Harden, T.K.; Sondek, J. Structural basis for the activation of PLC-γ isozymes by phosphorylation and cancer-associated mutations. *Elife* **2019**, *8*, doi:10.7554/eLife.51700.

227. Ensembl Gene: PLCG1 ENSG00000124181 Available online: https://jul2022.archive.ensembl.org/Homo_sapiens/Gene/Summary?db =core;g=ENSG00000124181;r=20:41136960-41196801;t=ENST00000473632.

228. Tsirimonaki, E.; Fedonidis, C.; Pneumaticos, S.G.; Tragas, A.A.; Michalopoulos, I.; Mangoura, D. PKCε Signalling Activates ERK1/2, and Regulates Aggrecan, ADAMTS5, and miR377 Gene Expression in Human Nucleus Pulposus Cells. *PLoS One* **2013**, *8*, e82045, doi:10.1371/journal.pone.0082045.

229. Cai, H.; Qu, N.; Chen, X.; Zhou, Y.; Zheng, X.; Zhang, B.; Xia, C. The inhibition of PLCγ1 protects chondrocytes against osteoarthritis, implicating its binding to Akt. *Oncotarget* **2018**, *9*, 4461–4474,

163

doi:10.18632/oncotarget.23286.

230. Kim, J.-Y.; Park, S.-H.; Baek, J.M.; Erkhembaatar, M.; Kim, M.S.; Yoon, K.-H.; Oh, J.; Lee, M.S. Harpagoside Inhibits RANKL-Induced Osteoclastogenesis via Syk-Btk-PLCγ2-Ca 2+ Signaling Pathway and Prevents Inflammation-Mediated Bone Loss. *J. Nat. Prod.* **2015**, *78*, 2167–2174, doi:10.1021/acs.jnatprod.5b00233.

231. Baker, J.; Falconer, A.M.D.; Wilkinson, D.J.; Europe-Finner, G.N.; Litherland, G.J.; Rowan, A.D. Protein kinase D3 modulates MMP1 and MMP13 expression in human chondrocytes. *PLoS One* **2018**, *13*, e0195864, doi:10.1371/journal.pone.0195864.

232. Liu, Z.; Cai, H.; Zheng, X.; Zhang, B.; Xia, C. The Involvement of Mutual Inhibition of ERK and mTOR in PLCγ1-Mediated MMP-13 Expression in Human Osteoarthritis Chondrocytes. *Int. J. Mol. Sci.* **2015**, *16*, 17857–17869, doi:10.3390/ijms160817857.

233. Mariano, A.; Di Sotto, A.; Leopizzi, M.; Garzoli, S.; Di Maio, V.; Gullì, M.; Vedova, P.D.; Ammendola, S.; Scotto d'Abusco, A. Antiarthritic effects of a root extract from harpagophytum procumbens DC: Novel insights into the molecular mechanisms and possible bioactive phytochemicals. *Nutrients* **2020**, *12*, 2545, doi:10.3390/nu12092545.

234. Mariano, A.; Bigioni, I.; Mattioli, R.; Di Sotto, A.; Leopizzi, M.; Garzoli, S.; Mariani, P.F.; Dalla Vedova, P.; Ammendola, S.; Scotto d'Abusco, A. Harpagophytum procumbens Root Extract Mediates Anti-Inflammatory Effects in Osteoarthritis Synoviocytes through CB2 Activation. *Pharmaceuticals* **2022**, *15*, 457, doi:10.3390/ph15040457.

Appendix

A. Scientific publications during the PhD course (2019-2022)

Article

Nanostructured TiC Layer is Highly Suitable Surface for Adhesion, Proliferation and Spreading of Cells

Mariangela Lopreiato [1], **Alessia Mariano** [1], **Rossana Cocchiola** [1,†], **Giovanni Longo** [2], **Pietro Dalla Vedova** [3], **Roberto Scandurra** [1] and **Anna Scotto d'Abusco** [1,*]

[1] Department of Biochemical Sciences, Sapienza University of Roma, P.le Aldo Moro, 5, 00185 Roma, Italy; mariangela.lopreiato@uniroma1.it (M.L.); alessia.mariano@uniroma1.it (A.M.); rossana.cocchiola@gmail.com (R.C.); roberto.scandurra@fondazione.uniroma1.it (R.S.)

[2] Consiglio Nazionale delle Ricerche-Istituto di Struttura della Materia, Via del Fosso del Cavaliere, 100, 00133 Rome, Italy; giovanni.longo@artov.ism.cnr.it

[3] UOC di Ortopedia e Traumatologia, Ospedale Santa Scolastica di Cassino, ASL di Frosinone, Via S. Pasquale, 03043 Cassino, Italy; pietro.dallavedova@aslfrosinone.it

* Correspondence: anna.scottodabusco@uniroma1.it; Tel.: +39-06-4991-0947

† Current affiliation: Clinical Trial Unit, Bambino Gesù Children's Hospital, IRCSS, P. Sant'Onofrio 4, 00100 Roma, Italy.

check for updates

Abstract: Cell culture is usually performed in 2D polymer surfaces; however, several studies are conducted with the aim to screen functional coating molecules to find substrates more suitable for cell adhesion and proliferation. The aim of this manuscript is to compare the cell adhesion and cytoskeleton organization of different cell types on different surfaces. Human primary fibroblasts, chondrocytes and osteoblasts isolated from patients undergoing surgery were seeded on polystyrene, poly-D-lysine-coated glass and titanium carbide slides and left to grow for several days. Then their cytoskeleton was analyzed, both by staining cells with phalloidin, which highlights actin fibers, and using Atomic Force Microscopy. We also monitored the production of Fibroblast Growth Factor-2, Bone Morphogenetic Protein-2 and Osteocalcin, using ELISA, and we highlighted production of Collagen type I in fibroblasts and osteoblasts and Collagen type II in chondrocytes by immunofluorescences. Fibroblasts, chondrocytes and osteoblasts showed both an improved proliferative activity and a good adhesion ability when cultured on titanium carbide slides, compared to polystyrene and poly-D-lysine-coated glass. In conclusion, we propose titanium carbide as a suitable surface to cultivate cells such as fibroblasts, chondrocytes and osteoblasts, allowing the preservation of their differentiated state and good adhesion properties.

Keywords: titanium carbide surface; human primary fibroblasts; human primary chondrocytes; human primary osteoblasts; Atomic Force Microscopy; cell differentiation; cell adhesion

1. Introduction

In the last years, the in vitro cell culture fields have undergone significant developments, especially in their application to a wide range of research areas, such as screening of molecules to be used in the treatments of pathologies, toxicology and disease studies [1]. A number of concerns has been raised regarding the quality of cell cultures, with particular focus on the surfaces used to propagate cells. While plastic flasks and dishes have been available since the 1960s, to perform in vitro cell culture, nowadays, most of these vessels are in polystyrene, a long carbon chain polymer with benzene rings attached to carbons. This material can be easily bent to form any kind of container or support, which has excellent optical clarity and simple sterilization processes. The main disadvantage is the

Article

Platelet Rich Fibrin (PRF) and Its Related Products: Biomolecular Characterization of the Liquid Fibrinogen

Giorgio Serafini [1,*], Mariangela Lopreiato [2], Marco Lollobrigida [1,*], Luca Lamazza [1], Giulia Mazzucchi [1], Lorenzo Fortunato [1], Alessia Mariano [2], Anna Scotto d'Abusco [2], Mario Fontana [2] and Alberto De Biase [1]

[1] Department of Oral and Maxillo Facial Sciences, "Sapienza" University of Rome, Via Caserta 6, 00161 Rome, Italy
[2] Department of Biochemical Sciences "Alessandro Rossi Fanelli", "Sapienza" University of Rome, Piazzale Aldo Moro 5, 00185 Rome, Italy
*   Correspondence: giorgio.serafini@uniroma1.it (G.S.); marco.lollobrigida@uniroma1.it (M.L.)

Abstract: Liquid fibrinogen is an injectable platelet concentrate rich in platelets, leukocytes, and fibrinogen obtained by blood centrifugation. The aim of this study was to analyze the release of different growth factors in the liquid fibrinogen at different times and to assess possible correlations between growth factors and cell counts. The concentration of transforming growth factor beta 1 (TGF-β1), platelet-derived growth factor-AB (PDGF-AB), platelet-derived growth factor-BB (PDGF-BB), bone morphogenetic protein 2 (BMP-2), fibroblast growth factor 2 (FGF-2) and vascular endothelial growth factor (VEGF) released by liquid fibrinogen were examined with ELISA at three time points (T0, time of collection; T7, 7 days; T14, 14 days). The cellular content of the liquid fibrinogen and whole blood was also calculated for each volunteer. A mean accumulation of platelets of almost 1.5-fold in liquid fibrinogen compared to whole blood samples was found. An increase of TGF-β1, PDGF-AB, FGF-2, and VEGF levels was detected at T7. At T14, the level of TGF-β1 returned to T0 level; PDGF-AB amount remained high; the levels of FGF-2 and VEGF decreased with respect to T7, but remained higher than the T0 levels; PDGF-BB was high at all time points; BMP-2 level was low and remained constant at all time points. TGF-β1, PDGF-AB, and PDGF-BB showed a correlation with platelet amount, whereas BMP-2, FGF-2, and VEGF showed a mild correlation with platelet amount. Due to the high concentration of platelets, liquid fibrinogen does contain important growth factors for the regeneration of both soft and hard tissue. The centrifugation protocol tested in this study provides a valid solution to stimulate wound healing in oral and periodontal surgery.

Keywords: liquid fibrinogen; platelet concentrate; growth factors; platelet rich fibrin; PRF; platelets; leukocyte

1. Introduction

The focus of regenerative medicine is the restoration of damaged tissues [1]. A stable fibrin clot is the first step of the healing process as it provides a provisional matrix for the migration of mesenchymal cells, fibroblasts, and epithelial cells. This has been the rationale for using platelet gel and fibrin glues in oral and maxillofacial surgery [2,3].

Research and development of new protocols to enhance hemostasis and wound healing is, however, a common focus for all surgical disciplines. The interest for innovative techniques has been particularly evident in the development of autologous platelets concentrates for surgical use,

Antiarthritic Effects of a Root Extract from *Harpagophytum procumbens* DC: Novel Insights into the Molecular Mechanisms and Possible Bioactive Phytochemicals

Alessia Mariano [1], Antonella Di Sotto [2], Martina Leopizzi [3], Stefania Garzoli [4], Valeria Di Maio [3], Marco Gullì [2], Pietro Dalla Vedova [5], Sergio Ammendola [6] and Anna Scotto d'Abusco [1,*]

[1] Department of Biochemical Sciences, Sapienza University of Roma, P.le Aldo Moro 5, 00185 Roma, Italy; alessia.mariano@uniroma1.it
[2] Department of Physiology and Pharmacology, Sapienza University of Rome, P.le Aldo Moro 5, 00185 Rome, Italy; antonella.disotto@uniroma1.it (A.D.S.); marco.gulli@uniroma1.it (M.G.)
[3] Department of Medico-Surgical Sciences and Biotechnologies, Polo Pontino-Sapienza University, 04100 Latina, Italy; martina.leopizzi@uniroma1.it (M.L.); dimaiovaleria@libero.it (V.D.M.)
[4] Department of Drug Chemistry and Technologies, Sapienza University of Rome, P.le Aldo Moro 5, 00185 Rome, Italy; stefania.garzoli@uniroma1.it
[5] UOC di Ortopedia e Traumatologia, Ospedale Santa Scolastica di Cassino, ASL di Frosinone, Via S. Pasquale, 03043 Cassino, Italy; pietro.dallavedova@aslfrosinone.it
[6] Ambiotec S.A.S. Via Appia Nord 47, 04012 Cisterna di Latina (LT), Italy; ambiotec@libero.it
* Correspondence: anna.scottodabusco@uniroma1.it; Tel.: +39-06-4991-0947

Abstract: *Harpagophytum procumbens* (Burch.) DC. ex Meisn. is a traditional remedy for osteoarticular diseases, including osteoarthritis (OA), although the bioactive constituents and mechanisms involved are yet to be clarified. In the present study, an aqueous *H. procumbens* root extract (HPE; containing 1.2% harpagoside) was characterized for its effects on synoviocytes from OA patients and phytochemical composition in polyphenols, and volatile compounds were detected. HPE powder was dissolved in different solvents, including deionized water (HPE$_{H2O}$), DMSO (HPE$_{DMSO}$), 100% v/v ethanol (HPE$_{EtOH100}$), and 50% v/v ethanol (HPE$_{EtOH50}$). The highest polyphenol levels were found in HPE$_{DMSO}$ and HPE$_{EtOH50}$, whereas different volatile compounds, mainly β-caryophyllene and eugenol, were detected in all the extracts except for HPE$_{H2O}$. HPE$_{H2O}$ and HPE$_{DMSO}$ were able to enhance CB2 receptor expression and to downregulate PI-PLC β2 in synovial membranes; moreover, all the extracts inhibited FAAH activity. The present results highlight for the first time a multitarget modulation of the endocannabinoid system by HPE, likely ascribable to its hydrosoluble compounds, along with the presence of volatile compounds in *H. procumbens* root. Although hydrosoluble compounds seem to be mainly responsible for endocannabinoid modulation by HPE, a possible contribution of volatile compounds can be suggested, strengthening the hypothesis that the entire phytocomplex can contribute to the *H. procumbens* healing properties.

Keywords: osteoarthritis; nutraceuticals; polyphenols; volatile compounds; β-caryophyllene; eugenol; FAAH; cannabinoid receptors; phospholipases

1. Introduction

Osteoarthritis (OA) is a pathology of the whole joint structure, involving several cellular and molecular processes, in different types of cells, such as chondrocytes, osteoblasts, synoviocytes, and

Article

Biochemical and Computational Studies of the Interaction between a Glucosamine Derivative, NAPA, and the IKKα Kinase

Mariangela Lopreiato [1,2,†], Samuele Di Cristofano [3,†], Rossana Cocchiola [1,4], Alessia Mariano [1], Libera Guerrizio [1], Roberto Scandurra [1], Luciana Mosca [1], Domenico Raimondo [3,*,‡] and Anna Scotto d'Abusco [1,*,‡]

1   Department of Biochemical Sciences, Sapienza University of Roma, P.le Aldo Moro 5, 00185 Rome, Italy; mariangela.lopreiato@gmail.com (M.L.); rossana.cocchiola@gmail.com (R.C.); alessia.mariano@uniroma1.it (A.M.); liberagtab3@gmail.com (L.G.); roberto.scandurra@fondazione.uniroma1.it (R.S.); luciana.mosca@uniroma1.it (L.M.)
2   Department of Medicina Sperimentale, Università Magna Graecia, Campus S. Venuta, 88100 Catanzaro, Italy
3   Department of Molecular Medicine, Sapienza University of Rome, Viale Regina Elena 291, 00161 Rome, Italy; dicristofano.1665448@studenti.uniroma1.it
4   Clinical Trial Unit, Bambino Gesù Children's Hospital, IRCSS, P. Sant'Onofrio 4, 00165 Rome, Italy
*   Correspondence: domenico.raimondo@uniroma1.it (D.R.); anna.scottodabusco@uniroma1.it (A.S.d.)
†   These authors contributed equally to this work.
‡   These authors contributed equally to this work as senior co-authors.

Abstract: The glucosamine derivative 2-(N-Acetyl)-L-phenylalanylamido-2-deoxy-β-D-glucose (NAPA), was shown to inhibit the kinase activity of IKKα, one of the two catalytic subunits of IKK complex, decreasing the inflammatory status in osteoarthritis chondrocytes. In the present work we have investigated the inhibition mechanism of IKKα by NAPA by combining computational simulations, in vitro assays and Mass Spectrometry (MS) technique. The kinase in vitro assay was conducted using a recombinant IKKα and IKKtide, a 20 amino acid peptide substrate derived from IκBα kinase protein and containing the serine residues Ser32 and Ser36. Phosphorylated peptide production was measured by Ultra Performance Liquid Chromatography coupled with Mass Spectrometry (UPLC-MS), and the atomic interaction between IKKα and NAPA has been studied by molecular docking and Molecular Dynamics (MD) approaches. Here we report that NAPA was able to inhibit the IKKα kinase activity with an IC_{50} of 0.5 mM, to decrease the K_m value from 0.337 mM to 0.402 mM and the V_{max} from 0.0257 mM·min^{-1} to 0.0076 mM·min^{-1}. The computational analyses indicate the region between the KD, ULD and SDD domains of IKKα as the optimal binding site explored by NAPA. Biochemical data indicate that there is a non-significant difference between K_m and K_i whereas there is a statistically significant difference between the two V_{max} values. This evidence, combined with computational results, consistently indicates that the inhibition is non-competitive, and that the NAPA binding site is different than that of ATP or IKKtide.

Keywords: IKK; NAPA; osteoarthritis; chondrocytes; UPLC-MS; molecular docking; molecular dynamics

1. Introduction

The IκB kinase (IKK) complex is involved in several cellular pathways, among them the activation of Nuclear Factor-κB family, (NFκB) which is involved in several aspects of both normal and disease physiology [1]. IKK complex is a high molecular weight multi-subunits complex, which comprises two catalytic subunits, IKKα and IKKβ, and a regulatory subunit, IKKγ/NEMO [2].

The IKKα and IKKβ proteins share high amino acid sequence identity, almost 50%, and their 3D structure presents a kinase catalytic domain (KD) at N-terminal region, a ubiquitin-like domain (ULD) in the middle, followed by an α-helical scaffold/dimerization domain

169

Chitosan scaffolds with enhanced mechanical strength and elastic response by combination of freeze gelation, photo-crosslinking and freeze-drying

Ilaria Silvestro [a], Riccardo Sergi [a], Anna Scotto D'Abusco [b], Alessia Mariano [b], Andrea Martinelli [a], Antonella Piozzi [a], Iolanda Francolini [a,*]

[a] Department of Chemistry, Sapienza University of Rome, Italy
[b] Department of Biochemical Sciences, Sapienza University of Rome, Italy.

ARTICLE INFO

ABSTRACT

In this study, a new scaffold fabrication method based on the combination of a series of stabilization processes was set up to obtain chitosan scaffolds with improved mechanical properties for regeneration of load-bearing tissues. Specifically, thermally induced phase separation (TIPS) of chitosan solutions was used to obtain an open structure which was then stabilized by freeze-gelation and photo cross-linking. Freeze-gelation combined with freeze-drying permitted to obtain a porous structure with a 95 μm-mean pore size suitable for osteoblast cells' housing. Photo-crosslinking improved by ca. three times the scaffold compressive modulus, passing from 0,8 MPa of the uncrosslinked scaffolds to 2,2 MPa of the crosslinked one. Hydrated crosslinked scaffolds showed a good elastic response, with an 80% elastic recovery for at least 5 consecutive compressive cycles. The herein reported method has the advantage to not require the use of potentially toxic cross-linking agents and may be extended to other soft materials.

1. Introduction

Tissue engineering is a very promising approach to in vivo regenerate damaged tissues. Such approach relies on the seeding of cells into biocompatible and biodegradable porous scaffolds, acting as temporary biological and mechanical supports for cell adhesion and tissue growth. The structure of the scaffolds plays a pivotal role for the success of tissue regeneration since it should provide an environment able to mimicking the extracellular matrix in terms of porosity, pore interconnection and mechanical stability. Specifically, under a functional point of view, the scaffold should keep a structural integrity for all tissue regeneration course and ensure a mechanical response coherent with the replaced tissue. A proper mechanical response is crucial for regeneration of load-bearing tissues, like bones or cartilages, but also for replacement of non-load bearing soft tissues submitted to repeated and cyclical stresses like heart valves. Besides that, recently, a correlation between scaffold stiffness and cell behavior has been also demonstrated (Dado & Levenberg, 2009).

Polysaccharides are considered among the best materials for tissue regeneration because of their excellent biodegradability, biocompatibility, and bioactivity. However, these soft materials often suffer from poor mechanical resistance and low stability in water environment, which may compromise their in-use performance. That's also the case of chitosan, a natural polycation deriving from the partial deacetylation of chitin, largely investigated for biomedical applications, because of its outstanding biological properties including mucoadhesivity and anti-microbial properties (Amato et al., 2018; Cuzzucoli Crucitti et al., 2018; Francolini, Donelli, Crisante, Taresco, & Piozzi, 2015; Silvestro et al., 2020; Wang et al., 2020). Additionally, more than other natural polymers, chitosan triggers a minimal foreign-body response and fibrous encapsulation (Bhattarai, Edmondson, Veiseh, Matsen, & Zhang, 2005; Jayakumar, Prabaharan, Nair, & Tamura, 2010; Kim et al., 2008). Chitosan has been shown to be especially attractive as a scaffold material for bone regeneration due to its in vitro ability to support adhesion and proliferation of osteoblasts as well as promote formation of mineralized bone matrix (Aguilar et al., 2019; Seol et al., 2004). Indeed, chitosan, together with hydroxyapatite, is among the very few osteoconductive materials considered promising for bone tissue engineering (Venkatesan

Article

Metabolomic Profiling of Fresh Goji (*Lycium barbarum* L.) Berries from Two Cultivars Grown in Central Italy: A Multi-Methodological Approach

Mattia Spano [1,†], Alessandro Maccelli [1,†], Giacomo Di Matteo [1], Cinzia Ingallina [1], Mariangela Biava [1], Maria Elisa Crestoni [1,*], Jean-Xavier Bardaud [2], Anna Maria Giusti [3], Alessia Mariano [4], Anna Scotto D'Abusco [4], Anatoly P. Sobolev [5,*], Alba Lasalvia [1], Simonetta Fornarini [1] and Luisa Mannina [1]

[1] Department of Chemistry and Technology of Drugs, Sapienza University of Rome, Piazzale Aldo Moro 5, 00185 Rome, Italy; mattia.spano@uniroma1.it (M.S.); alessandro.maccelli@uniroma1.it (A.M.); giacomo.dimatteo@uniroma1.it (G.D.M.); cinzia.ingallina@uniroma1.it (C.I.); mariangela.biava@uniroma1.it (M.B.); alba.lasalvia@uniroma1.it (A.L.); simonetta.fornarini@uniroma1.it (S.F.); luisa.mannina@uniroma1.it (L.M.)
[2] Institut de Chimie Physique, CLIO, Université Paris Saclay, Bât 200, BP34, CEDEX, 91898 Orsay, France; j.xavier.bardaud@gmail.com
[3] Department of Experimental Medicine, Sapienza University of Rome, P.le Aldo Moro 5, 00185 Rome, Italy; annamaria.giusti@uniroma1.it
[4] Department of Biochemical Sciences, Sapienza University of Roma, P.le Aldo Moro 5, 00185 Rome, Italy; alessia.mariano@uniroma1.it (A.M.); anna.scottodabusco@uniroma1.it (A.S.D.)
[5] Institute for Biological Systems, Magnetic Resonance Laboratory "Segre-Capitani", CNR, Via Salaria Km 29.300, 00015 Monterotondo, Italy
* Correspondence: mariaelisa.crestoni@uniroma1.it (M.E.C.); anatoly.sobolev@cnr.it (A.P.S.)
† These authors contributed equally to this work.

Abstract: The metabolite profile of fresh Goji berries from two cultivars, namely Big Lifeberry (BL) and Sweet Lifeberry (SL), grown in the Lazio region (Central Italy) and harvested at two different periods, August and October, corresponding at the beginning and the end of the maturation, was characterized by means of nuclear magnetic resonance (NMR) and electrospray ionization Fourier transform ion cyclotron resonance (ESI FT-ICR MS) methodologies. Several classes of compounds such as sugars, amino acids, organic acids, fatty acids, polyphenols, and terpenes were identified and quantified in hydroalcoholic and organic Bligh-Dyer extracts. Sweet Lifeberry extracts were characterized by a higher content of sucrose with respect to the Big Lifeberry ones and high levels of amino acids (glycine, betaine, proline) were observed in SL berries harvested in October. Spectrophotometric analysis of chlorophylls and total carotenoids was also carried out, showing a decrease of carotenoids during the time. These results can be useful not only to valorize local products but also to suggest the best harvesting period to obtain a product with a chemical composition suitable for specific industrial use. Finally, preliminary studies regarding both the chemical characterization of Goji leaves generally considered a waste product, and the biological activity of Big Lifeberry berries extracts was also investigated. Goji leaves showed a chemical profile rich in healthy compounds (polyphenols, flavonoids, etc.) confirming their promising use in the supplements/nutraceutical/cosmetic field. MG63 cells treated with Big Lifeberry berries extracts showed a decrease of iNOS, COX-2, IL-6, and IL-8 expression indicating their significant biological activity.

Keywords: Goji berries; metabolite profile; NMR; FT-ICR MS; Goji leaves; biological assays

1. Introduction

Goji berries or wolfberries (*Lycium* fruits) are healthy fruits of closely related shrubs from the genus *Lycium*, belonging to the Solanaceae family. *L. barbarum* and *L. chinense*

Article

Role of Caryophyllane Sesquiterpenes in the Entourage Effect of Felina 32 Hemp Inflorescence Phytocomplex in Triple Negative MDA-MB-468 Breast Cancer Cells

Silvia Di Giacomo [1,*], Alessia Mariano [2], Marco Gullì [1], Caterina Fraschetti [3], Annabella Vitalone [1], Antonello Filippi [3], Luisa Mannina [3], Anna Scotto d'Abusco [2] and Antonella Di Sotto [1,*]

[1] Department of Physiology and Pharmacology "V. Erspamer", Sapienza University of Rome, P.le Aldo Moro 5, 00185 Rome, Italy; marco.gulli@uniroma1.it (M.G.); annabella.vitalone@uniroma1.it (A.V.)

[2] Department of Biochemical Sciences, Sapienza University of Rome, P.le Aldo Moro 5, 00185 Rome, Italy; alessia.mariano@uniroma1.it (A.M.); anna.scottodabusco@uniroma1.it (A.S.d.)

[3] Department of Drug Chemistry and Technologies, Sapienza University of Rome, P.le Aldo Moro 5, 00185 Rome, Italy; caterina.fraschetti@uniroma1.it (C.F.); antonello.filippi@uniroma1.it (A.F.); luisa.mannina@uniroma1.it (L.M.)

* Correspondence: silvia.digiacomo@uniroma1.it (S.D.G.); antonella.disotto@uniroma1.it (A.D.S.)

Abstract: *Cannabis sativa* L. crops have been traditionally exploited as sources of fibers, nutrients, and bioactive phytochemicals of medical interest. In the present study, two terpene-rich organic extracts, namely FOJ and FOS, obtained from Felina 32 hemp inflorescences collected in June and September, respectively, have been studied for their in vitro anticancer properties. Particularly, their cytotoxicity was evaluated in different cancer cell lines, and the possible entourage effect between nonintoxicating phytocannabinoids (cannabidiol and cannabichromene) and caryophyllane sesquiterpenes (β-caryophyllene, β-caryophyllene oxide and α-humulene), as identified at GC/MS analysis, was characterized. Modulation of cannabinoid CB1 and CB2 receptors was studied as a mechanistic hypothesis. Results highlighted marked cytotoxic effects of FOJ, FOS, and pure compounds in triple negative breast cancer MDA-MB-468 cells, likely mediated by a CB2 receptor activation. Cannabidiol was the main cytotoxic constituent, although low levels of caryophyllane sesquiterpenes and cannabichromene induced potentiating effects; the presence in the extracts of unknown antagonistic compounds has been highlighted too. These results suggest an interest in Felina 32 hemp inflorescences as a source of bioactive phytocomplexes with anticancer properties and strengthen the importance of considering the possible involvement of minor terpenes, such as caryophyllane sesquiterpenes, in the entourage effect of hemp-based extracts.

Keywords: hemp inflorescences; phytocannabinoids; cannabidiol; cannabichromene; β-caryophyllene; β-caryophyllene oxide; α-humulene; chemosensitizing effects; triple negative breast cancer; entourage effect

1. Introduction

Cannabis sativa L. (Fam. Cannabaceae) is a plant cultivated since the ancient times as a multipurpose crop: it is exploited all over the world to produce fiber, oil, and biomass that are used in different materials such as clothing, net, paper, canvas, varnishes, inks, biofuel, material for phytoremediation, food and animal feed, nutraceuticals, and cosmetics [1]. Recently, the interest in its medical uses is growing, owing to the highlighted therapeutic potential of its phytoconstituents, particularly Δ9-tetrahydrocannabinol (Δ9-THC or THC) and cannabidiol (CBD), which have been shown to possess numerous bioactivities, among which anticancer properties [2–4]. Based on the THC and CBD content, different crops of hemp have been approached for medical purposes; among them, type I Cannabis, characterized by high levels of THC (>85% w/w), and type II crops, mainly containing CBD, with relative high amounts of THC, have been limited due to the psychoactive effects

Article

Pheomelanin Effect on UVB Radiation-Induced Oxidation/Nitration of L-Tyrosine

Alessia Mariano [1], Irene Bigioni [1], Anna Scotto d'Abusco [1], Alessia Baseggio Conrado [2], Simonetta Maina [1], Antonio Francioso [1], Luciana Mosca [1] and Mario Fontana [1,*]

[1] Department of Biochemical Sciences, Sapienza University of Rome, Piazzale Aldo Moro 5, 00185 Rome, Italy; alessia.mariano@uniroma1.it (A.M.); bigioni.1639690@studenti.uniroma1.it (I.B.); anna.scottodabusco@uniroma1.it (A.S.d.); simonetta.maina@yahoo.it (S.M.); antonio.francioso@uniroma1.it (A.F.); luciana.mosca@uniroma1.it (L.M.)

[2] National Heart & Lung Institute, Imperial College London, Norfolk Place, London W2 1PG, UK; a.baseggio-conrado@imperial.ac.uk

* Correspondence: mario.fontana@uniroma1.it; Tel.: +39-06-4991-0948

Abstract: Pheomelanin is a natural yellow-reddish sulfur-containing pigment derived from tyrosinase-catalyzed oxidation of tyrosine in presence of cysteine. Generally, the formation of melanin pigments is a protective response against the damaging effects of UV radiation in skin. However, pheomelanin, like other photosensitizing substances, can trigger, following exposure to UV radiation, photochemical reactions capable of modifying and damaging cellular components. The photoproperties of this natural pigment have been studied by analyzing pheomelanin effect on oxidation/nitration of tyrosine induced by UVB radiation at different pH values and in presence of iron ions. Photoproperties of pheomelanin can be modulated by various experimental conditions, ranging from the photoprotection to the triggering of potentially damaging photochemical reactions. The study of the photomodification of L-Tyrosine in the presence of the natural pigment pheomelanin has a special relevance, since this tyrosine oxidation/nitration pathway can potentially occur in vivo in tissues exposed to sunlight and play a role in the mechanisms of tissue damage induced by UV radiation.

Keywords: pheomelanin; nitrotyrosine; dityrosine; photooxidation; photosensitizer

1. Introduction

Pheomelanin is one of the existing forms of the natural pigment melanin. Melanin is present in the skin in two forms: eumelanin and pheomelanin. Eumelanin is a heterogeneous polymer composed mainly of dihydroxyindole units derived from tyrosinase-catalyzed oxidation of tyrosine or 3,4-dihydroxyphenylalanine (DOPA) to dopaquinone. Compared to eumelanin, pheomelanin structure differs due to non-enzymatic addition of cysteine to dopaquinone during the pathway of pigment biosynthesis. DOPA-derivatives with cysteine, such as 5'-S-cysteinyldopa and in minor amount 2'-S-cystenyldopa, are incorporated into the pigment in the form of 1,4-benzothiazine units (Figure 1) [1]. Before being incorporated into pheomelanin, a minor part of 1,4-benzothiazine units may undergo further structural modifications with formation of benzothiazole moiety which copolymerizes with benzothiazine units [2–4]. Interestingly, slight variations in the monomer composition of pigment polymer skeleton have been shown to determine significant differences in light absorption, antioxidant activity, redox behavior, and metal chelation [5].

It is commonly believed that melanin plays an important role in the modulation of the photochemical reactions that occur in the skin. Numerous experimental and clinical evidences have shown a protective role of eumelanin on the damage triggered by UV irradiation on the skin [6]. A lower incidence of UV-induced skin diseases is observed in individuals with darker skin pigmentation, where eumelanin is present. Conversely, a higher incidence of UV-induced skin diseases was found in red-haired individuals with pale

173

Article

One-Pot Preparation of Hydrophilic Polylactide Porous Scaffolds by Using Safe Solvent and Choline Taurinate Ionic Liquid

Anna Clara De Felice [1], Valerio Di Lisio [1], Iolanda Francolini [1], Alessia Mariano [2], Antonella Piozzi [1], Anna Scotto d'Abusco [2], Elisa Sturabotti [1,*] and Andrea Martinelli [1,*]

[1] Department of Chemistry, Sapienza University of Rome, P.le Aldo Moro 5, 00185 Rome, Italy; annaclara.defelice@gmail.com (A.C.D.F.); valerio.dilisio@dipc.org (V.D.L.); iolanda.francolini@uniroma1.it (I.F.); antonella.piozzi@uniroma1.it (A.P.)

[2] Department of Biochemical Sciences, Sapienza University of Rome, P.le Aldo Moro 5, 00185 Rome, Italy; alessia.mariano@uniroma1.it (A.M.); anna.scottodabusco@uniroma1.it (A.S.d.)

* Correspondence: elisa.sturabotti@uniroma1.it (E.S.); andrea.martinelli@uniroma1.it (A.M.)

Abstract: Polylactides (PLAs) are a class of polymers that are very appealing in biomedical applications due to their degradability in nontoxic products, tunable structural, and mechanical properties. However, they have some drawbacks related to their high hydrophobicity, lack of functional groups able to graft bioactive molecules, and solubility in unsafe solvents. To circumvent these shortcomings, porous scaffolds for tissue engineering were prepared by vigorously mixing a solution of isotactic and atactic PLA in nontoxic ethyl acetate at 70 °C with a water solution of choline taurinate. The partial aminolysis of the polymer ester bonds by taurine $-NH_2$ brought about the formation of PLA oligomers with surfactant activity that stabilized the water-in-oil emulsion. Upon drying, a negligible shrinking occurred, and mechanically stable porous scaffolds were obtained. By varying the polymer composition and choline taurinate concentration, it was possible to modulate the pore dimensions (30–50 μm) and mechanical properties (Young's moduli: 1–6 MPa) of the samples. Furthermore, the grafted choline taurinate made the surface of the PLA films hydrophilic, as observed by contact angle measurements (advancing contact angle: 76°; receding contact angle: 40°–13°). The preparation method was very simple because it was based on a one-pot mild reaction that did not require an additional purification step, as all the employed chemicals were nontoxic.

Keywords: polylactide; porous scaffold; tissue engineering; ethyl acetate; choline taurinate; ionic liquid

1. Introduction

Polylactides or polylactic acids (PLAs) are one of the most studied and employed synthetic polymer classes in many medical specialties, including orthopedic, general and plastic surgery, dentistry, and pharmacology. The market offers a wide variety of PLA-based commercial devices [1,2], and a very wide range of scientific literature suggests PLAs for the preparation of temporary prostheses and devices, drug-delivery systems, and scaffolds for tissue engineering as well. This results from the combination of the typical advantages of synthetic polymers, such as tunable chemical and physical properties, and PLAs' specific features. In fact, by selecting the proper ratio between the two enantiomeric monomers in the polymerization feed, isotactic poly(L-lactide) (PLLA) and poly(D-lactide) (PDLA) or completely atactic poly(DL-lactide) (PDLLA) polymer, as well as polymers with different D-L contents, can be obtained. Therefore, according to their composition, PLAs' crystallinity and chemical, physical, thermal, and mechanical properties are easily modulated. Moreover, PLAs are biocompatible and biodegradable, and the degradation rate can be tuned by crystallinity. In body tissues, PLAs are resorbed with small or negligible adverse response, and are approved by national and international agencies (FDA, EMA) for medical uses [3].

174

Harpagophytum procumbens Root Extract Mediates Anti-Inflammatory Effects in Osteoarthritis Synoviocytes through CB2 Activation

Alessia Mariano [1], Irene Bigioni [1], Roberto Mattioli [1], Antonella Di Sotto [2], Martina Leopizzi [3], Stefania Garzoli [4], Pier Francesco Mariani [5], Pietro Dalla Vedova [6], Sergio Ammendola [7] and Anna Scotto d'Abusco [1,*]

[1] Department of Biochemical Sciences, Sapienza University of Rome, 00185 Roma, Italy; alessia.mariano@uniroma1.it (A.M.); irene.bigioni@uniroma1.it (I.B.); roberto.mattioli@uniroma1.it (R.M.)
[2] Department of Physiology and Pharmacology, Sapienza University of Rome, 00185 Rome, Italy; antonella.disotto@uniroma1.it
[3] Department of Medico-Surgical Sciences and Biotechnologies, Polo Pontino-Sapienza University, 04100 Latina, Italy; martina.leopizzi@uniroma1.it
[4] Department of Drug Chemistry and Technologies, Sapienza University of Rome, 00185 Rome, Italy; stefania.garzoli@uniroma1.it
[5] Casa di Cura Villa Stuart, 00135 Rome, Italy; pierfrancescomariani@pec.it
[6] UOC di Ortopedia e Traumatologia, Ospedale Santa Scolastica di Cassino, ASL di Frosinone, 03043 Cassino, Italy; pietro.dallavedova@aslfrosinone.it
[7] Ambiotec S.A.S., 04012 Cisterna di Latina (LT), Italy; ambiotec@libero.it
[*] Correspondence: anna.scottodabusco@uniroma1.it; Tel.: +39-06-4991-0947

Abstract: The endocannabinoid system is involved in the nociceptive and anti-inflammatory pathways, and a lowered expression of CB2 receptors has been associated with inflammatory conditions, such as osteoarthritis (OA). This suggests that CB2 modulators could be novel therapeutic tools to treat OA. In the present study, the involvement of *Harpagophytum procumbens* root extract, a common ingredient of nutraceuticals used to treat joint disorders, in CB2 modulation has been evaluated. Moreover, to clarify the effects of the pure single components, the bioactive constituent, harpagoside, and the main volatile compounds were studied alone or in a reconstituted mixture. Human fibroblast-like synoviocytes, extracted by joints of patients, who underwent a total knee replacement, were treated with an *H. procumbens* root extract dissolved in DMSO (HPE$_{DMSO}$). The effectiveness of HPE$_{DMSO}$ to affect CB2 pathways was studied by analyzing the modulation of cAMP, the activation of PKA and ERK MAP kinase, and the modulation of MMP-13 production. HPE$_{DMSO}$ was able to inhibit the cAMP production and MAP kinase activation and to down-regulate the MMP-13 production. Pure compounds were less effective than the whole phytocomplex, thus suggesting the involvement of synergistic interactions. Present findings encourage further mechanistic studies and support the scientific basis of the use of *H. procumbens* in joint disorders.

Keywords: osteoarthritis; fibroblast-like synoviocytes; endocannabinoid system; CB2; devil's claw; harpagoside; volatile compounds; β-caryophyllene; eugenol; α-humulene

1. Introduction

Osteoarthritis (OA) is a degenerative and inflammatory disease that affects the joints of the patients, causing pain and functional limitations. This is a pathology of the cartilage, a specialized tissue with a support function, which lubricates the articular surface and allows the sliding between the two joint heads. The degeneration of cartilage provokes strong friction of the subchondral bones in the joints, causing pain, swelling, and bone remodeling, in particular the formation of osteophytes. The joints mainly affected are those of the knees, hips, and fingers [1]. A growing body of evidence suggests that inflammation is strongly

Efficacy of Combined Mechanical and Chemical Decontamination Treatments on Smooth and Rough Titanium Surfaces and Their Effects on Osteoconduction: An Ex Vivo Study

Marco Lollobrigida, DDS, PhD[1]/Luca Lamazza, MD, DDS, PhD[1]/Marisa Di Pietro, Mchem, PhD[2]/
Simone Filardo, MD, PhD[2]/Mariangela Lopreiato, CTF, PhD[3]/Alessia Mariano, CTF, PhD Student[3]/
Giuseppina Bozzuto, MBiolSci, PhD[4]/Agnese Molinari, MBiolSci[4]/
Francesca Menchini, MPhys, PhD Student[5]/Adriano Piattelli, MD, PhD[6]/Alberto De Biase, MD[1]

Purpose: The aim of this ex vivo study was to assess the ability to remove oral biofilm by different combinations of mechanical and chemical treatments on smooth and rough titanium surfaces, as well as their impact on osteoconduction. *Materials and Methods:* Forty-eight sandblasted acid-etched (SLA) and 48 machined titanium disks were contaminated with oral bacterial biofilm and exposed to the following treatments: *(1)* titanium brush (TB), *(2)* TB + 40% citric acid (CA), *(3)* TB + 5.25% sodium hypochlorite (NaOCl), *(4)* air polishing with glycine powder (AP), *(5)* AP + 40% CA, and *(6)* AP + 5.25% NaOCl. Residual bacteria and chemical contamination were assessed using viable bacterial count assay, scanning electron microscopy (SEM), and x-ray spectroscopy (XPS). Human primary osteoblast (hOB) adhesion and osteocalcin (OC) release were also evaluated. *Results:* The microbiologic, SEM, and XPS analysis indicate a higher biofilm removal efficiency of combined mechanical-chemical treatments compared with exclusively mechanical approaches, especially on SLA surfaces. SEM analysis revealed significant alterations of surface microtopography on the disks treated with TB, while no changes were observed after AP treatment. OC release by hOBs was mainly decreased on disks treated with CA and NaOCl. *Conclusion:* The combination of mechanical and chemical treatments provides effective oral biofilm removal on both SLA and machined implant surfaces. NaOCl and CA may have a negative effect on osteoblasts cultured on SLA samples. *Int J Oral Maxillofac Implants 2022;37:57–66. doi: 10.11607/jomi.9105*

Keywords: antiseptics, implant decontamination, peri-implantitis, surface decontamination

Peri-implantitis has become an increasingly common condition among patients undergoing implant-prosthetic rehabilitations. In a recent retrospective cohort study, it was found that approximately one-third of the patients and one-fifth of all implants experienced peri-implantitis.[1]

Peri-implantitis is a complex multifactorial disease characterized by tissue inflammation and progressive bone loss. Though many factors are involved in disease pathogenesis, it is well established that the primary cause of peri-implantitis is the bacterial colonization of the implant surface.[2–5] Therefore, biofilm removal is assumed to be crucial for peri-implantitis treatment.

Different approaches have been proposed to eliminate bacterial biofilm from implant surfaces, including mechanical, chemical, and combined treatments. Mechanical treatments disrupt the biofilm by means of a direct physical action of the instrument, or a medium, on the implant surface. These include curettes of different materials, air polishing, and ultrasonic and rotary instruments (burs and brushes).[6] Due to the intrinsic limitations of these instruments in achieving a complete biofilm removal, chemical agents are often used as an adjunctive treatment,[7] including chlorhexidine, citric or orthophosphoric acid, and sodium hypochlorite.[8]

[1]Department of Oral and Maxillo Facial Sciences, Sapienza University of Rome, Rome, Italy.
[2]Department of Public Health and Infectious Diseases, Section of Microbiology, Sapienza University of Rome, Rome, Italy.
[3]Department of Biochemical Sciences, Sapienza University of Rome, Rome, Italy.
[4]National Centre of Drug Research and Evaluation, Istituto Superiore di Sanità, Rome, Italy.
[5]Energy Technology Department, ENEA, Casaccia Research Center, Rome, Italy.
[6]Department of Medical, Oral and Biotechnological Sciences, University of Chieti-Pescara, Chieti, Italy.

Correspondence to: Dr Luca Lamazza, Department of Oral and Maxillo Facial Sciences, Sapienza University of Rome, Via Caserta 6 - 00161 Rome, Italy. Email: luca.lamazza@uniroma1.it

Review

The Nutraceuticals as Modern Key to Achieve Erythrocyte Oxidative Stress Fighting in Osteoarthritis

Alessia Mariano [1,†], Irene Bigioni [1,†], Francesco Misiti [2,*], Luigi Fattorini [3], Anna Scotto d'Abusco [1] and Angelo Rodio [2]

[1] Department of Biochemical Sciences, Sapienza University of Rome, 00185 Rome, Italy
[2] Department of Human Sciences, Society and Health, University of Cassino and Southern Lazio, 03043 Cassino, Italy
[3] Department of Physiology and Pharmacology, Sapienza University of Rome, 00185 Rome, Italy
* Correspondence: f.misiti@unicas.it
† These authors contributed equally to this work.

Abstract: Osteoarthritis (OA), the most common joint disease, shows an increasing prevalence in the aging population in industrialized countries. OA is characterized by low-grade chronic inflammation, which causes degeneration of all joint tissues, such as articular cartilage, subchondral bone, and synovial membrane, leading to pain and loss of functionality. Erythrocytes, the most abundant blood cells, have as their primary function oxygen transport, which induces reactive oxygen species (ROS) production. For this reason, the erythrocytes have several mechanisms to counteract ROS injuries, which cause damage to lipids and proteins of the cell membrane. Oxidative stress and inflammation are highly correlated and are both causes of joint disorders. In the synovial fluid and blood of osteoarthritis patients, erythrocyte antioxidant enzyme expression is decreased. To date, OA is a non-curable disease, treated mainly with non-steroidal anti-inflammatory drugs and corticosteroids for a prolonged period of time, which cause several side effects; thus, the search for natural remedies with anti-inflammatory and antioxidant activities is always ongoing. In this review, we analyze several manuscripts describing the effect of traditional remedies, such as *Harpagophytum procumbens*, *Curcumin longa*, and *Boswellia serrata* extracts, in the treatments of OA for their anti-inflammatory, analgesic, and antioxidant activity. The effects of such remedies have been studied both in in vitro and in vivo models, considering both joint cells and erythrocytes.

Keywords: oxidative stress; erythrocytes; osteoarthritis; nutraceuticals; *Harpagophytum procumbens*; *Boswellia serrata*; *Curcuma longa*

1. Introduction

Osteoarthritis (OA) is a chronic, degenerative, and inflammatory disease that affects articular joints, causing pain and functional limitation in patients. Knee, hip, and the small articular joints in the hand are mainly involved [1]. For several years, OA disease was called Arthrosis and considered only a pathology linked to the aging process. Recently, scientific studies demonstrated the involvement of inflammation in OA pathogenesis, which now is officially recognized as Osteoarthritis. The desinence "itis" indicates quantitatively variable inflammation, which is present in each phase of the disease [2]. OA affects more than 20% of the general population [3] and is significantly increased among retired elite athletes, with prevalence rates as high as 95% [4]. The incidence of OA increases with age, and women have higher rates than men, especially after age 50. A leveling off or decrease in incidence occurs at all joint sites around the age of 80 [5]. The prevalence and incidence of OA across studies vary greatly. It depends on the population sampled (primary versus tertiary care) and risk factors, such as age, sex, obesity, and geographical region [1].

Nowadays, there is no cure for OA disease; all the therapies are aimed to reduce pain and inflammation and improve the patient quality of life. Drugs mainly administered are

Acknowledgements

First and foremost, I am extremely grateful to my Supervisor, Prof. Anna Scotto d'Abusco for her valuable advice, continued support and patience during my PhD study. Thank you for guiding and encouraging me throughout my academic research by challenging me to grow as a scientist.

My sincere thanks also go to my labmates. I would like to thank Dr. Mariangela Lopreiato and Dr. Irene Bigioni for the cherished time spent together in the lab, for their support and friendship.
This journey would not have been the same without you!

I am very grateful to Prof. Francesco Malatesta, our PhD Coordinator, for his valuable guidance, wise teachings, and keen interest in our education.

Finally, I would like to express my gratitude to all our scientific collaborators who have contributed to my personal and professional evolution during my PhD experience.